Energy-efficient Control of a Smart Grid with Sustainable Homes based on Distributing Risk

by

Masahiro Ono

S.B., Aeronautics and Astronautics,
The University of Tokyo (2005)
S.M., Aeronautics and Astronautics,
Massachusetts Institute of Technology (2007)

MASSACHUSETTS INSTITUTE OF TECHNOLOGY
FEB 0 1 2012
LIBRARIES

ARCHIVES

Submitted to the Engineering Systems Division
in partial fulfillment of the requirements for the degree of

Master of Science in Technology and Policy

at the

MASSACHUSETTS INSTITUTE OF TECHNOLOGY

February 2012

© Massachusetts Institute of Technology 2012. All rights reserved.

Author .....
Engineering Systems Division
Jan 20, 2012

Certified by .....
Brian C. Williams, Ph.D.
Professor of Aeronautics and Astronautics
Thesis Supervisor

Accepted by .....
Dava J. Newman, Ph.D.
Professor of Aeronautics and Astronautics and Engineering Systems
Director, Technology and Policy Program

Energy-efficient Control of a Smart Grid with Sustainable Homes based on Distributing Risk

by

Masahiro Ono

Submitted to the Engineering Systems Division
on Jan 20, 2012, in partial fulfillment of the
requirements for the degree of
Master of Science in Technology and Policy

Abstract

The goal of this thesis is to develop a distributed control system for a smart grid with sustainable homes. A central challenge is how to enhance energy efficiency in the presence of uncertainty.

A major source of uncertainty in a smart grid is intermittent energy production by renewable energy sources. In the face of global climate change, it is crucial to reduce dependence on fossil fuels and shift to renewable energy sources, such as wind and solar. However, a large-scale introduction of wind and solar generation to an electrical grid poses a significant risk of blackouts since the energy supplied by the renewables is unpredictable and intermittent. The uncertain behavior of renewable energy sources increases the risk of blackouts. Therefore, an important challenge is to develop an intelligent control mechanism for the electrical grid that is both reliable and efficient.

Uncertain weather conditions and human behavior pose challenges for a smart home. For example, autonomous room temperature control of a residential building may occasionally make the room environment uncomfortable for residents. Autonomous controllers must be able to take residents' preferences as an input, and to control the indoor environment in an energy-efficient manner while limiting the risk of failure to meet the residents' requirements in the presence of uncertainties.

In order to overcome these challenges, we propose a distributed robust control method for a smart grid that includes smart homes as its building components. The proposed method consists of three algorithms: 1) market-based contingent energy dispatcher for an electrical grid, 2) a risk-sensitive plan executive for temperature control of a residential building, and 3) a chance-constrained model-predictive controller with a probabilistic guarantee of constraint satisfaction, which can control continuously operating systems such as an electrical grid and a building. We build the three algorithms upon the chance-constrained programming framework: minimization of a given cost function with chance constraints, which bound the probability of failure to satisfy given state constraints.

Although these technologies provide promising capabilities, they cannot contribute

to sustainability unless they are accepted by the society. In this thesis we specify policy challenges for a smart grid and a smart home, and discuss policy options that gives economical and regulatory incentives for the society to introduce these technologies on a large scale.

Thesis Supervisor: Brian C. Williams, Ph.D.
Title: Professor of Aeronautics and Astronautics

妻に捧ぐ

This thesis is for my wife, Eriko.

Acknowledgments

I would like to express my gratitude to all who have supported me in completion of this thesis.

First, I would like to express my most profound gratitude for my advisor, Prof. Brian C. Williams. Three years ago when I consulted with him about starting a second degree in the Technology and Policy Program (TPP), he greatly encouraged me to do so and supported my application to the program. He offered me a wonderful opportunity to work on a research topic that is both interesting and important, namely, smart grid and building control. I was able to complete this research thanks to his insightful guidance and enthusiastic support. Also, I am very thankful for his hard work on the weekend right before the thesis deadline to give me feedback on time.

I would like to thank Prof. William J. Mitchell and Prof. Federico Casalegno at the MIT Mobile Experience Laboratory (MEL) for providing me the opportunity to join their Connected Sustainable Home project. Through this fruitful collaboration, I was able to connect my research to real-world problems and thus create an impact on society. It was very unfortunate that Prof. Mitchell passed away before witnessing the completion of his own vision. Like all who know the creative visionary, I greatly miss him.

I also thank my colleagues and collaborators for their support. Wesley Graybill worked hard to deploy p-Sulu OL on a Connected Sustainable Home. All the collaborators at MEL and the Fondazione Bruno Kessler, particularly Dr. Sotirios Kotsopoulos, Dr. Orkan Telhan, Bob Hsiung, Wei Dong, Carl Yu, Laurène Barlet, Leonardo Benuzzi, and Dr. Carla Farina, gave me helpful feedback from an architectural perspective. It was a joyful and inspiring experience to work with people from different disciplines. I also thank all colleagues at the Model-based and Embedded Robotics Group.

I am grateful for my parents not only that they gave birth to me, but for all the love, support, and respect I have gotten from them over the years. I also thank my sister Asumi for being a cheerful companion. Lastly and most importantly, I

thank my wonderful wife Eriko, who was a classmate at TPP and became my lifelong partner during the program. This achievement would have been impossible without your constant encouragement, support, and love.

This research was funded by the National Science Foundation under Grant No. IIS-1017992 and Siemens AG under Addendum ID MIT CKI-2010-Seed_Fund-008. Any opinions, findings, and conclusions or recommendations expressed in this material are those of the author and do not necessarily reflect the views of the sponsoring agencies.

Contents

List of Figures

List of Tables

Chapter 1

Introduction

Climate change is currently one of society's most pressing challenges. Engineering efforts to address this challenge have largely focused on development and refinement of mechanical, electrical, and material technologies that generate and store renewable energy, such as solar arrays, wind turbines, and fuel cells. In recent years, growing attention has been drawn to computational methods, such as control theory, artificial intelligence, and operations research, that are essential for the energy-efficient and reliable operation of these systems. Two areas where computational methods play particularly important roles are grid and building operation. In both, a central challenge is how to enhance energy efficiency in the presence of uncertainty. For example, uncertain electricity supply by wind and solar may increases risk of blackouts; building controllers may fail to provide a comfortable environment due to uncertain weather conditions. The ultimate goal of our work is to develop a risk-sensitive computational method that overcome this challenge and contribute to realize a smart, sustainable society.

1.1 Visions

We envision a smart electrical grid whose operation is tightly integrated with renewable generation and smart homes in order to achieve energy efficiency, reliability, and reduced reliance on fossil fuels. In this section we present the vision of a smart grid,

as well as of a smart home project, called the Connected Sustainable Home [64, 65].

1.1.1 Smart Grid

According to the U.S. Department of Energy, a smart grid is defined as an "electricity delivery system, from point of generation to point of consumption, integrated with communications and information technology for enhanced grid operations, customer services, and environmental benefits[1]." The objective for a smart grid is three-fold: climate, reliability, and economy.

1. **Climate** - The smart grid's first objective is to reduce greenhouse gas emissions by optimizing grid operation and allowing the large-scale introduction of renewable energy production. According to an estimate by the Electric Power Research Institute (EPRI), the emissions reduction impact of a smart grid in the U.S. will be 60 to 211 million metric tons of CO_2 per year in 2030 [26]. This is equivalent to 1.0 to 3.9% of the total greenhouse gas emissions by the U.S. in 2008. Transition to renewable energy sources is also an urgent issue in Japan, which was hit by a devastating earthquake and a subsequent nuclear accident in 2011. Before the earthquake, the Japanese government had planned to reduce greenhouse gas emissions by increasing dependence on nuclear energy to 53% by 2030. After the earthquake, nuclear is no longer a viable option. In light of this situation, a large-scale introduction of renewable energy sources seems to be the only acceptable solution to address both environmental and security issues.

2. **Reliability** - The smart grid's second objective is to improve the security and reliability of the power grid. Blackout prevention is a particularly important challenge in the U.S., since the blackout probability there is comparatively high among industrialized countries. For example, in 2006, the average household in

[1]The Electric GridSmart and Getting Smarter. Prepared by Ken Huber at PJM Interconnection for DOE ARPA-E Grid Workshop on December 13, 2010.

the U.S. experienced 97 minutes of blackout.[2] An increasingly aging infrastructure is the main cause of reduced reliability in the U.S. The economic cost of power interruptions to U.S. electricity consumers is estimated to have been $79 billion in 2002 [53]. Therefore, enhancing the reliability of the electrical grid brings significant benefits to society.

3. **Economy** - The smart grid's third objective is to boost the economy. A smart grid can impact the economy in two ways. First, it enhances the efficiency of energy production by reducing the peak load. Reduction of peak load enables to depend more on cost-efficient baseload plants, instead of peaking plants. As a result, it is estimated that the average household could reduce its annual electric bill by 10% [30]. Second, a smart grid creates a new market for smart meters, sensors, and other IT hardware and software. The estimated size of the market in the U.S. is $17 billion in 2014 [78]. The economic impact of a smart grid has been particularly emphasized since the financial crisis of 2007-2008. For example, in the U.S., the American Recovery and Reinvestment Act of 2009 (also known as the "stimulus bill") provides $4.3 billion in funding for smart grid-related technologies, such as smart meters, IT-based energy management systems, and advanced energy storage systems, in the hope of contributing to both the economy and the environment.

1.1.2 The Connected Sustainable Home

The Connected Sustainable Home is a concept developed by William J. Mitchell and Federico Casalegno, within the School of Architecture at MIT[3] [64, 65]. The vision of the Connected Sustainable Home (Figure 1-1) is three-fold, to provide sustainable, comfortable, and convenient living. Each of the three items are discussed in detailed

[2]For comparison, the average blackout duration in Japan was 19 minutes in the same year. The statistics are report by Japanese Ministry of Economy, Trade, and Industry. 2010. Available online at `http://www.meti.go.jp/report/downloadfiles/g100426a02j.pdf` (Japanese). Retrieved on November 22, 2011.

[3]Connected Sustainable Home Project webpage: `http://mobile.mit.edu/fbk/` (Retrieved on January 15, 2012.)

below. A Connected Sustainable Home is connected to other Sustainable Connected Homes through a symmetric micro-grid, in order to form a sustainable community.

Figure 1-1: Artist's concept of the Connected Sustainable Home [64]. A full-scale prototype will be built in Rovereto, Italy in 2012. Image courtesy of the MIT Mobile Experience Laboratory.

Figure 1-2: Interior view of the dynamic window of the Connected Sustainable Home [64]. The variable configuration of the windows makes it possible to dynamically reconfigure clear, opaque, open, and closed elements to achieve the current optimum or the desired performance. Image courtesy of the MIT Mobile Experience Laboratory.

1. **Sustainability**

   Improving the energy efficiency of residential buildings plays a significant role in addressing the global climate challenge. In the U.S., for example, 27.3% of the total greenhouse gas emission is attributed to buildings in 2003[4], where res-

[4]U.S. GHG Emissions Flow Chart. Created by World Resources Institute based on the emissions data comes from the Inventory of U.S. Greenhouse Gas Emissions and Sinks: 1990-2003, U.S. EPA. Available on-line at `http://pdf.wri.org/us_greenhouse_gas_emissions_flowchart.pdf`. Retrieved on January 15, 2012.

idential and commercial buildings account for 15.3% and 12.0%, respectively. Heating and cooling accounted for the largest portion of residential energy consumption, that is, 7.99 quadrillion Btu or 38.2% [87]. Of the energy consumption by the residential sector, only 0.41 quadrillion Btu, that is, 1.9%, was supplied from renewable energy sources [87].

While current buildings consume non-renewable energy, they do not fully utilize locally available renewable energy, that is, sunlight. As shown in Figure 1-3, the average insolation (solar radiation energy received on a given surface area) in the U.S. is typically above 5 kWh/m^2/day. Hence, an average household in the U.S., with 1646 square feet or 152.9 m^2 area [87], receives about 750 kWh/day. This significantly exceeds the energy consumption by the average household, 153.7 kWh/day [87]. Hence, most of the energy consumed by average household can be covered by fully utilizing sunlight.

Energy conversion efficiency of commonly used silicon solar cells is typically 14-19%[5], while solar thermal systems can capture up to 30% of the solar energy[6]. When heating a room, it can be more efficient to use sunlight directly, rather than converting solar energy to electricity and run an HVAC system. This can be achieved by having a large south-facing window. Furthermore, if the incoming solar heat input is controllable, room temperature can be controlled without using HVAC systems.

The Connected Sustainable Home is designed to achieve significant reductions in non-renewable energy consumption by controlling incoming sunlight through a south-facing glass facade, called a *dynamic window*, as shown in Figure 1-2 [64]. By incorporating electrochromic and PDLC film with the glass, the opacity and tint of the dynamic window can be controlled. This feature allows the Connected Sustainable Home to minimize the use of an HVAC system, particularly in winter, by controlling the indoor temperature using solar heat

[5]National Renewable Energy Laboratory (NREL)

[6]"Sandia, Stirling Energy Systems set new world record for solar-to-grid conversion efficiency" (Press release). Sandia National Laboratories. 2008-02-12

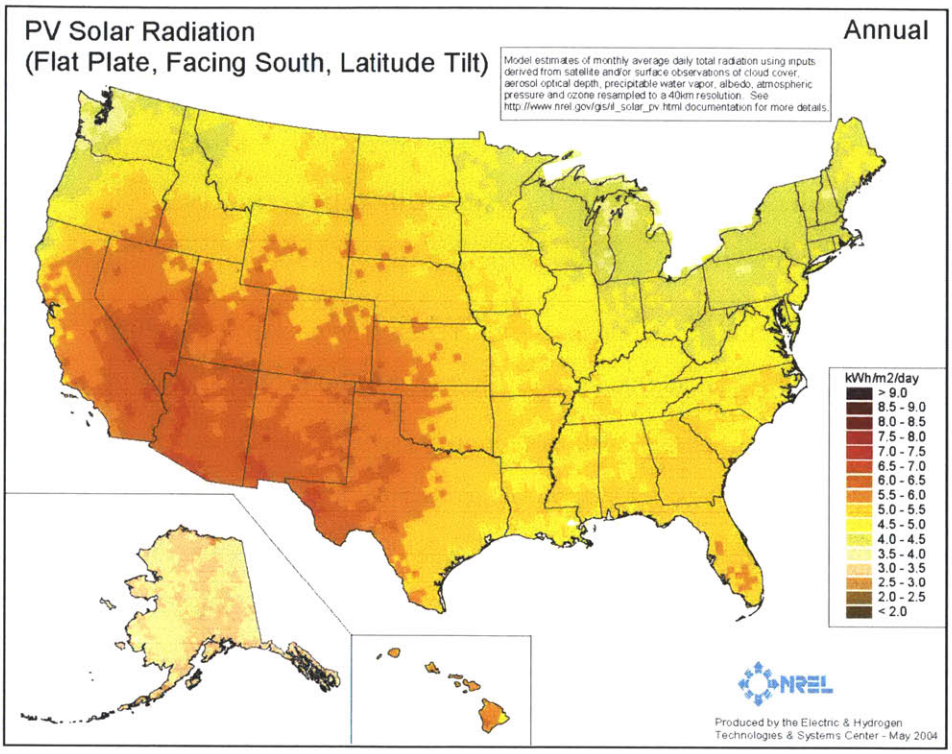

Figure 1-3: US annual average solar energy received by a latitude tilt photovoltaic cell. Image produced by the Electric and Hydrogen Technologies and Systems Center in May, 2004.

input in place of a heater. The Connected Sustainable Home achieves further enhancement in energy efficiency by exploiting its large thermal capacity. For example, it can store heat energy from sunlight in the day and use it to maintain the indoor temperature at night. In Summer, air conditioners can cool the building at night when electricity is cheap and minimize power consumption in the day as the house will warm slowly. Such economical features contribute to reduce peak demand for electricity, and support efficient operation of a power grid. Another feature of the Connected Sustainable Home is a solar array on its roof, which enables further reduction in non-renewable energy consumption.

2. **Comfort** The Connected Sustainable Home improves living comfort, instead of sacrificing it for energy efficiency. It allows residents to specify comfortable indoor conditions, such as room temperature and illumination, and it auto-

matically maintains the indoor environment within the desired range whenever the building is occupied. However, uncertainty in weather and occupancy patterns poses a risk of failure to keep the environment within the specified range. Moreover, optimal temperature control that minimizes energy usage can be susceptible to risk. For example, when the residents are absent in the winter the energy consumption can be minimized by turning off the heating, but it involves a risk that pipes freeze. The Connected Sustainable Home limits these risk by explicitly considering safety constraints and uncertain factors.

3. **Convenience** Advanced capabilities of the Connected Sustainable Home must be conveniently accessible to the residents. To this end, it will provide an intuitive interface for the residents to specify their requirements on indoor environment, as well as on energy efficiency.

1.2 Challenges

To realize both energy efficiency and robustness within a smart grid comprised of sustainable homes, a number of challenges must be overcome.

1.2.1 Challenges in a Smart Grid

Renewable energy sources cannot be directly substituted for conventional energy sources due to their uncontrollable and intermittent nature. In an electrical grid, power generation must be matched to varying power consumption at all times. Although demand is uncertain, conventional power plants can supply controllable and stable energy. Hence, in the current electrical grid, the demand-supply balance is achieved by adjusting the output of load-following power plants, such as gas turbine and hydroelectric power plants.

Unlike conventional power plants, the output of wind and solar power plants are not controllable (these are referred to as *non-dispatchable* plants). Moreover, they are intermittent, meaning that the energy produced at a future point in time cannot

be predicted with certainty. Figure 1-4 shows typical daily solar and wind generation profiles, which are highly intermittent [95]. In the current electrical grid, conventional load-following and peaking power plants absorb intermittent energy generation from wind and solar power plants in the same way as they absorb the uncertainty of energy demand. Such a strategy works because renewable energy production currently accounts for only a very small portion of the total energy generation, typically a few percent in most power grids. Denmark, where wind power provided 18.9 % of energy production in 2008, purchases power from its neighboring countries when necessary. There is no consensus about how much percentage of intermittent energy sources can be accepted to the current grid systems.

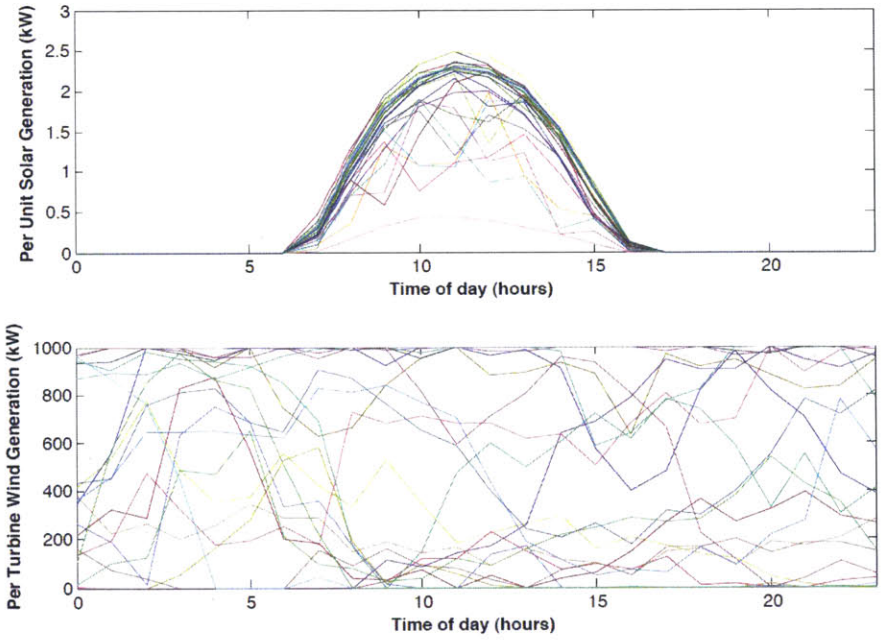

Figure 1-4: Daily solar generation profiles in Long Beach, CA (top) and wind generation profiles on an island near Santa Barbara, CA (bottom). Figure reprinted from [95].

Many governments have set ambitious goals for the penetration of renewable energies. For example, the European Union's Directive on Electricity Production from Renewable Energy Sources, which took effect in 2001 and was amended in 2009, re-

quires its members to increase the share of renewable domestic energy production to 20% by 2020[7]. In the U.S., 24 states and the District of Columbia have set a Renewable Portfolio Standard (RPS), a regulation that requires the increased production of energy from renewable energy sources up to a specified goal.[8] Among them, 22 states have set the goal of a more than 15% renewable penetration by 2025.

Such a high penetration level of intermittent renewable energy raises the two challenges, discussed below.

Risk of brownouts and blackouts Increased uncertainty in the power supply immediately affects the quality of power. Demand-supply imbalance in an electrical grid due to uncertainty results in changes to AC frequency; the frequency drops when load exceeds generation. Similarly, imbalance in reactive power, which represents stored energy due to inductance and capacitance of a grid, results in voltage fluctuation. Degraded power quality is particularly unfavorable for industry customers who operate sensitive electrical equipment. The quality of electricity has become increasingly important as society becomes ever more reliant on digital circuitry [28]. According to the report by [28], three sectors of the U.S. economy that are particularly sensitive to power disturbances are the digital economy, continuous process manufacturing, and fabrication and essential services. These three sectors account for approximately 40 percent of the GDP of the U.S. The report estimates that these industries lose $6.7 billion each year to power quality phenomena. A significant drop in voltage, often called a brownout, can also affect home appliances.

Uncertainty in energy supply also poses a risk of blackout. Large fluctuations in AC frequency forces power generators to shut down. Each component of an electrical grid, such as a substation or transmission line, typically has a safety mechanism that automatically shuts itself down when its capacity is exceeded. In most cases, such shutdowns result in local blackouts. In the worst case, a single failure cascades through the grid, causing a large-scale blackout. For example, the Northeast blackout of 2003,

[7]Directive 2009/28/EC on the promotion of the use of energy from renewable sources and amending and subsequently repealing Directives 2001/77/EC and 2003/30/EC

[8]Web page of U.S. Department of Energy. Retrieved from `http://apps1.eere.energy.gov/states/maps/renewable_portfolio_states.cfm` on January 14, 2012.

which affected more than 50 million people in the U.S. and Canada, was initiated by a single fault in a transmission line, which caused a chain of failure over a large area [86].

It is an important challenge for a smart grid to allow large-scale penetration of renewable energy while reducing the risk of brownouts and blackouts.

Cost of operational reserve and energy storage One way to deal with increased uncertainty is to increase operational reserve and energy storage, but this solution comes at significant cost.

Operational reserve refers to generation capacity that is available to the grid within a short interval of time, and is used to meet varying demand. There are two types of operational reserves: spinning reserve and non-spinning reserve. Spinning reserve is the extra generation capacity that is made available by increasing the power output of generators that are already connected to the power system. Non-spinning or supplemental reserve is the extra generating capacity that is not currently connected to the system, but which can be brought online after a short delay. Since the output of wind and solar generation changes quickly, having enough spinning reserve is particularly important. As a result, if wind and solar energy is introduced on a large scale to the grid, a sufficient number of conventional plants must be kept operational. The need for spinning reserve limits the penetration of renewables. Currently there is no consensus about how much spinning reserve is necessary or how much renewable penetration can be accepted by the current grid system. Due to this uncertainty, an electrical grid needs to be operated conservatively. Construction, maintenance, and operation cost of facilities for spinning reserve will increase overall energy cost.

Energy imbalance can also be absorbed by energy storage. The vast majority of current grid energy storage is composed of pumped-storage hydroelectricity. A pumped-storage hydroelectric plant consists of two reservoirs at different elevations. It stores energy by pumping water up from the lower reservoir to the higher reservoir when the grid has excess energy available. When demand is high, it generates energy by releasing the water from the higher reservoir to the lower. Pumped storage

recovers about 75% of the energy it receives, and is currently the most cost-effective form of mass power storage. The chief problem with pumped storage is geographical constraint, since it requires two nearby reservoirs at considerably different elevations. Hence, suitable sites for pumped storages tend to be in mountain areas, which are often very far from major cities.

Another option is battery storage, which is not constrained by geographical limitations. However, battery storage provides much smaller capacity than pumped-storage hydroelectricity. The largest battery-based storage facility in the world, located in Fairbanks, Alaska, has only 7 MWh capacity, while major pumped hydro reservoirs have giga-watt-hour scale capacity. Moreover, batteries are generally expensive, have high maintenance cost, and have limited lifespans.

In sum, in order to accept a high penetration of renewables, we must face significant uncertainty in intermittent energy supply and grid stability, as well as difficulty in expanding reserves. Absorbing the uncertainty of increased renewables through added storage requires significant cost. Instead, this needs to be addressed by the controller's ability to manage the risk incurred by fluctuations while minimizing greenhouse gas emission.

1.2.2 Challenges in the Connected Sustainable Home

An autonomous controller for a residential building must be able not only to minimize green house gas emission, but also to intelligently adapt to the changing needs of the residents. Currently most buildings are run inefficiently due to the non-adaptable nature of their control systems, and it is considered that savings of up to 35% are possible by optimizing operation of HVAC systems [31]. The inefficiency is mainly due to uncertainty in occupants' behavior. Typically, rooms are occupied only for a small fraction of time. For example, Figure 1-5 shows occupancy data, collected by a study conducted by Xerox PARC [27]. The study showed that the rooms were occupied only for about 20% of the time, and the occupancy patterns significantly varied from room to room. It is a significant loss of energy to heat or cool empty rooms during regular business hours. Although a centralized HVAC system has higher energy efficiency

than decentralized ones, it is hard to adapt to uncertain occupation pattern. On the other hand, decentralized HVAC systems, such as conventional window unit ACs, can manually achieve room-by-room control by simply enforcing occupants to turn it off when they leave a room. However, in reality, it is hard to enforce occupants to take such an energy efficient behaviors. Moreover, occupants may want to have a comfortable temperature when they enter a room, instead of start heating or cooling when they enter. Furthermore, Vastamäki et al. [90] found that occupants' poor understanding of temperature controllers, as well as their wrong mental models about good indoor temperatures, can degrade energy efficiency. For example, [90] finds that many people think a good temperature set point is always between 19-21 degrees Celsius, which is usually uncomfortably cool during the summer time.

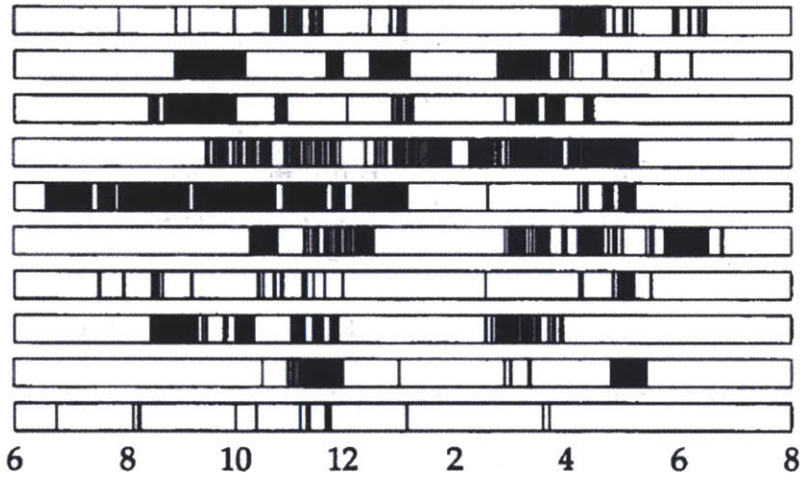

Figure 1-5: Occupancy data for ten different offices over the course of a single day. Each bar is shaded when the corresponding office is occupied and blank when the office is vacant. Image is taken from [27].

Another source of uncertainty is weather conditions. The dynamics of buildings are in general highly affected by environmental disturbances, particularly by the outside temperature. Using weather forecasts, a building can enhance energy efficiency by being "prepared."[9] For example, an energy efficient strategy would be to let the solar radiation heat up the structure of the building if it is going to be cold during

[9]The Building Control Group, ETH. `http://control.ee.ethz.ch/~building/research.php`

the next few days. However, a major challenge with using weather forecasts lies in their inherent uncertainty due to the stochastic nature of atmospheric processes, and the imperfect knowledge of the weather models initial conditions, as well as modeling errors [68].

Given the uncertainty and restrictions described above, the Connected Sustainable Home must achieve the challenging task of maximizing energy efficiency and providing comfortable environment in the presence of significant uncertainty in human behaviors and weather conditions. Our proposed system is distinct from existing building management systems in that it can reason over stochastic plant model in order to deal with the uncertainty.

Chapter 2

Risk Allocation Approach

In the previous chapter we present the visions of a smart grid and the Connected Sustainable Home, as well as their challenges. Recall that the main technical challenge is how to limit risk of energy imbalance and violation of residents' requirements in the presence of uncertainty. In this chapter we overview our approach to overcome this challenge.

2.1 Approach: Risk Allocation Approach for Chance-constrained Programming

Our overall approach to overcoming the challenges stated in Chapter 1 is to frame problems as *chance-constrained programming* framework, and solve them by a novel *risk allocation approach* [71].

Originally developed by [18], chance constraint programming specifies a constrained optimization problem that minimizes a given cost function defined for a stochastic system, while limiting the probability of violating constraints to a user-specified bound. In the case of a smart grid, we frame the problem as minimizing the operational cost of an electrical grid, for example, while limiting the annual probability of blackout to a certain risk bound, such as 0.001% per year[1]. In the case of a

[1]As mentioned in Section 1.1.1, average household in the U.S. experiences 97 minutes of blackout annually. This is about 0.02% of the time.

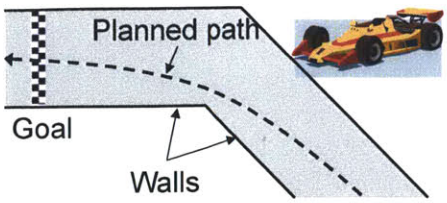

Figure 2-1: Risk allocation in a race car path planning.

sustainable home, we minimize non-renewable energy use, for example, while limiting the risk of bringing the room temperature outside of the specified range to 1% per day. By choosing an acceptable level of risk, users can balance cost efficiency and reliability in the presence of uncertainty.

In our previous work we developed the *risk allocation approach* [71], which enables efficient solution to chance constrained optimal planning problems. In order to understand the concept of risk allocation intuitively, consider the path planning example shown in Figure 2-1. In this example a race car driver wants to plan a path to get to the goal as fast as possible, while limiting the probability of a crash to 0.01%. An intelligent driver would plan a path as shown in Figure 2-1, which runs mostly in the middle of the straightaway, but gets close to the wall at the corner. This is because taking a risk by approaching the wall at the corner results in a greater time saving than taking the same risk along the straightaway; in other words, the utility of taking risk is greater at the corner than the straightaway. Therefore, the optimal path plan allocates a large portion of risk to the corner, while allocating little to the straightaway. As illustrated by this example, risk allocation needs to be optimized across the constraints in order to minimize cost.

Risk allocation approach reformulates a chance-constrained optimization problem into a resource allocation problem by distributing risk to individual constraints. Consider another path planning example in Figure 2-2. A chance constraint requires the vehicle to limit the probability of crashing into the obstacles to 10%. In other words, the vehicle is allowed to take 10% risk throughout the plan. The risk allocation approach distributes this risk among time steps in the plan, as shown in Figure 2-2-(a). If the probabilities of a crash at each time step are within these allocated risk bounds,

then the original 10% risk bound is guaranteed to be satisfied. The 4% risk that is allocated to the time step $t = 2$ is again distributed among constraints (i.e., obstacles) as in Figure 2-2-(b). Such a decomposition is obtained from Boole's inequality [76]. For example, let A be an event of colliding with the left obstacle at $t = 2$, and B be an event of colliding with the right obstacle at $t = 2$. Then, by Boole's inequality

$$\Pr(A) + \Pr(B) \geq \Pr(A \cup B).$$

Therefore, by allocating the risk A and B so that the left-hand side of the equation is equal to 4%, the right hand side is guaranteed to be less than or equal to 4%. That is, the total risk taken at $t = 2$ is less than or equal to 4%.

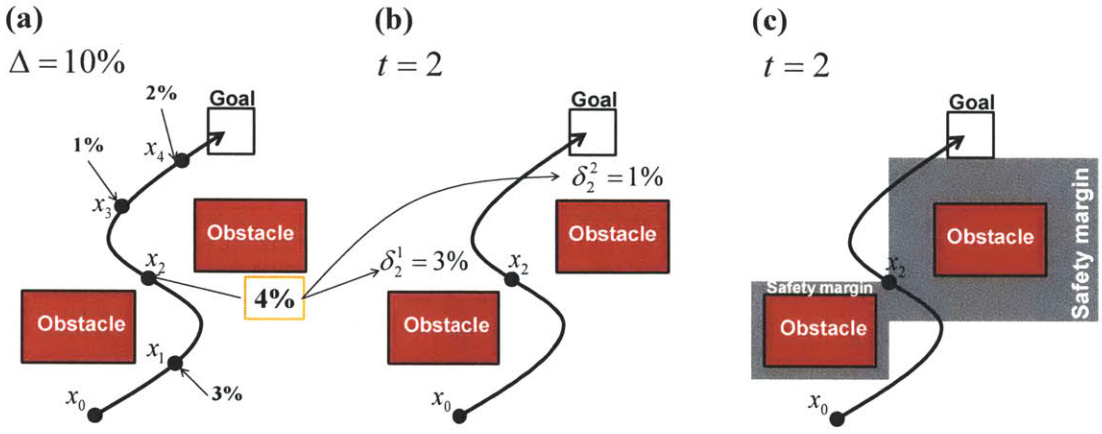

Figure 2-2: Overview of risk allocation approach. (a) The 10% of risk is allocated to time steps in the plan. (b) The 4% of risk allocated to $t = 2$ is distributed again among constraints (i.e., obstacles). (c) Safety margin is set around the constraints according to the risk allocation.

Once risk is allocated to every single constraint, a safety margin that guarantees the risk bound can be found as in Figure 2-2-(c). By planning the nominal path to remain outside of the safety margin for all time steps, the executive can guarantee the satisfaction of the original chance constraint. Note that planning a *nominal* path outside of safety margins is a deterministic optimization problem, which can be solved efficiently using existing approaches. Such a decomposition of a chance constraint makes the stochastic optimization significantly easier, hence allowing the

executive to compute the optimal control sequence efficiently. While our example involves vehicle path plaining, the underlying principle applies to the broad family of chance-constrained optimization problems, and in particular is well suited to the control of the grid and homes.

As a second example, consider the problem of controlling the set point of an office, given that data on occupancy is uncertain, as shown in Figure 2-3. More specifically, we assume that the occupancy pattern is uncertain, but the probability that the office is occupied at a given time in a day is known. Then, by turning off an HVAC within a time interval t involves risk δ_t, which is equivalent to the occupancy probability p_t. By applying the risk allocation approach, we can guarantee that the risk of failure to provide comfortable temperature when the office is occupied is below Δ, by distributing the risk so that $\sum_t \delta_t \leq \Delta$.

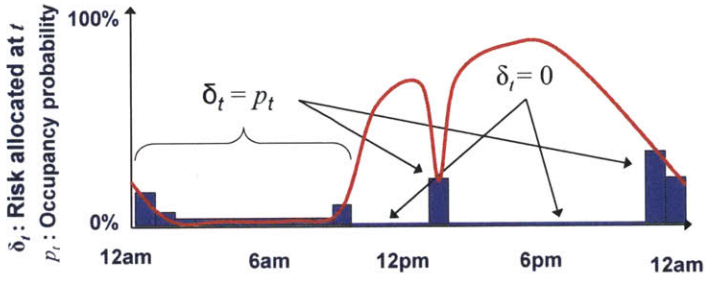

Figure 2-3: Risk allocation for temperature control of an office with uncertain occupancy data.

2.2 Solution: Distributed Robust Grid Control

In order to overcome the challenges in a smart grid and sustainable homes presented in Sections 1.2, we propose a distributed control system composed of three algorithms, as illustrated in Figure 2-4. In this section, we first present the overall architecture of the proposed control system, followed by a description of the three algorithms.

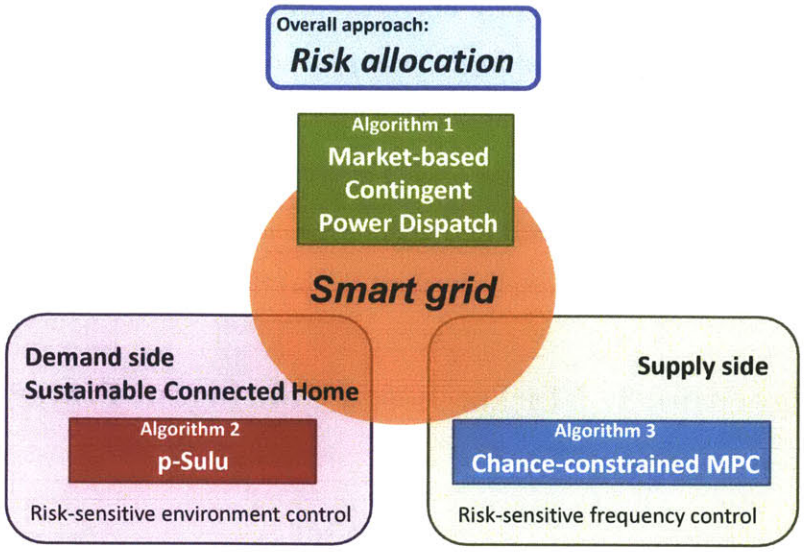

Figure 2-4: Overall architecture of the proposed distributed control method of a smart grid with Sustainable Connected Homes.

2.2.1 Overall Architecture

An electrical grid is a gigantic interconnected network, composed of numerous suppliers and consumers. In regions where electricity is deregulated, such as the U.S. and Europe, grid operation is quite decentralized, meaning that multiple decision makers are coordinated through a market-based mechanism. In a wholesale market, electricity supply companies and utility companies are the decision makers that choose output levels and supply levels, based on the wholesale price of the energy. Consumers are also decision makers since they decide the amount of energy to consume based on the retail price.

In order to fit with such a distributed nature of electrical grids, we also employ a distributed architecture in our proposed system. As shown in Figure 2-4, our first algorithm, *Market-based Contingent Power Dispatch*, optimally dispatches energy over a grid in a distributed manner. Thus, this algorithm plays a role in the system to coordinate distributed components, such as generators and buildings. Each of the distributed components, both loads and generators, are controlled by our second and third algorithms. The second algorithm, a risk-sensitive plan executive called

probabilistic Sulu[2] *(p-Sulu)*, robustly operates Sustainable Connected Homes. The third algorithm is a *chance-constrained model predictive control* that can operate each generator. Although our intended application of the algorithm is frequency control of generators, it can also be applied to a wide spectrum of robust constrained optimal control problems, both on the load and generation sides We elaborate on these three algorithms in the following three subsections, respectively.

2.2.2 Algorithm 1: Market-based Contingent Power Dispatch for a Smart Grid

Required Capabilities

In order to overcome the challenges described in previous sections, we specify three attributes that our power dispatch algorithm must have: 1) market-based distributed control, 2) optimal control with minimum cost and energy efficiency, and 3) robust control within a bounded risk.

Market-based distributed control As discussed in the previous subsection, grid operation must be distributed. Moreover, the building components of a grid must be coordinated by a market-based mechanism in order to fit with the current structure of an electrical grid. In a typical wholesale electricity market, the price is determined by matching offers from generators to bids from consumers in a day-ahead market, usually on an hourly interval. Likewise, our power dispatch algorithm must also determine the price through a market mechanism, while each generators and consumers choose its optimal supply or demand level depending on the price.

Optimal control with minimum cost and energy efficiency Recall that the three objectives of a smart grid are to 1) address the climate challenge, 2) improve reliability, and 3) contribute to the economy, as we discussed in Section 1.1.1. The first

[2]Sulu is a deterministic plan executive developed by [55]. The name of the executive was taken from Hikaru Sulu, a character in the science fiction drama *Star Trek*. In the story, Sulu serves as a helmsman of the starship USS Enterprise. The plan executive was named after him because its role is to "steer a ship" in order to achieve a given plan.

and the third objectives require minimization of energy and cost efficiency through optimal operation of a grid. Furthermore, the controller must achieve optimality in a distributed manner, instead of a straight forward centralized optimization.

Robust control with a bounded risk In order to achieve the second objective of a smart grid, we need to make a grid tolerant to uncertainties. Risk of energy shortage can be eliminated by operating an amount of spinning reserve sufficient to provide a "100% backup" for intermittent generators in order to prepare for the worst case. More concretely, the worst case scenario is that all wind turbines and solar cells have no output at all when the energy demand is at the highest possible level. One can guarantee zero probability of failure to meet energy demand by preparing spinning reserve and stored energy that is equivalent to the highest possible level of energy demand. Of course, such a conservative operation is very inefficient. First of all, as we mentioned in Section 1.2, energy storage is very costly. Second of all, since conventional plants, such as gas turbines, have minimum output level, maintaining spinning reserve requires consumption of fuels. These inefficiencies undermine the benefit of renewable energies.

In fact, real-world electrical grids typically do not operate the same amount of spinning reserve as the amount of intermittent generation[3]. However, although such operation without a "100% backup" is cost and energy efficient, it involves risk of energy imbalance. Therefore, the grid must be operated robustly to limit such a risk below an acceptable level.

Algorithm Overview

Our Market-based Contingent Power Dispatch optimally allocates generation to power plants within a bounded risk of power imbalance. The objective of the algorithm is to achieve the most cost-effective power dispatch in a futures market, while limiting the risk of power imbalance between supply and demand in the presence of uncertainty.

[3]American Wind Energy Association. 20% Wind Energy by 2030: Wind, Backup Power, and Emissions. Available on-line at `http://www.awea.org/learnabout/publications/upload/Backup_Power.pdf` Retrieved on January 16, 2012.

A key idea in this approach is to allocate uncertain power generation separately from nominal power generation. When electricity is traded in a futures market (e.g., a day-ahead market), there is uncertainty in future electricity demand, as well as supply from non-dispatchable generators, such as solar cells and wind turbines, which is treated as negative demand. We refer to the deviation of net electricity demand from the nominal as *contingent power*. In our algorithm, each dispatchable generator sells not only future electricity supply for nominal demand, but also a percentage of contingent power that it will provide. For example, assume that a generator has sold 100 MWh nominal power and 1% contingent power in a day-ahead market. If the net demand at the time of dispatch turns out to be 1 GWh more than the nominal, then the generator is responsible to provide 110 MWh - 100 nominal and 10% of 1 GWh.

This approach allows each generator to analytically evaluate the risk of exceeding generation capacity because the probability distribution of the demand on the generator can be obtained from the probability distribution of the net electricity demand, which is assumed to be available. Hence, each generator can decide the optimal amount of nominal and contingent energy to sell in a futures market through chance-constrained programming. Moreover, by employing a price adjustment mechanism called tâtonnement, our iterative algorithm is guaranteed to converge to the globally optimal allocation of nominal and contingent energy generation in a distributed manner. The algorithm can achieve energy efficiency by including greenhouse gas emission in the cost function.

Inputs

Predictions of intermittent energy supply and demand The algorithm takes the predicted net electricity demand as an input, where net demand is defined as demand minus intermittent supply. Moreover, in order to evaluate risk quantitatively, it requires the probability density function of the net demand.

Cost function Each generator must know its own cost function. Note that the cost function can include not only financial cost, but also environmental cost.

Risk bounds Each generator takes its own risk level as an input. By applying the risk allocation approach, the risk of the entire grid can be bounded by the summation of the individual risks taken by the generators.

Outputs

Nominal power allocation Our algorithm allocates nominal generation to each power plant, like the current electricity market.

Contingent power allocation Our algorithm also allocates contingent power to each power plant. Each plant decides the optimal level of nominal and contingent power by optimizing over a given cost function while respecting the given risk bound.

Next we turn to controlling the grid components, starting with sustainable homes.

2.2.3 Algorithm 2: p-Sulu for the Connected Sustainable Home

Required Capabilities

By breaking down the challenges of developing a Connected Sustainable Home described in Section 1.2.2, we specify three required technical capabilities: 1) Goal-directed planning with continuous effects and temporally extended goals (TEGs), 2) optimal planning, and 3) robust planning with risk bounds. We explain each item in detail below.

Goal-directed planning with continuous effects and temporally extended goals (TEGs) The Connected Sustainable Home must allow residents to specify desired ranges of room temperature (i.e., state constraints in a continuous domain). Moreover, it must be able to handle a *flexible* temporal constraints, instead of a fixed set-point schedule that existing temperature controllers take, in order to allow flexibility in schedule. For example, the temperature that a resident feel comfortable when she is asleep may be different than when she is awake. Although she knows she

needs at least 7 hours of sleep, the time to go to bed and wake up can be flexible. These requirements are represented as a sequence of TEGs, which must be executed in a goal-directed manner.

Optimal Planning While guaranteeing that the TEGs are achieved, the Connected Sustainable Home must also minimize the use of non-renewable energy consumption. In other words, it must solve a constrained optimal control problem.

Robust planning with risk bounds Optimal plan execution is susceptible to risk when uncertainty is introduced. For example, the Connected Sustainable Home involves a risk of failure to maintain the room temperature within a specified range due to unexpected climate changes. When the residents are absent in the winter the energy consumption can be minimized by turning off the heating, but it involves a risk that pipes freeze. Such risks must be limited to acceptable levels specified by the residents. The plan executive guarantees that the system is able to operate within these bounds. Such constraints are called *chance constraints.*

Algorithm Overview

As mentioned above, p-Sulu provides a robust plan execution capability with a bounded risk. The input to p-Sulu is a schedule and requirements of the residents, as well as risk bounds. For example, a resident specifies when to wake up in the following morning, what range of temperature she finds comfortable, and her acceptable level of risk of failure to satisfy the requirements. The schedule, requirements, and risk bounds are represented by a temporal plan representation, called a *chance-constrained qualitative state plan (CCQSP)*, which encodes both TEGs and chance constraints. Given a CCQSP, p-Sulu optimally controls the dynamic window and HVAC of the Connected Sustainable Home so that energy consumption is minimized while the risk of failure to satisfy resident's requirements is within the specified risk bounds. In this subsection we give informal definition of the inputs and outputs. They are rigorously defined in Sections 4.3.2 and 4.3.3.

Inputs

Initial Condition p-Sulu plans a control sequence starting from the current state, which is typically obtained from sensor measurements.

Stochastic Plant Model p-Sulu takes as an input a discrete-time, continuous-state stochastic plant model, which specifies probabilistic state transitions in a continuous domain. Although we limit our focus to Gaussian-distributed uncertainty, the algorithms presented in this thesis can be extended to a broader classes of distributions.

Chance-constrained qualitative state plan (CCQSP) A CCQSP is a formalism to express TEGs and chance constraints [13]. It is an extension of qualitative state plan (QSP), developed and used by [14, 40, 56]. CCQSP specifies a desired evolution of the plant state over time, and is defined by a set of discrete *events*, a set of *episodes*, which impose constraints on the plant state evolution, a set of *temporal constraints* between events, and a set of *chance constraints* that specify reliability constraints on the success of sets of episodes in the plan.

A CCQSP may be depicted as an acyclic directed graph, as shown in Figure 2-5. The circles represent events and squares represent episodes. Flexible temporal constraints are represented as a simple temporal network (STN) [25], which specifies upper and lower bounds on the duration of episodes (shown as the pairs of numbers in parentheses). The figure describes a typical plan for the Connected Sustainable Home, which can be stated informally as:

> "Maintain a comfortable sleeping temperature until I wake up. After I wake up, maintain room temperature until I go to work. No temperature constraints while I am at work, but when I get home, maintain room temperature until I go to sleep. Maintain a comfortable sleeping temperature while I sleep. The probability of failure of these episodes must be less than 1%. Always make sure the house does not get so cold that the pipes freeze. Limit the probability of such a failure to 0.01%."

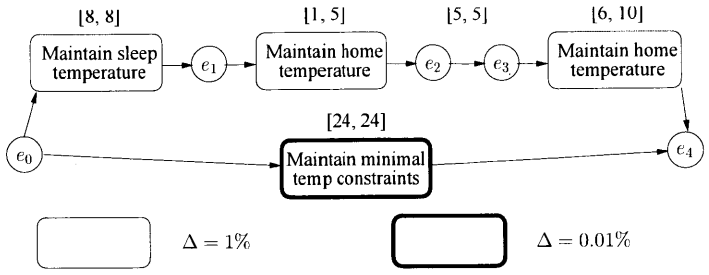

Figure 2-5: An example of a CCQSP for a resident's schedule in a planning problem for the Connected Sustainable Home

Outputs

Optimal executable control sequence One of the two outputs of p-Sulu is an executable control sequence that minimizes a given cost function and satisfies all constraints specified by the input CCQSP. In the case of the Connected Sustainable Home, the outputs are the opaqueness of the dynamic window, as well as the heat output of HVAC.

Optimal schedule The other output of p-Sulu is the optimal schedule, which consists of a set of execution time steps for events in the input CCQSP. In the case of the Connected Sustainable Home, a schedule specifies when to change the opaqueness of the windows and when to turn on the HVAC system.

The two outputs – the optimal control sequence and the optimal schedule – must be consistent with each other: the TEGs are achieved on the optimal schedule by applying the optimal control sequence to the given initial conditions.

2.2.4 Algorithm 3: Chance-constrained Model Predictive Control with Probabilistic Resolvability

As we discussed in Section 1.2, stabilizing AC frequency of a grid has a critical importance. Currently each individual power plant has its own AC frequency controller, which is based on classical PID control [4]. Recently, applications of model-predictive control (MPC) to primary frequency control have been proposed [6, 85].

MPC, also known as receding horizon control, is a closed-loop control approach that solves a finite-horizon optimal control problem at each time step starting from the current initial state. Only the first step in the resulting optimal control sequence is executed, and then a finite-horizon optimal control problem is solved again for the latest state [32]. Initially developed for process industries, MPC is distinguished from classical control approaches by its capability to explicitly consider state constraints while optimizing a control sequence to minimize a given cost function. MPC is suitable for power grid control because a power grid has a number of constraints, such as the capacities of generation plants, substations and transmission lines, as well as the acceptable range of frequency and voltage deviations. When applied to primary frequency control, MPC enables more energy efficient operation while guaranteeing the satisfaction of operational constraints, compared to classical controllers. MPC is also effectively applied to building control [69]. However, conventional MPCs do not typically consider stochastic uncertainty. The objective of our third algorithm is to extend the MPC approaches to allow stochastic uncertainties in an electrical grid. Such an extension to MPC is called a chance-constrained MPC (CCMPC) [79]. Our CCMPC algorithm is distinct from existing ones in that it guarantees probabilistic resolvability, as we explain shortly.

Required Features

CCMPC must have the following two features in order to be applied to grid components, such as frequency control and building control: 1) probabilistic resolvability and 2) tractability.

Probabilistic Resolvability A failure to find a feasible solution during the operation of a power plant or an electrical grid may result in a catastrophic failure. Existing robust model predictive control (RMPC) algorithms that assumes *bounded* uncertainty guarantees resolvability (also known as recursive feasibility), meaning that existence of feasible solution in the future is guaranteed given a feasible solution at the current time [50, 19, 80, 51, 1, 2, 21]. However, when the probability distribu-

tion of uncertainty is not bounded or has long tails, it is impossible or, at the best, extremely inefficient to guarantee resolvability. Alternatively, we propose a new concept of *probabilistic resolvability*, which provides a lower bound on the probability of solution existence. Probabilistic resolvability is a particularly important feature when controlling a social infrastructure that must operate continuously such as an electrical grid, because a failure to find a feasible solution poses a serious risk to a society, such as cascading blackouts. In order to limit such a risk, the proposed CCMPC algorithm must guarantee probabilistic resolvability with a specified risk bound.

Tractability MPC requires solving a constrained optimization problem at every control cycle, where control frequency is typically above 1 Hz. This means that the constrained optimization problem must be solved within one second. Hence, tractability is an important feature. More specifically, we require the constrained optimization problem to be a convex program.

Algorithm Overview

Our CCMPC algorithm is built upon the risk allocation approach. It distributes risk over time steps within a control horizon. We denote by $\delta_{\tau|k}$ the risk allocated to the τth time step in the kth control horizon. The CCQSP solves a constrained optimization problem at each time step, where the final state is required to be within an ϵ-robust control invariant set. An ϵ-robust control invariant set is a probabilistic counterpart of the robust control invariant set used by RMPC to guarantee resolvability. It is a set such that, if the state is within the set, then there exists a control law that keeps the state in the same set at the next time step with at least the probability of $1 - \epsilon$. Hence, in the next time step, a feasible solution can be constructed by applying the control law, with an additional risk ϵ. The CCMPC algorithm also require that $\delta_{\tau|k} \geq \epsilon$ at all time steps τ within the control horizon. With these requirements, feasibility of the next time step is guaranteed with a probability of $\delta_{k|k}$ because the newly added risk ϵ is always less than the risk that is taken at the current step, $\delta_{k|k}$, and hence the chance constraint can be satisfied, as illustrated in Figure

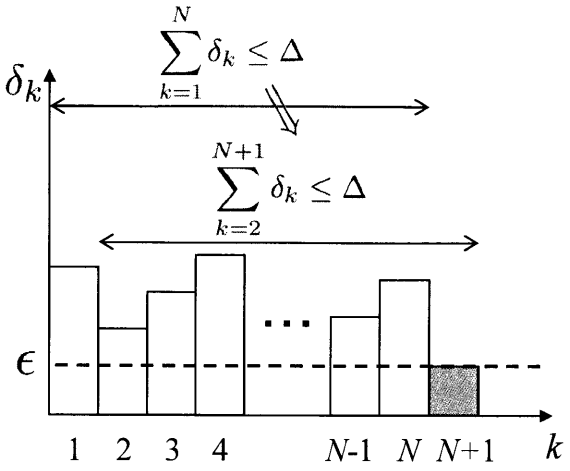

Figure 2-6: The proposed MPC algorithm requires that the terminal state is in an ϵ-robust control invariant set, so that the terminal state can stay within the set in the next time step with the probability of $1 - \epsilon$. Probabilistic resolvability is guaranteed by ensuring that risk allocation to each time step is greater than ϵ.

2-6. Recursive application of this argument proves probabilistic resolvability. The constrained optimization problem solved by the algorithm at each time step is convex under a moderate conditions.

Inputs

Risk bounds The algorithm takes two risk bounds as inputs. One of them is a regular risk bound Δ that sets an upper bound on the probability of constraint violation. In our algorithm, Δ also corresponds to the upper bound on the probability that feasible solutions do not exist over a control horizon. The other risk bound is ϵ, which specifies the upper bound on probability that a state in an ϵ-robust control invariant set cannot stay within the same set in the next time step.

Cost function The algorithm takes a cost function, which typically represents energy cost and financial cost.

Output

The CCMPC algorithm outputs an optimal control sequence that guarantees constraint satisfaction and solution existence over every control horizon with a probability of Δ, while minimizing the given cost function.

The three algorithms introduced in this section work together to control an electrical grid with sustainable homes in a distributed manner. With risk-sensitive control capability, the distributed grid control system can limit risks in the presence of uncertainty. The three algorithms are described in detail in Chapters 3-5.

2.3 Organization of the Thesis

The rest of the thesis is organized as follows. Chapters 3, 4, and 5 describe the three risk-constrained algorithms: Market-based Contingent Energy Dispatch for the electrical grid, p-Sulu for the Connected Sustainable Home, and a chance-constrained model-predictive control with probabilistic resolvability. Chapter 6 presents a policy analysis, and Chapter 7 concludes the thesis.

Chapter 3

Market-based Contingent Power Dispatch

3.1 Overview

In this chapter we propose a new market-based power dispatch algorithm, which optimally allocates generation to power plants with a bounded risk of power imbalance. The two key ideas behind the proposed algorithms are 1) to allocate uncertain power generation separately from nominal power generation, and 2) to optimize the allocations of both nominal and uncertain power generation concurrently in a decentralized manner using a market-based mechanism. This approach enables to bound probability of constraint violations quantitatively, while minimizing cost. In the proposed algorithm, two kinds of power are traded in a market: nominal power and *contingent power*. Contingent power is interpreted as insurance. Each plant sells an insurance contract to provide extra power out of its spinning reserve when demand is higher than forecast; when demand is lower than forecast, the contracted plant provides less power than the committed nominal power generation.

Regarding the first idea, contingent power is different from a regular insurance contract in that it promises to supply the *standard deviation* of the uncertain power that the plant provides, instead of setting the upper bound of the uncertain supply. This mechanism enables the ability to bound the risk of energy imbalance since each

plant can quantitatively evaluate the risk of exceeding capacity from the probability distribution. Contingent power dispatch also allows energy storage, such as pumped-hydro energy storage and batteries, to operate with bounded risk of exceeding capacity of or exhausting the stored energy. The idea of contingent power dispatch is explained in detail in Sections 3.3 and 3.4.

Turning to the second key idea, our algorithm finds optimal allocations of nominal and contingent power in a decentralized manner through an iterative market-based resource allocation mechanism called *tâtonnement* or a *Walrasian auction* [84]. Roughly speaking, *tâtonnement* follows the following process:

1) Increase the price if aggregate demand exceeds supply, or

   decrease the price if supply exceeds aggregate demand.

2) Repeat until supply and demand are balanced.

We use a subgradient method to concurrently optimize two prices: prices of nominal and contingent power. Mathematically, this allocation mechanism corresponds to a distributed optimization method called dual decomposition. Under moderate conditions, dual decomposition-based distributed optimization results in the same optimal solution as centralized optimization. The market-based decentralized algorithm is presented in Section 3.5.

3.2 Related Work

Optimal power dispatch problem, also known as economic dispatch problem, is to find the most cost-efficient allocation of generation in a power system. It has been an active topic of research since 1970s. Major work in this field is summarized in review articles, such as [37, 22]. A closely related area of study is optimal power flow problem, which adds constraints on transmission line capacity to the optimal power dispatch problem. Both real and reactive power flow is considered to determine the optimal voltage angle and magnitude of each bus. Comprehensive surveys on his subject are provided in [41, 75, 77]. Our work is unique in that it handles uncertainty in power

dispatch problem by separating contingent power from nominal power. This approach allows distributed solution of power dispatch problem with chance-constraints, by using dual decomposition. So far our work does not consider power flow. Such an extension is our future work.

Dual decomposition is a method that decomposes a separable constrained optimization problem, and hence enables distributed optimization, by dualizing coupled constraints [17]. It is widely applied from resource allocation [91] to risk allocation [73, 74], and from inference [82] to optimal data routing [94]. When the original optimization problem is convex, which is the case in our problem, a distributed solution through dual decomposition is optimal since there is no duality gap. Using dual decomposition, our contingent power dispatch problem is transformed to a distributed optimization problem, where each generator decides its output level by minimizing its own cost function while a central module optimizes dual variables.

Dual decomposition can be interpreted as a market-based resource allocation mechanism, called tâtonnement or Walrasian auction [84], where the dual variable corresponds to the price of a resource. The price is iteratively adjusted to find the equilibrium price, where supply and demand are balanced. Tâtonnement has been successfully applied to various problems such as the distribution of heating energy in an office building[91], control of electrical power flow[43], and resource allocation in communication networks[44]. In economics, a simple linear price update rule has long been the main subject of study, but the convergence of price can only be guaranteed under a quite restrictive condition[84]. In order to substitute the linear price update rule, various root-finding methods have been employed in agent-based resource allocation algorithms, such as the bisection method[93], Newton method[96], and Broyden's method[91]. The market-based iterative risk allocation algorithm [74, 73] employs Brent's method [7] to provide guaranteed convergence with superlinear rate of convergence. In the proposed Market-based Contingent Power Dispatch, the price is optimized using a subgradient method.

3.3 Walk-Through of Contingent Power Market

We first present a walk-through example to explain our problem framing intuitively. The formal problem statement follows shortly.

We consider a grid with three dispatchable generators, as shown in Figure 3-1. Plant 1 is a base-load plant, which can produce a constant level of power (i.e., nominal power) with the lowest cost, but requires the largest cost to deviate the output (i.e., contingent power production) from the constant level. Plane 2 is a load-following plant, which has moderate cost to produce both nominal and contingent power. Plant 3 is a peaking plant, which has the highest cost of nominal power production, but the output can be easily adjusted with the least cost.

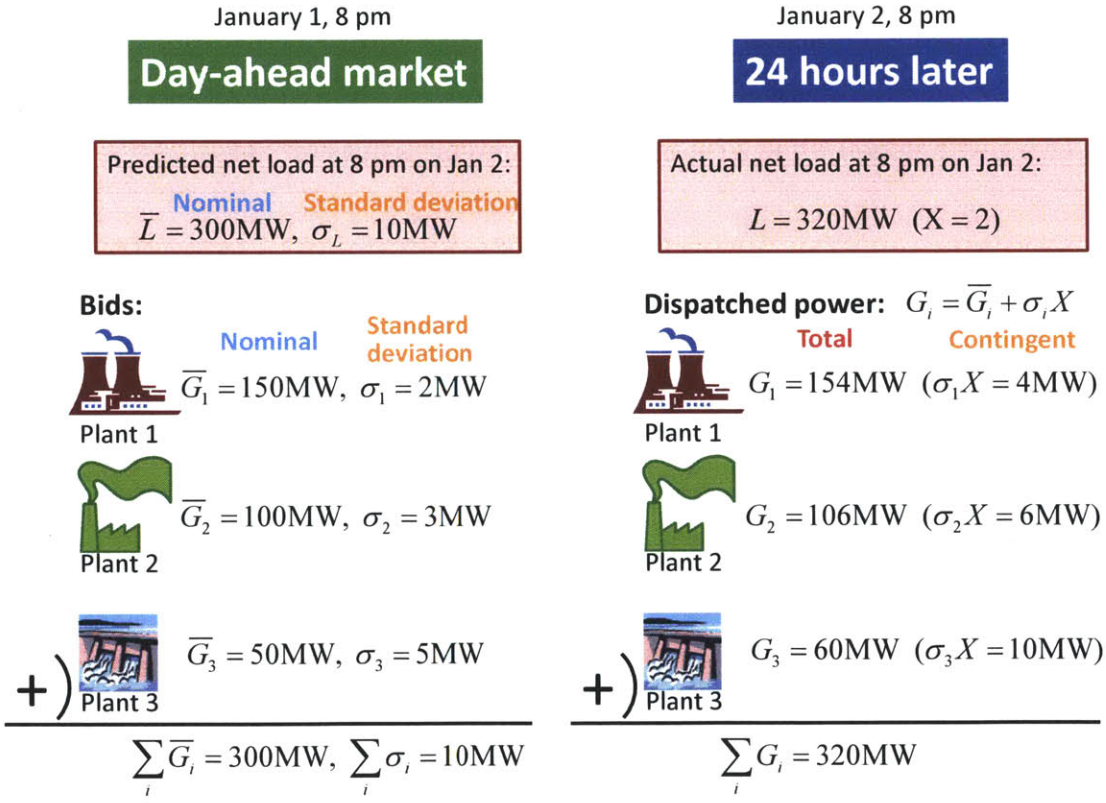

Figure 3-1: Walk-through example of contingent power dispatch for a grid with three dispatchable power plants. See Sections 3.4.1 and 3.4.2 for the notations used in this figure.

The predicted net load at 8:00 p.m., January 2nd, is 300 MWh, with a standard

deviation of 10 MWh. Hence, on the preceding day, January 1st, at 8:00 p.m., 300 MWh nominal power *and* 10 MWh standard deviation are demanded in the day-ahead market.

The three generators sell nominal power *and* coverage for the standard deviation to meet the uncertain demand. On the nominal market, Plant 1 sells 150 MWh nominal power, Plant 2 sells 100 MWh nominal power, and Plant 3 sells 50 MWh nominal power, which sum to 300 MWh. Plant 1 bids the highest amount of nominal power since it has the lowest cost of nominal power production. On the contingent market, Plant 1 sells 2 MWh standard deviation, Plant 2 sells 3 MWh standard deviation, and Plant 3 sells 5 MWh standard deviation. Plant 3 bids the highest amount of contingent power since it has the lower cost of contingent power production.

Then, 24 hours later, the actual net load turns out to be 320 MWh, resulting in 20 MWh excess load. We call the excess load as *contingent load.* The contingent load is allocated to each plant *proportionally* to the standard deviation it sold. Since the resulting excess load is twice as large as the standard deviation, Plants 1, 2, and 3 produce 4 MWh, 6 MWh, and 10 MWh of contingent power, respectively. Hence, the total power produced by each plant is 154 MWh, 106 MWh, and 60 MWh. These sum up to 320 MWh, which matches the actual load.

The problem that this chapter solves is how to find the optimal allocation of nominal power and standard deviation that minimizes the expected cost of energy production, while limiting the risk of exceeding capacity. We present the formal problem formulation in the next section.

3.4 Problem Formulation

We consider a power grid system where load is uncertain and uncontrollable, while generation is dispatchable and not intermittent. Wind and solar generation, which are non-dispatchable and intermittent, are considered as negative load. Recall that the goal of contingent power dispatch is to find the optimal allocation of nominal and contingent power generation to dispatchable power plants. Our approach is unique in

that the dispatchable generators commit to provide a fixed percentage of contingent load, which is defined as the deviation from the nominal load. We will explain this in detail in Section 3.4.2.

3.4.1 Net Load Prediction

In a deregulated wholesale electricity market, where generation is allocated through competitive bidding, electricity is traded in a futures market, typically a day-ahead market. The objective of the market is to balance the demand and supply of electricity, based on the predictions of future load and non-dispatchable generation. However, of course, such predictions cannot be perfect.

We assume that the prediction of future net load L, which is defined as the load minus non-dispatchable generation, is given in the following form:

$$L = \bar{L} + \sigma_L X \tag{3.1}$$

$$X \sim f(X) \tag{3.2}$$

where X is a zero-mean random variable with its standard deviation being one. Its probability density function (pdf) is assumed to be known and denoted by $f(X)$. In other words, we assume that the type of the probability distribution of the future electricity load is known. There are existing studies on the probability distribution of renewable energy generation. For example, it is known that a Weibull distribution gives a good approximation of the distribution of wind speed [88]. Leigh et al. [57] proposed a Gaussian process prior models for electrical load forecasting. The true value of X is known at the moment of dispatch. In the example shown in Figure 3-1, X turns out to be 2.

$\bar{L}$ and σ_L in (3.1) are deterministic parameters that represent the mean and the standard deviation of the predicted load, respectively, as shown in Figure 3-2. Intuitively, σ_L represents the confidence level of the prediction. A prediction with small σ_L means that the actual load L is likely to be close to the mean $\bar{L}$, indicating a high confidence in the prediction.

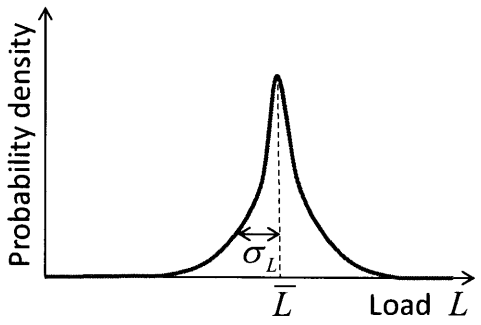

Figure 3-2: We assume that the prediction of future load is given by the mean $\bar{L}$ and the standard deviation, while the type of the distribution is known.

We call the first term in (3.1), $\bar{L}$s, nominal load, while referring to the second term, $\sigma_L X$, as *contingent load.*

3.4.2 Generation

We assume that there are N dispatchable generators in the grid. In the electricity market, the ith generator *commits* to produce the following amount:

$$G_i = \bar{G}_i + \sigma_i X \tag{3.3}$$

where X is the same random variable as (3.1). $\bar{G}_i$ is the nominal power production of the generator.

The second term, $\sigma_i X$, is the *contingent power production.* Since it shares X with (3.1), the ith generator is committed to provide a fixed portion σ_i/σ_L of the contingent load.

3.4.3 Contingent Electricity Market

The objective of the electricity market is to balance the load and generation, both of which are uncertain:

$$L = \sum_{i=1}^{N} G_i. \tag{3.4}$$

This can be achieved by ensuring that the nominal and contingent power productions of all dispatchable generators match the net nominal and contingent load, respectively:

$$\bar{L} = \sum_{i=1}^{N} \bar{G}_i \tag{3.5}$$

$$\sigma_L = \sum_{i=1}^{N} \sigma_i. \tag{3.6}$$

Hence, instead of directly balancing a random quantity as in (3.4), the market seeks to balance two deterministic quantities: nominal power (3.5) and standard deviation (3.6).

Note that the contingent power generation $\sigma_i X$ is *not* independent between plants since it shares a random variable X. The standard deviation of total contingent power generation is simply the summation of the standard deviations of all plants.

3.4.4 Cost and Capacity of Electricity Generation

We are interested in a grid system where generators are heterogeneous, meaning that each plant in the grid has different electricity generation cost and capacity. This is the case in real-world power grids, where various types of plants (e.g., gas, coal, hydro, nuclear, etc.) with different cost structures are connected. Typically, nuclear power plants are used for baseload plants since they can operate at a constant level with relatively low cost, but adjusting the output level is not easy. On the other hand, gas and hydro plants are often used for load-following and peaking plants since their output levels can be quickly adjusted.

Cost We assume that the cost of electricity generation of each plant J_i is a continuously differentiable convex function of nominal power $\bar{G}_i$ and standard deviation σ_i:

$$J_i = J_i(\bar{G}_i, \sigma_i). \tag{3.7}$$

For example, baseload plants are considered to have relatively small cost of nominal power production, while having very large cost of contingent power production. On

the other hand, peaking plants are considered to relatively have high cost of nominal power and low cost of contingent power production.

The cost function can include external costs, such as health and environmental costs. For example, according to a study by the U.S. National Research Council, the external cost of electricity produced from coal was 3.2 cents per kilowatt-hour in 2005, while that of natural gas was 0.16 cents per kilowatt-hour in the same year [83]. However, we note that the estimation of external costs varies widely from study to study.

The cost function only includes the *marginal* cost of electricity, since the problem that we solve is concerned with the allocation of electricity generation, *given* a set of available generation facilities. Fixed costs, such as capital investment and fixed maintenance costs, must be considered as sunk costs.

Capacity We assume that each generator has a generation capacity C_i, which is a positive real constant. Hence,

$$0 \leq \bar{G}_i + \sigma_i X \leq C_i. \tag{3.8}$$

Note that, when X is unbounded, it is not always to guarantee the satisfaction of constraint (3.8) in general. This means that there is a risk of power shortage when unexpectedly large electricity demand exceeds generation capacity. In the next subsection, we present a problem formulation that explicitly requires that such risk is below a user-specified risk bound.

3.4.5 Problem Statement

We frame contingent power dispatch problem a chance-constrained optimization problem, as shown below:

Problem 1: Centralized Contingent Power Dispatch

$$\min_{\bar{G}_{1:N},\sigma_{1:N}} \quad \sum_{i=1}^{N} J_i(\bar{G}_i, \sigma_i) \tag{3.9}$$

$$s.t. \quad \bar{L} = \sum_{i=1}^{N} \bar{G}_i \tag{3.10}$$

$$\sigma_L = \sum_{i=1}^{N} \sigma_i \tag{3.11}$$

$$\Pr\left[0 \leq \bar{G}_i + \sigma_i X\right] \geq 1 - \delta_i^l \qquad (i = 1 \cdots N) \tag{3.12}$$

$$\Pr\left[\bar{G}_i + \sigma_i X \leq C_i\right] \geq 1 - \delta_i^u \qquad (i = 1 \cdots N) \tag{3.13}$$

$$X \sim f(X), \tag{3.14}$$

where $f(\cdot)$ is a zero-mean probability density function with a standard deviation of one.

The problem is to find an optimal allocation of nominal power $\bar{G}_i$ and standard deviation σ_i to each of the generators that minimizes total cost (3.9). Constraints (3.10) and (3.11) ensure that demand and supply of electricity are balanced, as explained in Section 3.4.3. Finally, (3.12) and (3.13) are the chance constraints. δ_i^l and δ_i^u are the *risk bounds* that are specified by users, where δ_i^l bounds the risk of oversupply and δ_i^u bounds the risk of undersupply. Specifically, (3.12) requires that, when the contingent power turns out to be negative, the total power output is not negative with probability $1 - \delta_i^l$, while (3.13) requires that the resulting output level of each plant is within its capacity with probability $1 - \delta_i^u$.

The risk of oversupplying electricity does not have to be considered for conventional grids. However, we have to consider such risk when renewable energy sources, such as solar and wind, are introduced on a large scale. When those non-dispatchable generators produce more electricity than the demand, such a risk can be realized. This risk can be avoided by allowing dumping of electricity. However, for this study, we do not allow electricity to be dumped in order to be conservative.

Remark 1 *The overall risk of power imbalance in the grid is bounded by the total of*

δ_i^l *and* δ_i^u*:*

$$\Pr\left[\begin{array}{c} 0 \le \bar{G}_1 + \sigma_1 X \le C_1 \\ \wedge \quad 0 \le \bar{G}_2 + \sigma_2 X \le C_2 \\ \vdots \\ \wedge \quad 0 \le \bar{G}_N + \sigma_N X \le C_N \end{array}\right] \le 1 - \sum_{i=1}^{N} (\delta_i^l + \delta_i^u). \tag{3.15}$$

In other words, the risk that at least one generator in a grid fails to provide committed nominal and contingent power is at most $\sum_{i=1}^{N}(\delta_i^l + \delta_i^u)$. Hence, this remark provides a useful guideline to set δ_i^l and δ_i^u. For example, consider a case where a grid operator would like to limit the overall probability of power imbalance to 10^{-5} at the given time instance. This safety goal can be achieved by setting $\delta_i^l = \delta_i^u = 10^{-5}/2N$, where N is the number of generators.

The risk bounds δ_i^l and δ_i^u can be optimized, rather than fixed, by using the Iterative Risk Allocation algorithm (see Chapter 4 of [70]). This allows further reduction of the cost. However, the optimization of risk allocation is not the focus of this chapter.

3.4.6 Deterministic Reformulation

We next reformulate Problem 1 to a deterministic optimization problem.

Conversion to Deterministic Constraints

Let $F_X(\cdot)$ be the cumulative distribution function of X :

$$F_X(x) := \Pr[X \le y] = \int_{-\infty}^{y} f(X)dX.$$

We also denote by $F_X^{-1}(\delta)$ the inverse function of the cumulative distribution function:

$$F_X(y) = \delta \Longleftrightarrow F_X^{-1}(\delta) = y$$

Using these notations, the chance constraint (3.13) is transformed into an equiv-

alent deterministic constraint as follows:

$$\begin{aligned}
\Pr\left[\bar{G}_i + \sigma_i X \leq C_i\right] \geq 1 - \delta_i^u \quad &\Leftrightarrow \quad \Pr\left[X \leq \frac{C_i - \bar{G}_i}{\sigma_i}\right] \geq 1 - \delta_i^u \\
&\Leftrightarrow \quad F_X\left(\frac{C_i - \bar{G}_i}{\sigma_i}\right) \geq 1 - \delta_i^u \\
&\Leftrightarrow \quad C_i - \bar{G}_i \geq \sigma_i F_X^{-1}(1 - \delta_i^u)
\end{aligned}$$

The last equivalence is derived from the fact that a cumulative distribution function is always a non-decreasing function. (3.12) can also be transformed into an equivalent deterministic constraint in the same manner.

Figure 3-3 provides an intuition of this transformation. The integral of the probability distribution function of X above $\frac{C_i - \bar{G}_i}{\sigma_i}$ represents the probability of constraint violation. In order to satisfy the chance constraint (3.13), this area must be less than δ_i^u. Such a condition can be met by leaving a margin between the mean and the constraint boundary, and the necessary width of the margin is $F_X^{-1}(1 - \delta_i^u)$.

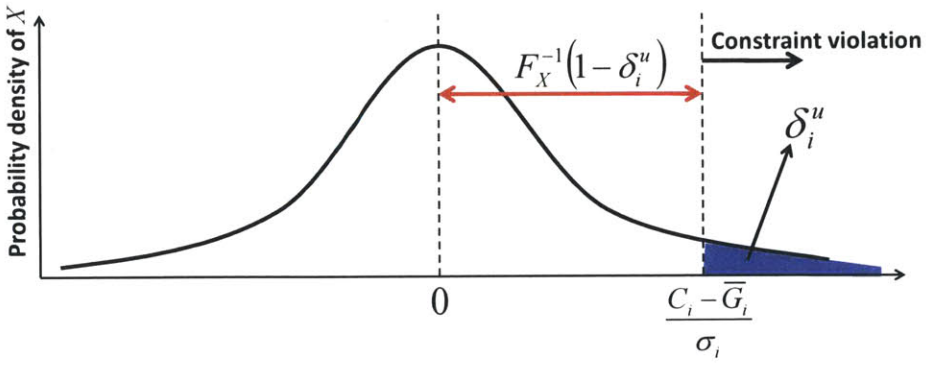

Figure 3-3: Transformation of an individual chance constraint into an deterministic constraint.

Deterministic Reformulation of Problem 1

By applying the deterministic transformation described above to Problem 1, we obtain the following deterministic optimization problem that is equivalent to Problem 1.

Problem 2: Deterministic Equivalent of the Centralized Contingent Power

Dispatch

$$\min_{\bar{G}_{1:N},\sigma_{1:N}} \quad \sum_{i=1}^{N} J_i(\bar{G}_i, \sigma_i) \tag{3.16}$$

$$s.t. \quad \bar{L} = \sum_{i=1}^{N} \bar{G}_i \tag{3.17}$$

$$\sigma_L = \sum_{i=1}^{N} \sigma_i \tag{3.18}$$

$$-\sigma_i F_X^{-1}(\delta_i^l) \leq \bar{G}_i \leq C_i - \sigma_i F_X^{-1}(1-\delta_i^u) \qquad (i = 1 \cdots N) \tag{3.19}$$

where F_X^{-1} is the cumulative distribution function of X.

Problem 2 is a convex optimization problem since we assume that J_i is a convex function of $\bar{G}_i$ and σ_i. Hence, this problem is tractable. Note that Problem 2 is a *centralized* optimization since the nominal power and standard deviation of all generators are decided by one optimization process. In the next section we present an algorithm to solve Problem 1 in a *decentralized* manner.

3.5 Market-based Decentralized Contingent Power Dispatch

In this section we present a decentralized solution to Problem 2 (3.16-3.19) that uses a market-based mechanism called *tâtonnement*. Our main reason to develop a decentralized optimization algorithm is because the real-world electricity market also works in a decentralized manner: providers and consumers bid their demand and supply to maximize their benefit; electricity is priced competitively. Likewise, in our decentralized algorithm, each provider decides its nominal and contingent power supply to maximize its own benefit at a given market price; the price is adjusted by the market to balance demand and supply. We show that, with moderate conditions, our decentralized algorithm results in a globally optimal solution for Problem 2.

3.5.1 Overview

We give an informal overview of our market-based decentralized contingent power dispatch algorithm in this subsection. Formal discussion follows in subsections 3.5.2 and 3.5.3.

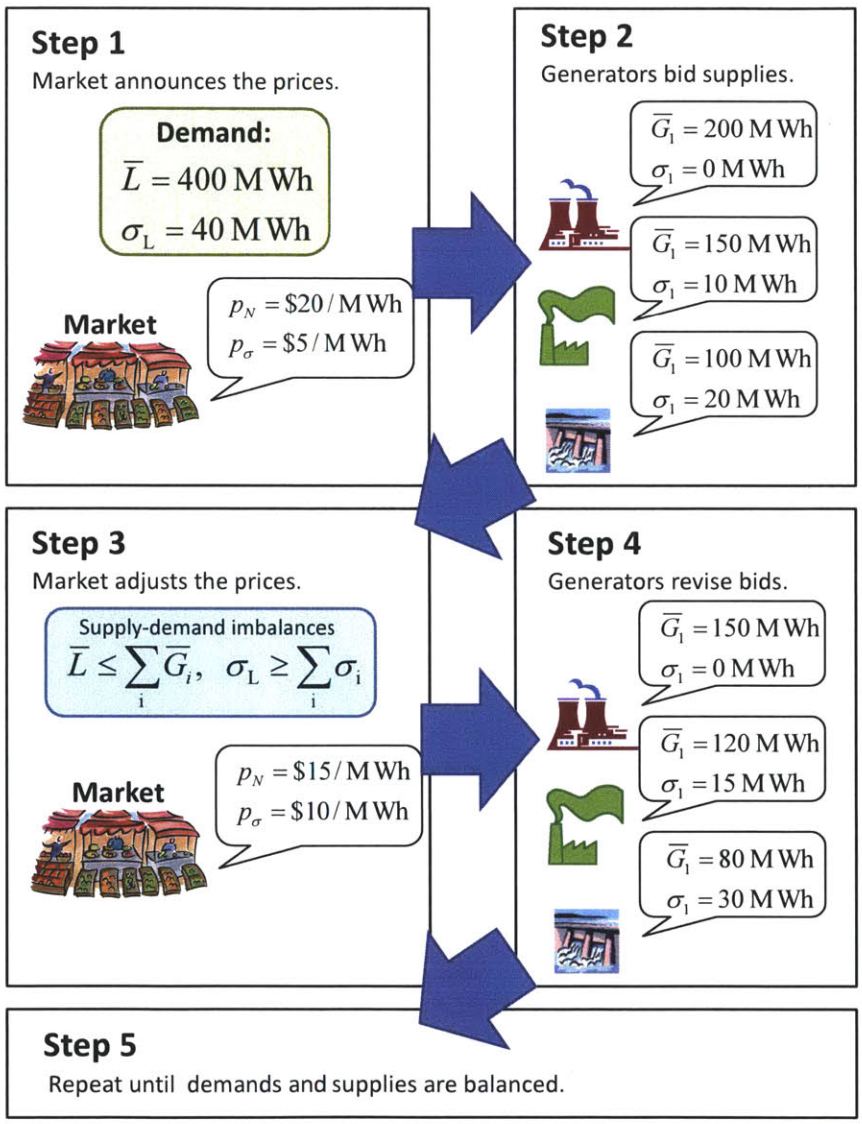

Figure 3-4: Overview of the market-based decentralized contingent power dispatch algorithm.

Figure 3-4 shows the overall process of the algorithm. The algorithm involves a market, which decides the prices, and generators, each of which decides its output

level, depending on the prices. In each iteration, the market announces the price of nominal power as well as the price of contingent power, that is, the price of standard deviation (Step 1). Then, each agent solves its own optimization problem in a decentralized manner in order to decide how much nominal and contingent power it wants to sell at the given prices (Step 2). In other words, each agent decides the supply level as a function of price. Then, the market compares the demands and aggregate supplies. In Step 2 of Figure 3-4, for example, there is excess supply of nominal power and excess demand for standard deviation, since $\bar{L} \leq \sum_{i=1}^{3} \bar{G}_i$ and $\sigma_L \geq \sum_{i=1}^{3} \sigma_i$. Therefore, in Step 3, the market lowers the price of nominal power and raises the price of standard deviation. Then, in Step 4, the generators revise the supply levels according to the updated price. The supplies and demands have not been balanced yet, but the gaps become smaller this time. We repeat this process until the supplies and demands of both quantities are balanced.

3.5.2 Dual Decomposition

We reformulate Problem 2 to a decentralized form by using dual decomposition. The decentralized formulation has two parts. The first part is a series of convex optimization problems, which are solved by each power provider in parallel, while the second part is a root-finding problem, which is solved by a central module, that is, a market.

We apply dual decomposition to Problem 2 to obtain the following Problem 3, which is the optimization problem solved by *each* power provider.

Problem 3: Optimal Contingent Power Supply Problem for the ith Generator (Primal)

$$q_i(p_N, p_\sigma) = \min_{\bar{G}_i, \sigma_i} \quad J_i(\bar{G}_i, \sigma_i) - p_N \bar{G}_i - p_\sigma \sigma_i \tag{3.20}$$

$$s.t. \quad -\sigma_i F_X^{-1}(\delta_i^l) \leq \bar{G}_i \leq C_i - \sigma_i F_X^{-1}(1 - \delta_i^u) \tag{3.21}$$

where p_N and p_σ are the prices of nominal power and standard deviation, given by the market. Note that, in (3.20), $p_N\bar{G}_i + p_\sigma\sigma_i$ represent the revenue of the ith generator obtained by selling $\bar{G}_i$ of nominal power and σ_i of standard deviation in the market. Hence, minimizing the objective function in (3.20) means maximizing the benefit (i.e., revenue less cost) of the ith generator. $q_i(p_N, p_\sigma)$ is the minimized net cost (i.e., negative benefit) of the ith generator at the given prices. Note that its sum, $\sum_i q_i(p_N, p_\sigma)$, corresponds to the dual objective function of Problem 2.

We denote the arguments of the optimal solution to Problem 3 by $\left[\bar{G}_i^\star(p_N, p_\sigma), \sigma_i^\star(p_N, p_\sigma)\right]$:

$$\begin{aligned}\left[\bar{G}_i^\star(p_N, p_\sigma), \sigma_i^\star(p_N, p_\sigma)\right] = \arg\min_{\bar{G}_i, \sigma_i} \quad & J_i(\bar{G}_i, \sigma_i) - p_N\bar{G}_i - p_\sigma\sigma_i \\ s.t. \quad & -\sigma_i F_X^{-1}(\delta_i^l) \leq \bar{G}_i \leq C_i - \sigma_i F_X^{-1}(1-\delta_i^u)\end{aligned}$$

These optimal solutions are functions of price. They can be considered as *supply functions*, which indicate the optimal level of supply by the ith generator at given prices. Note that Problem 3 involves only $\bar{G}_i$ and σ_i. Hence, this problem can be solved by the ith generator independent from all of the other generators. This enables parallel computation. Also note that the prices (p_N, p_σ) are treated as given constants in Problem 3.

The market finds the optimal prices (p_N, p_σ) by solving the following root-finding problem.

Problem 4: Optimal Contingent Power Pricing Problem (Dual)

Find (p_N, p_σ) such that:

$$\begin{aligned}\bar{L} &= \sum_{i=1}^{N} \bar{G}_i^\star(p_N, p_\sigma) \\ \sigma_L &= \sum_{i=1}^{N} \sigma_i^\star(p_N, p_\sigma).\end{aligned}$$

Problems 3 and 4 together solve the dual optimization problem of Problem 2. The sum of the optimal cost of all generators obtained from Problem 3, $\sum_{i=1}^{N} J_i\left(\bar{G}_i^\star(p_N, p_\sigma), \sigma_i^\star(p_N, p_\sigma)\right)$, corresponds to the dual objective function, while Problem 4 corresponds to the sta-

tionary conditions of the dual optimization problem.

We present an iterative algorithm that finds solutions to Problems 3 and 4 in the next section. For now, let us assume that optimal solutions to Problems 3 and 4 are available. Let $p_N^\star$, $p_\sigma^\star$, $\bar{G}_i^\star(p_N^\star, p_\sigma^\star)$, and $\sigma_i^\star(p_N^\star, p_\sigma^\star)$ be the optimal solutions. Then, the following theorem holds:

Theorem 1: Optimality of Decentralized Contingent Power Dispatch
Optimal solutions to Problems 3 and 4, $\bar{G}_i^\star(p_N^\star, p_\sigma^\star)$ and $\sigma_i^\star(p_N^\star, p_\sigma^\star)$, are also optimal solutions to Problem 2.

Proof: Problem 2 has no duality gap since J_i are continuously differentiable convex functions by assumption and all constraints in Problem 2 are linear. Therefore, dual optimal solution $\bar{G}_i^\star(p_N^\star, p_\sigma^\star), \sigma_i^\star(p_N^\star, p_\sigma^\star)$ corresponds to the primal optimal solution of Problem 2. ■

3.5.3 Decentralized Optimization Algorithm

In this subsection we present an iterative algorithm that finds optimal solutions to Problems 3 and 4. The algorithm solves Problem 4 by a subgradient method, while the supply functions $\bar{G}_i^\star(p_N, p_\sigma), \sigma_i^\star(p_N, p_\sigma)$ are evaluated in each iteration of the subgradient method by solving Problem 4 using an interior point method. Every generator solves Problem 4 in parallel.

In this subsection, we use a stronger assumption on the cost function: $J_i(\bar{G}_i, \sigma_i)$ is a *strictly* convex function. This assumption excludes linear objective functions. Such an assumption is required since, if the cost function is not strictly convex, the supply functions $\bar{G}_i^\star(p_N, p_\sigma), \sigma_i^\star(p_N, p_\sigma)$ can be discontinuous and a subgradient may not exist. We note that, even if the cost function is convex but not strictly convex, optimal solutions can still be obtained by the centralized optimization of Problem 2.

The proposed algorithm, shown in Algorithm 1, is based on a market-based price adjustment process, tâtonnement [84]. The algorithm is initialized with initial prices $[p_N^0, p_\sigma^0]$(Line 1). The initial step size α_0 and the discount factor of the step size λ are also set appropriately (Line 2). In each iteration, each agent solves Problem 3 to find

Algorithm 1 Market-based Contingent Power Dispatch

1: $p_N \leftarrow p_N^0$, $p_\sigma \leftarrow p_\sigma^0$
2: $\alpha \leftarrow \alpha_0$, set $\lambda \in (0, 1)$
3: $d_L \leftarrow \infty$, $d_\sigma \leftarrow \infty$
4: **while** $|d_L| > \epsilon_N \ \vee \ |d_\sigma| > \epsilon_\sigma$ **do**
5: The market announces the prices $[p_N, p_\sigma]$ to generators
6: Each agent computes $\bar{G}_i^\star(p_N, p_\sigma)$ and $\sigma_i^\star(p_N, p_\sigma)$ by solving Problem 3
7: $d_L \leftarrow \bar{L} - \sum_{i=1}^N \bar{G}_i^\star(p_N, p_\sigma)$
8: $d_\sigma \leftarrow \sigma_L - \sum_{i=1}^N \sigma_i^\star(p_N, p_\sigma)$
9: $[p_N, p_\sigma] \leftarrow [p_N, p_\sigma] + \alpha\,[d_L, d_\sigma]$
10: $\alpha \leftarrow \lambda\alpha$
11: **end while**

the optimal supply levels of nominal power and standard deviation at the given prices (Line 6). The market then compares the demands and the aggregate supplies (Lines 7 and 8). If their differences are within specified tolerance levels, the current prices are the solution to Problem 4, and the algorithm terminates (Line 4). If they are not balanced, the market adjusts the prices (Line 9) and repeats the iteration. The price adjustment is proportional to the difference between the demand and the aggregate supply $[d_L, d_\sigma]$. The step size α diminishes throughout iteration since $\lambda \in (0, 1)$ (Line 10).

Note that the difference between demand and aggregate supply corresponds to a subgradient of the dual objective function, $q(p_N, p_\sigma)$:

$$[d_L, d_\sigma] = \left[\bar{L} - \sum_{i=1}^N \bar{G}_i^\star(p_N, p_\sigma), \quad \sigma_L - \sum_{i=1}^N \sigma_i^\star(p_N, p_\sigma)\right] \in \partial q(p_N, p_\sigma)$$

In each iteration, the price adjustment is obtained by multiplying a diminishing step size α. Algorithm 1 is guaranteed to find an optimal solution since the convergence of the subgradient method with diminishing step size is guaranteed [12, 81].

3.6 Simulation Result

We demonstrate the Market-based Contingent Power Dispatch in a simulation.

3.6.1 Simulation Setting

We consider three electricity generators in this simulation: 1) a base load plant, 2) a load-following plant, and 3) a peaking plant. The base load plant has the lowest cost of nominal power and the highest cost of standard deviation. The peaking plant has the highest cost of nominal power and the lowest cost of standard deviation.

We assume that the cost function of each plant is a quadratic function of nominal power and standard deviation:

$$J_i(\bar{G}_i, \sigma_i) = a_i\bar{G}_i + b_i\bar{G}_i^2 + c_i\sigma_i + d_i\sigma_i^2,$$

where a_i, b_i, c_i, and d_i are constant parameters. Table 3.1 shows the parameter settings for each plant, as well as the capacity and the risk bounds. As for the step size of the subgradient method, we set $\alpha = 0.1$ and $\lambda = 0.995$.

Table 3.1: Parameter settings of the cost functions of the three plants. The cost function that we assume is: $J_i(\bar{G}_i, \sigma_i) = a_i\bar{G}_i + b_i\bar{G}_i^2 + c_i\sigma_i + d_i\sigma_i^2$.

		Nominal		Contingent	
i		a_i	b_i	c_i	d_i
1	Baseload plant	1.0	0.10	0	10^6
2	Load-following plant	1.5	0.15	0	0.10
3	Peaking plant	2.0	0.20	0	0.05

As shown in Figure 3-5, we run the simulation on six cases, (a)-(f), with different levels of demand for nominal power and standard deviation. Two nominal power demand levels are considered: 100 MWh and 200 MWh, as listed on the horizontal axis of Figure 3-5. We also consider three demand levels for standard deviation: 10 MWh, 20 MWh, and 200 MWh, as shown on the horizontal axis of the figure.

3.6.2 Result

The simulation results are shown in Figure 3-5.

The case (e) with 100 MWh nominal power and 30 MWh standard deviation

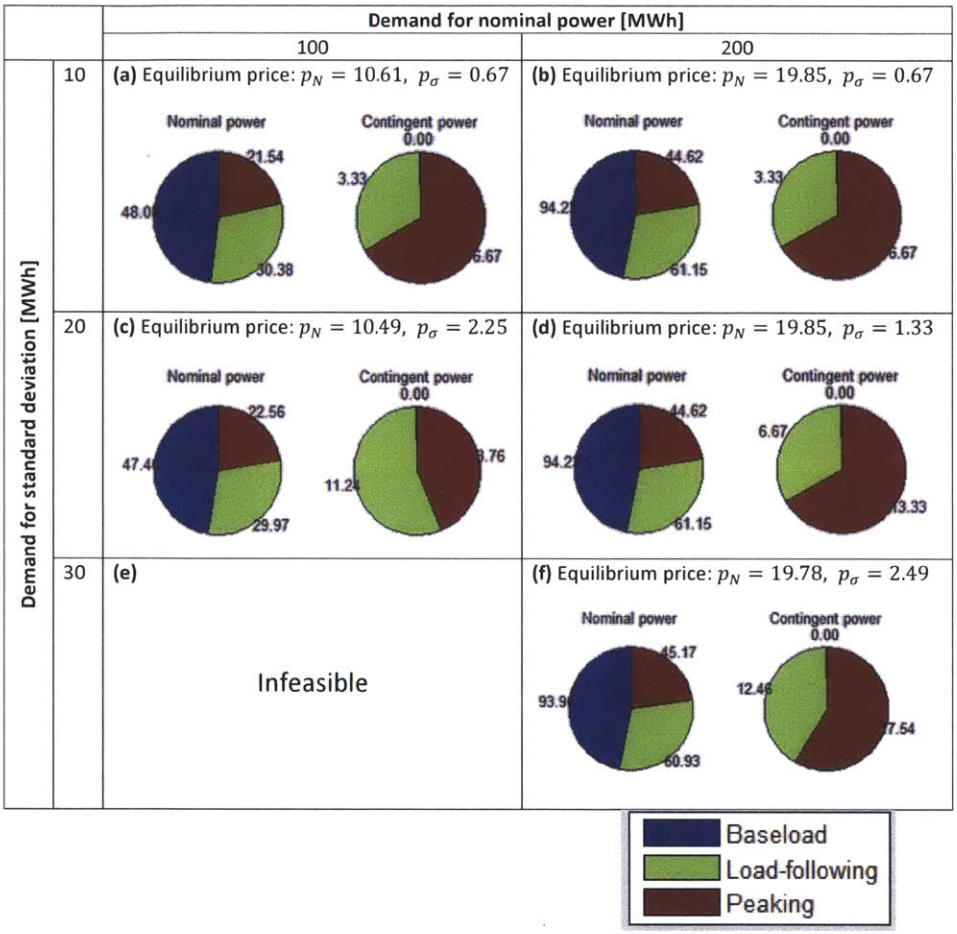

Figure 3-5: Simulation results of the Market-based Contingent Power Dispatch.

turned out to be infeasible. This is because the lower bound constraint (3.12) cannot be satisfied. Recall that (3.12) limits the risk of oversupplying electricity. Since the allocated nominal power $\bar{G}_i$ is small, there is not enough margin to guarantee the specified risk level.

Optimal solutions are obtained in all other cases. The base-load plant provides the largest portion of nominal power, while the peaking plant provides the largest portion of contingent power in all feasible cases, except for case (c). The reason for this exception is explained shortly.

Note the increasing tendency of the equilibrium price of nominal power as the demand for nominal power increases. Likewise, the price of standard deviation also

increases as the demand for standard deviation increases. There is a weak coupling between the two prices: compare the three cases in the right column in Figure 3-5 and notice that the price of nominal power is slightly changed, although the demand for nominal power is constant. Such an effect is called a substitution effect in economics. This substitution effect occurs because the optimizations of the supply levels of nominal power and standard deviation are coupled through Problem 3.

The substitution effect becomes significant when the demands are close to the boundary of the feasible region. For example, observe that, in the case (c) with the 100 MWh demand for nominal power and the 20 MWh demand for standard deviation, the load-following plant provides the largest portion of contingent power, even though its cost of standard deviation is higher than that of the peaking plant. This is explained by the substitution effect. In order for the peaking plant to provide a larger portion of contingent energy, it must also provide a larger amount of nominal energy, since otherwise the risk of undersupplying power will exceed the risk bound (i.e., violation of (3.12)). However, providing nominal energy is expensive for the peaking plant. Rather, it is cheaper to produce the necessary amount of contingent energy at the load-following plant, since it is already producing a larger portion of nominal energy. Therefore, the load-following plant produces a larger portion of contingent energy than the peaking plant in the particular case.

Chapter 4

Risk-sensitive Plan Execution for the Connected Sustainable Home

4.1 Introduction

In this chapter we present a robust plan executive, p-Sulu, and its application for the Connected Sustainable Home. Recall that p-Sulu takes a chance-constrained qualitative state plan (CCQSP) as an input, and continuously outputs control sequences and execution schedules. Also recall that, in Section 1.2.2, we specified three features that are required to control Connected Sustainable Home:

1. goal-directed planning with continuous effects and temporally extended goals (TEGs),
2. optimal planning, and
3. robust planning with bounded risk.

Our approach is to build p-Sulu upon the iterative risk allocation (IRA) algorithm [71], which can optimally plan with chance constraints. Hence, IRA can provide the second and third features listed above. However, IRA cannot handle TEGs. Moreover, its application has been limited to simple planning problems with *finite* duration, while building control must operate continuously.

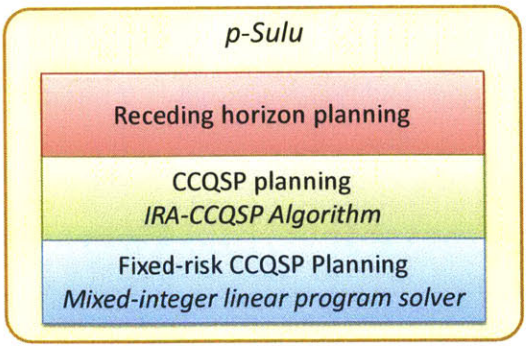

Figure 4-1: Architecture of p-Sulu. p-Sulu consists of two nested loops on top of the fixed-risk CCQSP planner.

Therefore, two major technical challenges for p-Sulu are 1) handling of TEGs and 2) continuous planning with infinite plan duration. The first challenge is overcome by a novel algorithm called IRA-CCQSP, which extends IRA to planning problems with TEGs. The second challenge is overcome by employing a receding horizon control approach, also known as model predictive control (MPC) [63], where a finite-horizon CCQSP planning problem is repeatedly solved by the IRA-CCQSP algorithm.

Figure 4-1 shows the architecture of p-Sulu, which consists of two nested loops on top of the fixed-risk CCQSP planner. The outer loop performs continuous receding horizon planning through repeated calls to a CCQSP planner. The receding horizon planner divides the time into multiple planning segments or planning horizons with a finite duration, which "recede" over time. For example, at time $t = 0$, a CCQSP planning problem with a planning horizon $t \in [0\ 10]$ is solved. Then, at time $t = 3$, a CCQSP planning problem is solved again with a planning horizon $t \in [3\ 13]$.

In each planning horizon the CCQSP planning problem is solved by the inner loop through the novel IRA-CCQSP algorithm. IRA-CCQSP finds an optimal allocation of risk through iterative solving of a fixed-risk CCQSP planning problem. The fixed-risk CCQSP planning problem is to find an optimal control sequence and a schedule that satisfy the given CCQSP, which involves TEGs and chance constraints. The fixed-risk CCQSP problem is encoded into a mixed-linear integer program (MILP), which is solved by a commercial MILP solver.

Three innovations are presented in this chapter. First, we formulate building climate control as a CCQSP planning problem. Second, we develop IRA-CCQSP algorithm. Furthermore, we show that IRA-CCQSP is an anytime algorithm. Third, we develop a new fixed-risk CCQSP planner, which is used in the IRA-CCQSP algorithm to deal with TEGs in a continuous domain.

4.2 Related Work

Application of AI methods to building control has been actively studied for several decades. For example, [62] employs a stochastic model-predictive control (SMPC) approach to significantly reduce energy consumption of a building, based on a stochastic occupancy model. Although our work is similar to theirs in that p-Sulu is also built upon SMPC, our problem differs in its guarantee to bound risk, and its formulation with chance-constraints. [48] models end user energy consumption in residential and commercial buildings. Another relevant work within the community is [58], which uses a robust plan executive to control autonomous underwater vehicles in order to perform ocean monitoring.

Application of MPC for building climate control has received considerable attention for its ability to minimize energy consumption with time-varying constraints [34, 38, 61]. [69] applied a chance-constrained MPC to deal with uncertain weather and occupancy predictions. Our approach differs from [69] in that p-Sulu can take *flexible* temporal constraints.

There is extensive literature on planning with discrete actions to achieve temporally extended goals (TEGs), such as TLPlan [8] and TALPlan [52]. However, since these TEG planners assume discrete state spaces, they cannot handle problems with continuous states and effects without discretization. Ignoring chance constraints, the representation of time evolved goals used by TLPlan and p-Sulu is similar. TlPlan uses a version of metric interval temporal logic (MITL) [3] applied to discrete states, while p-Sulu uses qualitative state plans (QSPs) [56, 40, 59] over continuous states. Kongming [59] plans with TEGs for hybrid systems, but it does not consider stochas-

tic uncertainty and chance constraints. Chance-constraint MDP [33] considers chance constraints, but out work is distinct from theirs in that p-Sulu is goal-directed, by which we mean that it achieves TEGs within user-specified temporal constraints.

4.3 Problem Formulation

Recall that p-Sulu takes as an input a CCQSP, which encodes both TEGs and chance constraints. Given a CCQSP, p-Sulu finds an optimal control sequence, which is an assignment to real-valued control variables, as well as a schedule, which is an assignment of execution time to events.

4.3.1 Stochastic Plant Model

An advantage of p-Sulu over existing deterministic plan executives is that it can explicitly reason over a stochastic plant model, which specifies probabilistic state transitions in a continuous domain in the following form:

$$\boldsymbol{x}_{t+1} = A_t \boldsymbol{x}_t + B_t \boldsymbol{u}_t + \boldsymbol{w}_t, \tag{4.1}$$

where $\boldsymbol{x}_t$ is a continuous state vector at time t, $\boldsymbol{u}_t$ is a continuous control vector at t, and $\boldsymbol{w}_t$ is a disturbance whose probability distribution is known.

4.3.2 Input: CCQSP

A CCQSP may be depicted as an acyclic directed graph. For example, the CCQSP shown in Figure 4-2 is interpreted in plain English as a series of episodes, as follows:

> "Maintain a comfortable sleeping temperature (18-22°C) until I wake up. After waking up, maintain a comfortable room temperature (20-25°C) until I go to work. I can do some work at home, but I have to do 5 hours of work in the office sometime between 9 a.m. and 6 p.m. No temperature constraints while I am away, but when I get home, maintain

the comfortable room temperature (20-25°C) until I go to sleep. The probability of failure of these episodes must be less than 1%. The entire time, make sure the house does not get so cold that the pipes freeze. Limit the probability of such a failure to 0.01%."

Formally, a **chance-constrained qualitative state plan** (*CCQSP*) is a four-tuple $P = \langle \mathcal{E}, \mathcal{A}, \mathcal{T}, \mathcal{C} \rangle$, where $\mathcal{E}$ is a set of discrete events, $\mathcal{A}$ is a set of *episodes*, $\mathcal{T}$ is a set of *simple temporal constraints*, and $\mathcal{C}$ is a set of *chance constraints.*

An **event**, illustrated as a circle in Figure 4-2, represents a point of time, to which an execution time is assigned.

An **episode**, depicted as a rectangle, specifies the desired state of the system under control over a time interval. It is a three tuple $a = \langle e_a^S, e_a^E, R_a \rangle$, where e_a^S and e_a^E are the start and end events of the episode, respectively. Each episode a has a feasible state region R_a. For example, R_a for the "Maintain sleep temperature" is a closed interval on the indoor temperature, $[18°C\ 22°C]$.

A **simple temporal constraint**, denoted by two numbers in a bracket as $[lb_e^{e'}\ ub_e^{e'}]$, specifies an upper bound $ub_e^{e'}$ and a lower bound $lb_e^{e'}$ on the temporal distance between two events $e, e' \in \mathcal{E}$. Note that $ub_e^{e'} = -lb_{e'}^{e}$.

Finally, a **chance constraint** specifies a lower bound on the probability of failing to satisfy a set of episodes during execution. It is a two-tuple, $c = \langle \Delta_c, \Psi_c \rangle$, where Δ_c is the risk bound and Ψ_c is the set of episodes associated with a chance constraint c. For example, in the CCQSP shown in Figure 4-2, the first chance constraint is associated with three episodes: a "Maintain sleep temperature" episode and two "Maintain home temperature" episodes.

4.3.3 Outputs

Optimal executable control sequence p-Sulu generates a control sequence $\boldsymbol{u}_0 \cdots \boldsymbol{u}_T$ that minimizes a given cost function and satisfies all constraints specified by the input CCQSP. In the case of the Connected Sustainable Home, the outputs are the opaqueness of the dynamic window, as well as the heat output of HVAC.

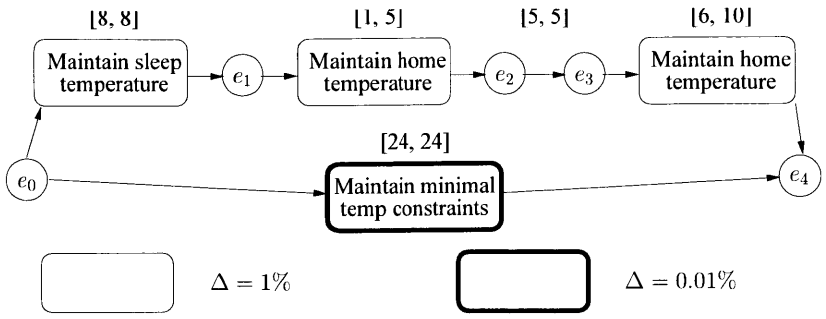

Figure 4-2: An example of a CCQSP for a resident's schedule in a planning problem for the Connected Sustainable Home.

Optimal schedule p-Sulu also outputs an optimal schedule. Let $s_e \in \mathbb{R}_+$ be an execution time of the event e, where $\mathbb{R}_+$ is the set of non-negative real numbers. A schedule s is an assignment of execution times to all events in $\mathcal{E}$.

4.3.4 CCQSP Planning Problem Encodings

In this subsection we encode the CCQSP planning problem that is solved at each planning horizon by the IRA-CCQSP algorithm. Recall that we employ a receding horizon approach. We denote by $\mathbb{T}_n := \{(n-1)N_E + 1 \cdots (n-1)N_E + N_P\}$ the set of discrete time steps included in the nth planning horizon, where N_E and N_P are the number of time steps in an execution horizon and a planning horizon, respectively. Note that $N_E \leq N_P$.

The temporal constraints in a CCQSP are encoded as follows:

$$\bigwedge_{e \in \mathcal{E}_u} \bigwedge_{e' \in \mathcal{E}, e' \neq e} lb_e^{e'} \leq s_{e'} - s_e \leq ub_e^{e'} \tag{4.2}$$

$$\bigwedge_{e \in \mathcal{E} \setminus \mathcal{E}_u} s(e) = \bar{s}_e, \tag{4.3}$$

where $\mathcal{E}_u$ is a set of unexecuted events. (4.2) imposes upper bound and lower bounds on arcs that involves unexecuted events. The schedule of the events that have already been executed, $e \in \mathcal{E} \setminus \mathcal{E}_u$, are fixed to their execution time $\bar{s}_e$, as in (4.3).

We next encode the episodes, as well as chance constraints. An episode a is satisfied if the state $\boldsymbol{x}_t$ is within the feasible region R_a whenever a is being executed (i.e., $s_{e_a^S} \leq t \leq s_{e_a^E}$). A chance constraint c is satisfied if all episodes in Ψ_c are satisfied with probability $1 - \Delta_c$. Hence, for all chance constraints in $\mathcal{C}$, the following must be satisfied:

$$\bigwedge_{c \in \mathcal{C}} \Pr \left[\bigwedge_{a \in \Psi_c} \bigwedge_{t \in \mathbb{T}} \left((s_{e_a^S} \leq t \leq s_{e_a^E}) \Longrightarrow \boldsymbol{x}_t \in R_a \right) \right] \geq 1 - \Delta. \tag{4.4}$$

The constraint (4.4) allows the plan executive to postpone the execution of a by setting $s_{e_a^S}$ larger than all the time steps in $\mathbb{T}_n$. Postponed episodes are executed in later planning horizons. However, whenever an episode can be executed at the current horizon, the executive should not postpone its execution since there is no guarantee that the episode is still feasible with regard to state and chance constraints at future time steps. Therefore, we penalize deferments of episode execution. Let p_a be the penalty, and M be a large positive constant. We require the following:

$$s_{e_a^S} > (n-1)N_E + N_P \Longrightarrow p_a = M. \tag{4.5}$$

Finally, we set the objective function. Let $J(\boldsymbol{u}, s)$ be a cost function, which is assumed to be a piecewise linear function of a control sequence $\boldsymbol{u}$ and a schedule s. The penalty p_a of all episodes must be added to the cost function. Hence, we minimize the following objective function:

$$\min_{\boldsymbol{u}, s} J(\boldsymbol{u}, s) + \sum_{a \in \mathcal{A}} p_a. \tag{4.6}$$

For each planning horizon $\mathbb{T}_n$, p-Sulu solves a CCQSP planning problem with the objective function (4.6) and constraints (4.1), (4.2), (4.4), and (4.5).

4.4 Robust Plan Executive: p-Sulu

Recall that p-Sulu consists of two nested loops. The outer loop performs continuous receding horizon planning through repeated calls to a stochastic CCQSP planner. The CCQSP planning is implemented by the inner loop through the novel IRA-CCQSP algorithm, which performs a series of fixed-risk CCQSP planning steps. We first walk through an example to give an intuitive overview of IRA-CCQSP. Next we transform the stochastic optimization problem stated in the previous section above to a deterministic optimization problem by using the risk allocation approach. We then present the formulation of the fixed-risk CCQSP planning problem, followed by the descriptions of the inner and outer loop algorithms.

4.4.1 Walk-Through of IRA-CCQSP

We walk through an example shown in Figure 4-3, a room temperature control problem with a 24-hour planning horizon in winter (hence the room must be heated). For simplicity of explanation, we assume a fixed schedule in this example, where the resident wakes up at 8 a.m., leaves home at 12 p.m., comes back home at 5 p.m., and goes to bed at 12 p.m. The room temperature is required to be within specified ranges according to the resident's state, as in Figure 4-3.

As we explained in Section 2.1, allocation of risk to each constraint must be optimized in order to optimally solve a joint chance constrained optimization problem. The IRA-CCQSP algorithm optimizes risk allocation for a CCQSP planning problem. It guarantees satisfaction of chance constraints by setting a safety margin (shown as shadowed areas in Figure 4-3) along the boundaries of the constraints, and planning a nominal state trajectory to remain outside of the margin. The width of the safety margin is determined so that the probability of constraint violation is below the risk allocated to each constraint. For example, in Figure 4-3-(a), the safety margin is uniform for all the time because the initial risk allocation is uniform.

IRA-CCQSP is initialized with an arbitrary feasible risk allocation, such as the uniform one in Figure 4-3-(a), and improves the risk allocation through iteration.

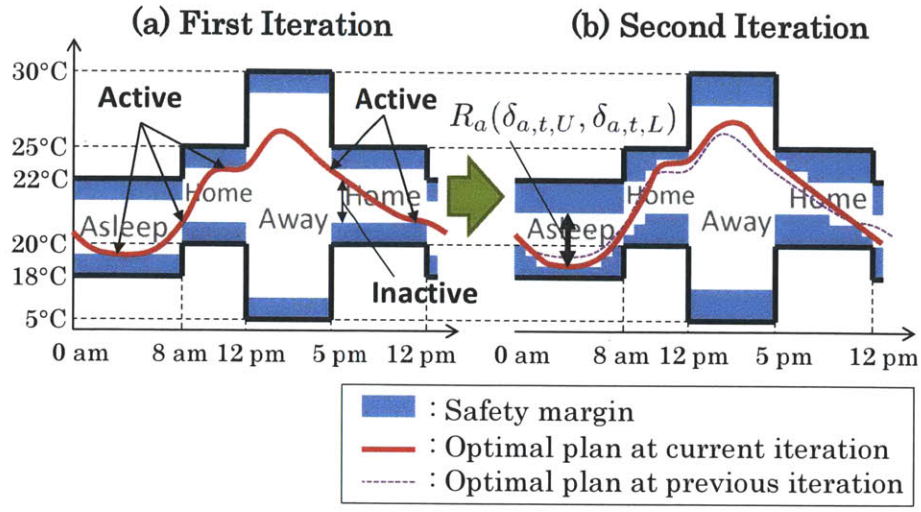

Figure 4-3: Intuitive explanation of the iterative risk allocation (IRA) algorithm.

In each iteration a fixed-risk CCQSP planning problem is solved in order to plan a nominal state trajectory that minimizes cost and does not violate the safety margin, as shown in Figure 4-3-(a). The plan minimizes energy consumption by lowering the temperature during the night, while heating the room using sunlight during the day. It heats the room to the maximum before the sunset at around 5 p.m. to store heat in the structure, so that the use of heater during the night can be minimized.

Note in Figure 4-3-(a) that, with this plan, constraints are active at a few points of time, while they are inactive at other points of time. To improve cost, IRA removes the risk that was allocated to the inactive constraints, and reallocates it to the active constraint. Note that reducing risk allocation results in a wider safety margin, while increasing risk allocation results in the opposite. Thus, the new risk allocation results in the safety margin shown in Figure 4-3-(b). The algorithm then solves the fixed-risk CCQSP planning problem again, in order to obtain the optimal plan that does not violate the new safety margin. The new plan is more energy efficient than the one in the previous iteration since the temperature can be lower during the night, while it is higher in the evening to store more heat. In this way, the algorithm reallocates the risk again from inactive constraints to active constraints at every iteration. It terminates when all constraints become active or all constraints are inactive. The

cost function value (i.e., energy consumption in this case) decreases monotonically during successive iterations. The path generated at each iteration always satisfies the chance constraint since it does not violate the safety margin.

4.4.2 Deterministic Transformation

In order to make the CCQSP planning problem tractable, we reformulate the stochastic constraints (4.4) to deterministic constraints. To this end, we first decompose the chance constraint. It follows from Boole's inequality that the following is a sufficient condition for (4.4):

$$\bigwedge_{c\in\mathcal{C}}\bigwedge_{a\in\Psi_c}\bigwedge_{t\in\mathbb{T}_n}\Pr\left[(s_{e_a^S}\leq t\leq s_{e_a^E})\Longrightarrow \boldsymbol{x}_t\in R_a\right]\geq 1-\delta_{a,t} \tag{4.7}$$

$$\bigwedge_{c\in\mathcal{C}}\sum_{a\in\Psi_c,t\in\mathbb{T}_n}\delta_{a,t}\leq\Delta_c, \tag{4.8}$$

where $\delta_{a,t}$ is the risk allocated to episode a at time step t. The above two constraints can be transformed into equivalent deterministic constraints on nominal states. For example, in the case of Connected Sustainable Home, the equivalent deterministic constraints are described as follows:

$$\bigwedge_{c\in\mathcal{C}}\bigwedge_{a\in\Psi_c}\bigwedge_{t\in\mathbb{T}_n}(s_{e_a^S}\leq t\leq s_{e_a^E})\Longrightarrow \bar{x}_t\in R_a(\delta_{a,t,U},\delta_{a,t,L}) \tag{4.9}$$

$$\bigwedge_{c\in\mathcal{C}}\sum_{a\in\Psi_c,t\in\mathbb{T}_n}\delta_{a,t,U}+\delta_{a,t,L}\leq\Delta_c, \tag{4.10}$$

where $\bar{x}_t$ is a *nominal* state, which is a deterministic variable defined as $\bar{x}_t = E[\boldsymbol{x}_t]$. $\delta_{a,t,U}$ and $\delta_{a,t,L}$ are the risk allocated to the upper and lower temperature bounds of episode a at time t. $R_a(\delta_{a,t,U},\delta_{a,t,L})$ is a range of temperature between the safety margins, as shown in Figure 4-3-(b). It is a closed interval on the indoor temperature,

$$R_a(\delta_{a,t,U},\delta_{a,t,L}) = [T_a^L + m_t(\delta_{a,t,L}) \quad T_a^U - m_t(\delta_{a,t,U})],$$

where T_a^U and T_a^L are the lower and upper bounds of the comfortable indoor temperature range for episode a, respectively. The function $m_t(\delta)$ represents the width of the safety margin at time step t given the risk allocation δ. For example, when the indoor temperature T_t^{in} has a Gaussian distribution with standard deviation σ_t, the safety margin width is given as:

$$m_{c,i}(\delta) = -F_{\sigma_t}^{-1}(\delta) = -\sqrt{2}\,\sigma_t^{\text{in}}\text{erf}^{-1}(1-2\delta),$$

where $F_{\sigma_t}^{-1}(\cdot)$ is an inverse cumulative distribution of a zero-mean Gaussian distribution with standard deviation σ_t, and $\text{erf}^{-1}(\cdot)$ is the inverse of the Gauss error function. Figure 4-4 provides an intuition of this transformation. The integral of the probability distribution function above T_a^U represents the probability of violating the upper bound. In order to satisfy the chance constraint, this area must be less than δ. Such a condition can be met by leaving a margin between the mean and the constraint boundary, and the necessary width of the margin is $-F_{\sigma_t}^{-1}(\delta)$.

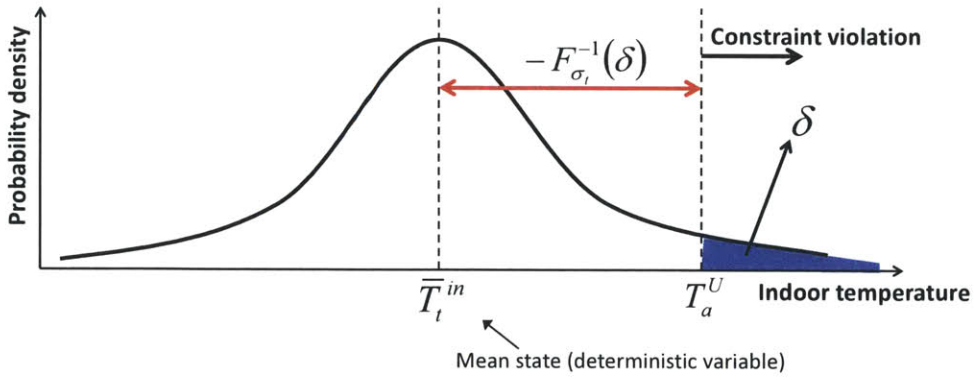

Figure 4-4: Transformation of an individual chance constraint into an deterministic constraint.

Finally, since $\boldsymbol{w}_t$ is assumed to have a zero-mean disturbance, the following nominal plant model is obtained from (4.1):

$$\bar{x}_{t+1} = A_t\bar{x}_t + B_t\boldsymbol{u}_t. \tag{4.11}$$

4.4.3 Fixed-risk CCQSP planning problem

In this subsection we formulate the fixed-risk CCQSP planning problem, which is solved in IRA-CCQSP to obtain nominal state trajectories with a given risk allocation. Let δ be a vector comprised of risk allocations $\delta_{a,t,j}$ for all $a \in \mathcal{A}$, $t \in \mathbb{T}_n$, and $j \in \{U, L\}$.

Definition 1 Fixed-risk CCQSP Planning Problem $\mathcal{P}_n(\delta)$ *is a constrained optimization problem with objective function (4.6) and constraints (4.2), (4.3), (4.5), (4.9), (4.10), and (4.11), given a fixed risk allocation* δ.

[56] showed that the logical implications ($\Rightarrow$) in (4.5) and (4.9) can be encoded to mixed-integer linear constraints. Thus, the fixed-risk CCQSP planning problem is a mixed-integer linear program, which can be efficiently solved by a commercial solver, such as CPLEX.

4.4.4 Inner Loop: CCQSP Planning using IRA-CCQSP

Next we present the IRA-CCQSP algorithm. IRA-CCQSP is described in Algorithm 2. Here, k is the index of iteration. We denote by $\delta^k_{a,t,j}$ the risk allocated to the constraint (a, t, j) at iteration k, and by δ^k the vector comprised of all risk allocations at iteration k. The algorithm is initialized with an feasible risk allocation δ^1 in Line 1. We assume that such a feasible risk allocation is known. A uniform risk allocation is typically used to initialize IRA-CCQSP. At each iteration, an optimal nominal state trajectory is obtained by solving the fixed-risk CCQSP planning problem with a risk allocation δ^k (Line 3). In Lines 5-12 the algorithm reallocates risk from inactive constraints to active constraints. It reduces the risk allocated to inactive constraints (Line 7), and deposits the amount of risk removed from the inactive constraints in γ_c. In Line 7, $0 < \alpha < 1$ is an interpolation coefficient, and $p_{a,t,j}(\bar{x}_t)$ is the probability of violating the constraint with index (a, t, j), given a nominal state $\bar{x}_t$. In the case of Connected Sustainable Home, $p_{a,t,j}(\cdot)$ is evaluated as follows:

$$p_{a,t,U}(\bar{T}^{in}_t) = 1 - F_t(T^U_a), \quad p_{a,t,L}(\bar{T}^{in}_t) = F_t(T^L_a),$$

where $\bar{T}_t^{in}$ is the nominal indoor temperature at time t, $F_t(\cdot)$ is the cumulative distribution function of the indoor temperature T_t^{in}, and T_a^U, T_a^L are the upper and lower bound of the comfortable temperature range of episode a. Intuitively, Line 7 obtains a new safety margin by interpolating the current safety margin and the current nominal state, as shown in Figure 4-5. The new risk bound δ^{k+1} is smaller than the current risk bound δ^k, but still greater than the risk of the current nominal state $p_{a,t,L}(\bar{T}_t^{in})$. Therefore, Line 7 guarantees that the new safety margin is not violated by the current nominal state trajectory. Then the algorithm reallocates the amount of risk saved in γ_c to the active constraints. It splits the deposit of risk equally to the N_c active constraints in Line 11. By going through one iteration, the risk allocation is updated from δ^k to δ^{k+1}.

Algorithm 2 IRA-CCQSP

1: Set initial risk allocation δ^1; $k \leftarrow 1$
2: **repeat**
3: Solve $\mathcal{P}_n(\delta^k)$
4: **for all** $c \in \mathcal{C}$ **do**
5: $\gamma_c \leftarrow 0$; $N_c \leftarrow$ number of active constraints in c
6: **for all** $a \in \Psi_c$, $t \in \mathbb{T}_n$, $j \in \{U, L\}$ such that the constraint with index (a, t, j) is inactive **do**
7: $\delta_{a,t,j}^{k+1} \leftarrow \alpha \delta_{a,t,j}^k + (1-\alpha) p_{a,t,j}(\bar{x}_t)$
8: $\gamma_c \leftarrow \gamma_c + (\delta_{a,t,j}^k - \delta_{a,t,j}^{k+1})$
9: **end for**
10: **for all** $a \in \Psi_c$, $t \in \mathbb{T}_n$, $j \in \{U, L\}$ such that the constraint with index (a, t, j) is active **do**
11: $\delta_{a,t,j}^{k+1} \leftarrow \delta_{a,t,j}^k + \gamma_c / N_c$
12: **end for**
13: **end for**
14: $k \leftarrow k + 1$
15: **until** $\forall_{c \in \mathcal{C}}\ N_c = 0$ **or** $\forall_{c \in \mathcal{C}}\ \gamma_c = 0$

Anytime Algorithm We now prove that IRA-CCQSP is an anytime algorithm, given that the initial risk allocation δ^1 is feasible. The following lemma holds:

Lemma 1: If $\mathcal{P}_n(\delta^k)$ has a feasible solution, then $\mathcal{P}_n(\delta^{k+1})$ also has a feasible solution.

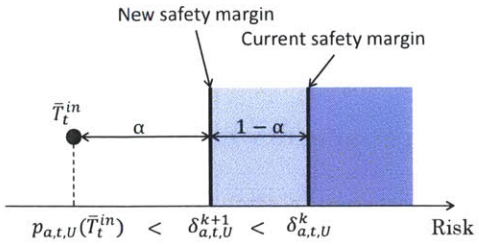

Figure 4-5: Constraint tightening of an inactive constraint in the IRA-CCQSP algorithm (Line 7). The new risk bound δ^{k+1} is smaller than the current risk bound δ^k, but still greater than the risk of the current nominal state $p_{a,t,L}(\bar{T}_t^{in})$. Therefore, the new safety margin is not violated by the current nominal state trajectory.

Intuitively, we prove the lemma by showing that the nominal state trajectory in the previous iteration, as shown as the dashed line in Figure 4-3-(b), does not violate the new safety margin.

Proof: Let $\bar{x}^\star$ be a feasible solution of $\mathcal{P}_n(\delta^k)$. Then, $\bar{x}^\star$ is also a feasible solution because the active constraints in $\mathcal{P}_n(\delta^k)$ are relaxed while Line 7 guarantees that tightened inactive constraints are not violated by $\bar{x}^\star$. ■

It immediately follows from the lemma that, given a feasible initial risk allocation, the fixed-risk CCQSP planning problem has a feasible solution for all iterations. The following lemma, which guarantees that the objective function value $J^\star$ (defined in (4.6)) monotonically decreases over iterations, is also derived from Lemma 1.

Lemma 2: Let $J^\star(\delta^k)$ the minimized objective function value of the fixed-risk CCQSP planning problem given a risk allocation δ^k. Then, $J^\star(\delta^{k+1}) \leq J^\star(\delta^k)$ for all $k \geq 1$.

Proof: Lemma 1 guarantees that an optimal solution of $\mathcal{P}_n(\delta^k)$ is also a feasible solution of $\mathcal{P}_n(\delta^{k+1})$. Hence, $J^\star(\delta^{k+1}) \leq J^\star(\delta^k)$. ■

It follows from Lemmas 1 and 2 that the IRA-CCQSP algorithm is an anytime algorithm. Each iteration constructs a feasible CCQSP sequence of actions. Every iteration improves the plan, hence iteration can be stopped at any point after the first call, while sacrificing optimality, but not correctness or incurring unacceptable risk.

4.4.5 Outer Loop: Receding Horizon Planning

We next present the outer loop of p-Sulu. The outer loop performs continuous receding horizon planning through repeated calls of IRA-CCQSP. It exploits the feature of IRA-CCQSP that it is an anytime algorithm by running as many IRA-CCQSP iterations as possible within each planning horizon, in order to obtain the best available solution for a given replanning interval. The outer loop is outlined in Algorithm 3.

Algorithm 3 p-Sulu

1: $\mathcal{E}_u \leftarrow \mathcal{E}$; $n \leftarrow 1$
2: **while** $\mathcal{E}_u \neq \emptyset$ **do**
3: Wait until $t = (n-1)N_E + 1$
4: $\boldsymbol{u} \leftarrow$ IRA-CCQSP$(n, \mathcal{E}_u)$
5: Execute the first N_E steps in $\boldsymbol{u}$
6: $\forall e \in \mathcal{E}_u$, remove e from $\mathcal{E}_u$ if e has been executed
7: $n \leftarrow n + 1$
8: **end while**

In Algorithm 3, we denote by N_E the number of time steps in an execution horizon and by $\mathcal{E}_u$ a set of unexecuted events. At the start of continuous planning and execution, $\mathcal{E}_u$ is initialized with the full set of events $\mathcal{E}$ in the given CCQSP(Line 1). The executive replans every N_E time steps. It waits until the next scheduled replanning time in Line 3. A CCQSP planning problem is solved at every planning cycle by IRA-CCQSP, in order to generate a sequence of optimal control inputs $\boldsymbol{u}$ (Line 4), of which the first N_E control inputs are executed in this horizon (Line 5). Finally, the events that are executed within this planning horizon are removed from $\mathcal{E}_u$ (Line 6). This iteration is repeated until all the events are executed and hence the set $\mathcal{E}_u$ becomes empty (Line 2).

In the application for Connected Sustainable Home, new events are continuously added to the CCQSP so that the algorithm operates without termination. This is a reasonable approach for Connected Sustainable Home since it is not realistic to specify episodes in far future. For example, a resident would not specify the time to go to bed

a year in advance. Instead, a resident are allowed to add episodes to CCQSP in order to specify her requirements in near future. The plan executive operates continuously with a CCQSP, which has a finite duration but is continuously extended. The same approach has been employed by Remote Agent [66] and Casper [47].

4.5 Application to Connected Sustainable Home

Building Model We obtain a stochastic plant model of Connected Sustainable Home in the form of (4.1) by using a lumped capacitance model for a thermal system [42]. The lumped capacitance model is analogous to an electrical circuit. Separate components, or "lumps", of a building store heat according to its heat capacity C_i similar to how an electrical capacitor stores charge. Heat transfers between lumps subject to a thermal resistance, which is a property of the materials. We break the home down into a single lump for the indoor air mass, as well as a lump for each wall and window, as shown in Figure 4-6. In total the house is decomposed into 11 lumps: 4 for windows, 6 for walls, and 1 for the indoor air mass. For each component i, the following holds for a short time interval Δt:

$$C^i(T^i_{t+1} - T^i_t) = \Delta Q^i_{\text{Cond},t} + \Delta Q^i_{\text{Conv},t} + \Delta Q^i_{\text{Rad},t}, \tag{4.12}$$

here, T^i_t is the temperature of the ith component at the time step t. $\Delta Q^i_{\text{Cond},t}$, $\Delta Q^i_{\text{Conv},t}$, and $\Delta Q^i_{\text{Rad},t}$ are heat inputs to the ith component during the time interval through conduction, convection, and radiation, respectively. The outdoor environment is treated as a heat source, similar to a voltage source in the circuit analogy.

The conductive heat input $\Delta Q^i_{\text{Cond},t}$ accounts for all heat transfer through each wall. For example, the conduction heat input for the indoor air mass component is:

$$\Delta Q^{\text{in}}_{\text{Cond},t} = \sum_i \frac{A_i}{R^{\text{in}}_i}(T^i_t - T^{\text{in}}_t)\Delta t, \tag{4.13}$$

where T^{in}_t is the indoor temperature, T^i_t is the temperature of wall i, A_i is the area of contact between components i and j, and R^j_i is the heat resistance (R-value) between

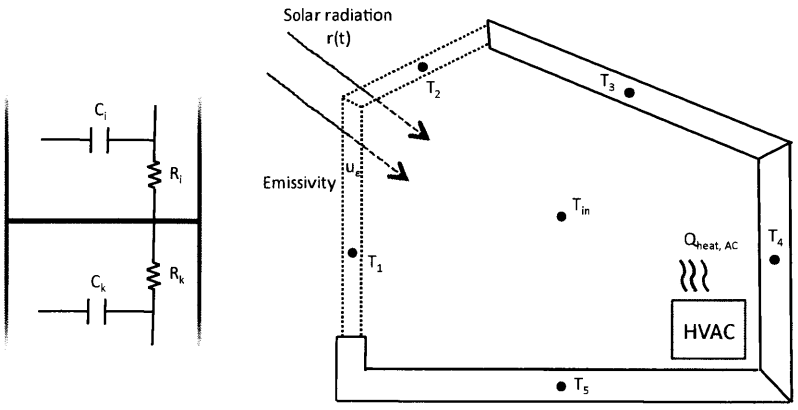

Figure 4-6: Model of temperature flow between lumps is analogous to an electric circuit (left). Depiction of state variables T_i and control variables $Q_{\text{Heat}}, Q_{\text{AC}}, u_t^{\text{DW}}$ (right).

components i and j. The convection term accounts for any heat transfer from the heater and air conditioner:

$$\Delta Q_{\text{Conv},t}^{\text{in}} = \Delta Q_t^{\text{Heat}} - \Delta Q_t^{\text{AC}}, \tag{4.14}$$

where ΔQ_t^{Heat} and ΔQ_t^{AC} are the outputs of the heater and air conditioner, respectively. Finally, the radiation term accounts for heat transfer from the sun through the glass facade:

$$\Delta Q_{\text{Rad},t}^{\text{in}} = A \cdot r(t) \cdot u_t^{\text{DW}} \Delta t, \tag{4.15}$$

where A is the area of the facade, r is the solar radiation, and u_t^{DW} is a control variable for the emissivity of the dynamic windows. By substituting (4.13)-(4.15) into (4.12), we obtain the following:

$$T_{t+1}^{\text{in}} = T_t^{\text{in}} + \frac{1}{C^{\text{in}}} \left(\sum_i \frac{A_i \Delta t (T_i - T_{\text{in}})}{R_i^{\text{in}}} + \Delta Q_t^{\text{Heat}} - \Delta Q_t^{\text{AC}} + A r(t) u_t^{\text{DW}} \Delta t \right). \tag{4.16}$$

Similarly, the thermal models for the walls is are obtained as follows:

$$T_{t+1}^i = T_t^i + \frac{1}{C^{\text{in}}} \left\{ \frac{A_i^{\text{in}} \Delta t (T_t^{\text{in}} - T_t^i)}{R_i^{\text{in}}} + \frac{A_i^{\text{out}} \Delta t (T_t^{\text{out}} - T_t^i)}{R_i^{\text{out}}} + \Delta Q_{\text{Rad},t}^i \right\}. \tag{4.17}$$

We assume that future outdoor temperature T_t^{out} has uncertainty, which is represented by a Gaussian distribution. Hence,

$$T_t^{\text{out}} = \overline{T}_t^{\text{out}} + w_t, \tag{4.18}$$

where $\overline{T}_t^{\text{out}}$ is a constant representing the predicted temperature at time t, and w_t is a random variable that has a zero-mean Gaussian distribution with a known standard deviation σ_t.

Finally, the stochastic plant model (4.1) is obtained from (4.16)-(4.18) by defining the state vector and the control vector as follows:

$$\boldsymbol{x}_t = [T_t^{\text{in}}, T_t^1, \ldots, T_t^{N-1}]^T, \boldsymbol{u}_t = [\Delta Q^{\text{Heat}_t}, \Delta Q_t^{\text{AC}}, u_t^{\text{DW}}]^T.$$

Cost Function The cost function J in (4.6) is the total energy consumption over a planning horizon, give as follows:

$$J(\boldsymbol{u}, s) = \sum_{t=1}^{N_P} \frac{\Delta Q_t^{\text{AC}}}{\eta^{\text{AC}}} + \frac{\Delta Q_t^{\text{Heat}}}{\eta^{\text{Heat}}}$$

where η^{AC} and η^{Heat} are the thermal efficiencies of the air conditioner and heater, respectively, and N_P is the number of time steps in a planning horizon.

4.6 Experimental Design

We demonstrate p-Sulu on simulations of Connected Sustainable Home. In our experiments, we assume the resident can specify one of the following three types of episodes: Home, Asleep, and Away. The temperature must be between 20 and 25°C while the resident is home, between 18 and 22°C while sleeping, and above 5°C while away to

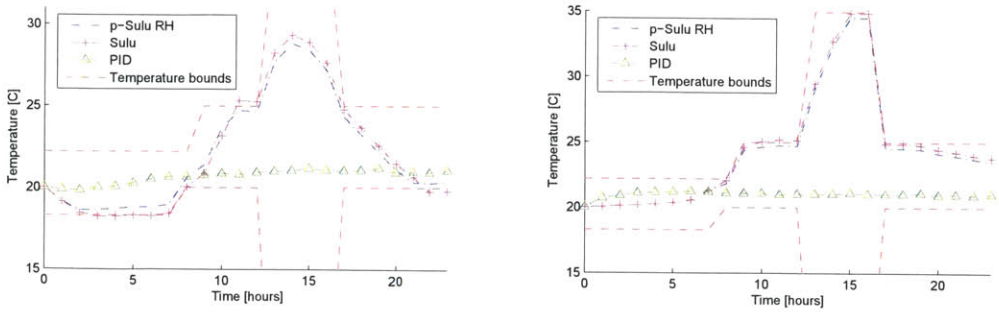

(a) January 1.

(b) July 1.

Figure 4-7: Planning results for January 1 and July 1.

ensure pipes don't freeze. We impose flexible temporal constraints and chance constraints shown in Figure 4-2. We introduce a disturbance w_t drawn from a Gaussian distribution with standard deviation $\sigma_t^{\text{in}} = 0.5°C$. p-Sulu is implemented in C++, and all trials were run on a machine with a Core i7 2.67 GHz processor and 8 GB of RAM.

We evaluate the performance of p-Sulu on the basis of both energy saved, and robustness to failure. We consider two baseline models for comparison: (a) a PID controller, and (b) Sulu, the deterministic predecessor to p-Sulu. We compare p-Sulu to the PID controller to illustrate the energy savings that comes from using a model-predictive control compared with a traditional heating controller. We then compare p-Sulu to Sulu to illustrate the robustness to failure that arises from risk-sensitive control. The setpoint of the PID controller was chosen to be 21°C, a point that is feasible in every state. For each controller, we plan according to an example resident CCQSP that spans a week. Each controller is evaluated on the basis of energy use and percentage of executions that fail due to constraint violations.

Figure 4-7 illustrates the results of a stochastic simulation over two different days in the year. Notice that Sulu plans right up to the edge of the constraints, often violating constraints when a disturbance is introduced, while p-Sulu leaves a margin.

In Table 4.1 we present the results of the stochastic simulation on the week-long scenario, averaged over 100 Monte Carlo trials each with $\Delta = 0.1$. Notice that the failure rate of p-Sulu is lower than the risk bound Δ. Out of the 400 trials of Sulu

Table 4.1: Comparison of energy use and failure rate. Values are the averages of 100 runs with randomly generated disturbances.

	Winter		Summer	
	Energy [J]	Pr(Fail)	Energy [J]	Pr(Fail)
p-Sulu	1.93×10^4	0.01	3.47×10^4	0.00
Sulu	1.65×10^4	1.00	–	1.00
PID	3.97×10^4	0.00	4.17×10^4	0.00
	Spring		Autumn	
	Energy [J]	Pr(Fail)	Energy [J]	Pr(Fail)
p-Sulu	3.37×10^4	0.00	3.81×10^4	0.00
Sulu	3.09×10^4	1.00	3.67×10^4	1.00
PID	3.98×10^4	0.00	3.99×10^4	0.00

across all seasons, 345 failed to complete due to infeasibility. Of the 55 trials that completed, every trial had constraint violations on at least 26 of the 168 time steps of the plan.

Although the PID controller did not violate any temperature constraints, the other two controllers performed drastically better in terms of energy consumption. In the winter, p-Sulu ($\Delta = 0.1$) yielded energy savings of 42.8% over the PID controller; in the spring, summer, and autumn, we saw 15.3%, 16.8%, and 4.4% savings respectively.

Planning in a risk-sensitive manner does require more energy. Compared to the Sulu runs that completed, we saw p-Sulu use 3.8% more energy in autumn, 8.9% more energy in spring, and 17.4% more energy in the winter.

Overall, our results show that p-Sulu achieves significant savings in energy compared with PID, while drastically reducing and even eliminating constraint violations compared with Sulu.

4.7 Conclusion

In this chapter, we have developed a novel risk-sensitive plan executive called p-Sulu, and applied to temperature control of Connected Sustainable Home. Simulation studies demonstrated that p-Sulu achieves as much as 42.8% energy savings over a traditional PID controller. p-Sulu exhibited drastically fewer constraint violations

than its deterministic predecessor, Sulu, under uncertainty.

Chapter 5

Joint Chance-Constrained Model Predictive Control with Probabilistic Resolvability

This chapter presents a fundamental control algorithm that can continuously operate an uncertain system, such as an electricity grid with renewable energy generations, with bounded risk. More specifically, we develop a joint chance-constrained model predictive control algorithm with *probabilistic resolvability*, which grantees the existence of feasible solutions with a given probability. Furthermore, with moderate conditions, we show that the optimization problem solved at each time step in the proposed algorithm is a convex optimization problem.

5.1 Introduction

Model predictive control (MPC), also known as receding horizon control, has been successfully applied to a range of energy-related problems, such as a building control to reduce peak electricity demand [69], power grid control [5], and AC frequency control [46]. It is distinguished from classical control approaches by its capability to explicitly consider state constraints, while optimizing a control sequence to minimize a given cost function. MPC is well suited to power grid control because a power grid

has number of constraints, such as the capacity of generation plants, substations and transmission lines, as well as bounds on the acceptable range of frequency and voltage deviations.

However, when uncertainty is present, MPC is susceptible to risk of constraint violation, since the optimal solution typically pushes against one or more constraint boundaries, and hence leaves no margin for error. When uncertainty is bounded by a compact set (i.e., roughly speaking, if there is a known upper bound on the level of uncertainty), robust model predictive control (RMPC) method can be used to provide a guarantee of solution existence, through the means of *resolvability*, also known as *recursive feasibility*. Recall that MPC computes control inputs by solving a constrained optimization problem at each time step. An MPC algorithm is resolvable if the optimization problem has a feasible solution in a future time given a feasible solution at the current time. Therefore, if one can find a feasible solution only at the initial time step, then a resolvable MPC algorithm is guaranteed to find feasible solutions at any given time in the future. Very roughly speaking, recursive feasibility can be achieved by leaving enough margin that the worst case scenario can be handled in the future.

However, in many practical cases, uncertainty is not bounded. Even if it is bounded, guaranteeing solution feasibility in the worst case scenario often results in a very conservative solution. In the case of an electricity grid, the worst case scenario is that all wind turbines and solar cells have no output at all when the energy demand is at its highest possible level. Assuming that the worst case can be bounded, one can attempt to achieve a zero probability of failure by preparing spinning reserve and stored energy, equivalent to the worst case demand. Of course, such a conservative operation is very inefficient. First of all, as we mentioned in Section 1.2, energy storage is very costly. Second of all, since conventional plants, such as gas turbines, have a minimum output level, maintaining spinning reserve requires consumption of fuel. These inefficiencies undermine the benefit of renewable energy.

A more balanced approach is to employ chance-constrained model predictive control (CCMPC) [79], which enhances efficiency by accepting a limited amount of risk.

A control input generated by CCMPC is guaranteed to satisfy a given set of constraints with a specified probability. However, existing CCMPC algorithms do *not* guarantee existence of such a control input when uncertainty is unbounded. Since a power grid is a social infrastructure that must operate *continuously*, a failure to find a feasible solution poses a serious risk to society. For example, assume a situation where grid energy storage become nearly depleted after discharging energy to compensate for unexpectedly low wind generation, at a certain point of time. Then in the next time step, CCMPC may fail to find a feasible solution that has enough back-up capacity to prepare for future uncertainty. Such a failure to find a feasible operating point can expose the consumers to an unacceptable risk of blackouts. In general, when considering an unbounded stochastic disturbance, such as (5.2), it can be impossible to guarantee resolvability, since there is a finite probability that the disturbance is large enough to make the future optimization problem infeasible.

However, although it is impossible to guarantee the existence of feasible solutions with 100% probability, resorting to a trial-and-error operation of a power grid is also unacceptable. Instead, we seek to provide a probabilistic guarantee; that is, a guarantee that feasible solutions for CCMPC exist with a certain probability, such as 99.9999%. More specifically, we define a new concept called *probabilistic resolvability*. A controller is probabilistically resolvable if there exists, with a specified probability, feasible solutions for the next n time steps, given that the state at the current time step is feasible (the formal definition of probabilistic resolvability is given in Section 5.3). A probabilistically resolvable CCMPC method will enable an electrical grid to operate with high efficiency within a given risk bound.

5.2 Related Work

This work is closely related to robust model predictive control (RMPC) with set-bounded uncertainty, which has been intensively studied over the past two decades (e.g., [50, 19, 80, 51, 1, 2, 21]). These RMPC algorithms assume that parametric and additive uncertainty are bounded in a compact set $\mathcal{W}$. Exploiting this assumption,

the RMPC algorithms compute control inputs that satisfy the given state and control constraints for *all* possible realizations of the disturbance $w \in \mathcal{W}$. Resolvability can be guaranteed by requiring that the terminal state at each horizon is within a robust control invariant set [45]. Literature on RMPC is well reviewed in [63]. For the reasons discussed earlier in this thesis, we pursue a stochastic approach to uncertainty, and employ constraint that bounds risk.

Chance-constrained MPC has recently received growing attention for its ability to handle *unbounded* uncertainty with a probability distribution, such as a Gaussian distribution. Stochastic uncertainty is a more natural model for exogenous disturbances than set-bounded uncertainty, for example, in the case of wind disturbances [9]. Schwarm et al. [79] studied an MPC method with individual chance constraints, which bound the probability of satisfying a scalar output constraint at individual time steps. Their approach transforms the individual chance constraints into equivalent deterministic constraints. Van Hessem [89] and Li et al. [60] developed a more general *joint* chance-constrained MPC method that bounds the probability of satisfying multiple constraints by using a conservative ellipsoidal relaxation. The particle control algorithm, developed by Blackmore et al. [16], approximates the joint probability by sampling. Oldewurtel et al. [67] incorporates the affine disturbance feedback approach [10] with chance-constrained MPC, in order to address the issue of conservatism in open-loop chance-constrained MPC. In our previous work [72], we presented the risk allocation approach, which reduces conservatism by optimally allocating risk bounds to individual state constraints.

Past research on chance-constrained MPC, including work reviewed above, mainly focuses on developing efficient solution methods for finite-horizon optimal control problems, while leaving the discussion of resolvability relatively undeveloped. This lack of guarantee is a significant weakness of chance-constrained MPC, compared to set-bounded RMPC. The primary purpose of the research in this chapter is to overcome this weakness.

The remainder of this chapter is organized as follows. Section 5.4 explains our overall approach. Section 5.5 presents a new joint chance-constrained MPC algorithm,

and proves its probabilistic resolvability. Section 5.6 proves the convexity of the optimization problem, and Section 5.7 presents a method to compute an ϵ-robust control invariant set, the probabilistic counterpart of the robust control invariant set. Finally, Section 5.8 presents simulation results.

5.3 Problem Statement

We consider MPC for the following discrete-time stochastic dynamics with a zero-mean additive Gaussian-distributed uncertainty:

$$x_{k+1} = Ax_k + Bu_k + Ew_k. \tag{5.1}$$

Without loss of generality, we assume that w_k has a n_w-dimensional standard Gaussian distribution:

$$w_k \sim \mathcal{N}(0, I_{n_w}), \tag{5.2}$$

where I_{n_w} is the n_w-dimensional identity matrix. We assume that w_k and w_j are independent for $k \neq j$.

We consider a state constraint $g(x) \preceq 0$, where $g(\cdot)$ is a vector-valued function and $\preceq$ is a componentwise inequality. For all time steps $k = 1, 2, \cdots$, we impose a joint chance constraint, which requires that the state constraint is satisfied with a probability $1 - \Delta$ over the next N time steps:

$$\Pr\left[\bigwedge_{\tau=k}^{k+N-1} g(x_\tau) \preceq 0\right] \geq 1 - \Delta, \ \forall k \in \mathbb{Z}^+ \tag{5.3}$$

where the constant $0 < \Delta < 1$ is a user-specified risk bound and $\mathbb{Z}^+$ is a set of positive integers. This is a more general formulation than individual chance constraints, which correspond to a special case of (5.3) with $N = 1$.

The objective of this chapter is to develop an MPC algorithm that satisfies the joint chance constraint (5.3) and has the following two properties:

1. Probabilistic Resolvability Recall that MPC computes the control inputs by solving a constrained optimization problem (i.e., a finite-horizon optimal control problem) at each time step. An MPC algorithm is resolvable if the optimization problem has a feasible solution in a future time, given a feasible solution at the current time. However, as argued earlier, when considering an unbounded stochastic disturbance, such as (5.2), it is typically impossible to guarantee resolvability, since there is a finite probability that the disturbance w_k is large enough to make the future optimization problem infeasible. Instead, we guarantee *probabilistic resolvability*, defined as follows:

Definition 1 : Probabilistic Resolvability
Let $\mathcal{P}_k$ be the optimization problem solved by a model-predictive controller at time step k. The controller is *probabilistically resolvable* if there is a positive integer n and a positive real-valued constant $0 < \alpha \leq 1$, such that $\mathcal{P}_{k+1} \cdots \mathcal{P}_{k+n}$ are feasible with a probability of at least α, given the feasibility of $\mathcal{P}_k$.

We prove that the proposed joint chance-constrained MPC algorithm is probabilistically resolvable with $n = N$ and $\alpha = 1 - \Delta$.

2. Convexity We show that, with moderate conditions, the optimization problem solved by the proposed MPC algorithm at each time step is a convex optimization problem. This result has a practical importance because a convex optimization problem can be solved in polynomial time by interior point methods.

5.4 Approach

In this section we give an informal overview of our key ideas. A formal discussion will follow in Section 5.5.

5.4.1 Risk Allocation Approach

Like p-Sulu OL presented in the previous section, out CCMPC algorithm is also build upon the risk allocation approach. However, in this chapter we give a slightly different definition of individual risk bound δ_k than in the previous sections. Here, δ_k is the upper bound on the *conditional* probability of violating state constraints at the next time step $k+1$, given the satisfaction of the constraints at the current time step k. At each time step, the proposed algorithm computes the control inputs, u_k, as well as δ_k. Later we prove that a sufficient condition of the joint chance constraint (5.3) is the following:

$$\sum_{\tau=k}^{k+N-1} \delta_\tau \leq \Delta, \quad \forall k \in \mathbb{Z}^+. \tag{5.4}$$

At each time k, the algorithm optimizes the sequence of risk allocation over the next N time steps with the above constraint. This problem can be viewed as a resource allocation problem. The available amount of resource for every N time step is limited to Δ, and the problem is to find the allocation of the resource within the horizon.

5.4.2 Probabilistic Resolvability and ϵ-Robust Control Invariant Set

As we discussed in Section 5.3, we seek to guarantee probabilistic resolvability. Most RMPC methods with set-bounded uncertainty guarantees resolvability by requiring that the terminal state at each planning horizon is within a robust control invariant set $\mathcal{R}_f$ [45], which has the following property:

$$x_k \in \mathcal{R}_f \Longrightarrow \exists \kappa(x_k) \in \mathcal{U} : x_{k+1} \in \mathcal{R}_f, \forall w_k \in \mathcal{W}.$$

In general, it is impossible to find such a robust control invariant set when w_k is unbounded.

Instead, we consider an *ϵ-robust control invariant set*, $\mathcal{R}_f(\epsilon)$, which has the fol-

lowing property for a given $0 < \epsilon < 1$:

$$\exists \kappa(x_{k+N}) \in \mathcal{U} : \Pr\left[x_{k+1} \in \mathcal{R}_f(\epsilon) \mid x_k \in \mathcal{R}_f(\epsilon)\right] \geq 1 - \epsilon.$$

In other words, if the state is within $\mathcal{R}_f(\epsilon)$, then there exists a control law $\kappa(x_{k+N})$ such that the state remains in $\mathcal{R}_f(\epsilon)$ at the next time step with at least probability $1 - \epsilon$. The proposed algorithm also requires the following:

$$\delta_k \geq \epsilon, \quad \forall k \in \mathbb{Z}^+. \tag{5.5}$$

With the above two conditions, we can guarantee probabilistic resolvability. Assume that the finite-horizon optimal control problem has a feasible solution at time k, which satisfies (5.4). Then, with probability at least $1 - \delta_k$, the solution is also feasible at time $k + 1$ with an additional control input $u_{k+N} = \kappa(x_{k+N})$ and a risk allocation $\delta_{k+N} = \epsilon$. Such a solution also satisfies the constraint (5.4) at time $k + 1$ because it follows from (5.5) that:

$$\sum_{\tau=k+1}^{k+N} \delta_\tau = \sum_{\tau=k}^{k+N-1} \delta_\tau + \epsilon - \delta_k \leq \Delta.$$

Intuitively, (5.4) is satisfied recursively because the newly added risk $\delta_{k+N} = \epsilon$ is less than δ_k, the risk that has been taken at the previous time step, as shown in Figure 5-1.

5.5 Method

5.5.1 The Algorithm

The proposed joint chance-constrained MPC algorithm is as follows.

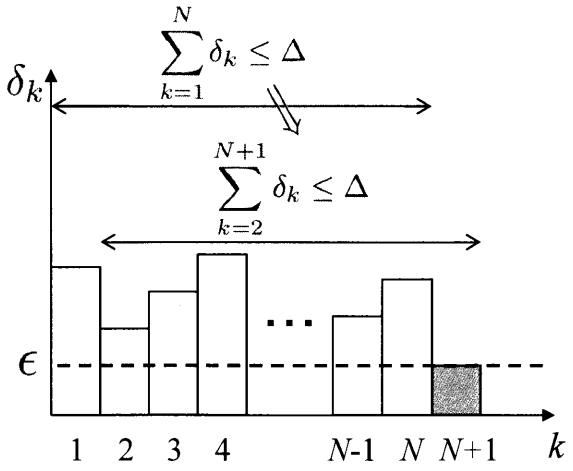

Figure 5-1: The proposed MPC algorithm requires that the terminal state is in an ϵ-robust control invariant set, so that the terminal state can stay within the set in the next time step with the probability of $1-\epsilon$. Probabilistic resolvability is guaranteed by ensuring that risk allocation to each time step is greater than ϵ.

Algorithm 4 Joint Chance-Constrained MPC

1: $k = 0$

2: $\delta_{-1} = 0,\ \delta_{-2} = 0, \cdots, \delta_{-N+1} = 0$

3: **loop**

4: Solve $\mathcal{P}_k$ with x_k and $[\delta_{k-N+1}, \delta_{k-N+2}, \cdots \delta_{k-1}]$

5: $u_k = u_{k|k}, \quad \delta_k = \delta_{k|k}$

6: Apply u_k

7: k = k+1

8: **end loop**

$\mathcal{P}_k$, the finite-horizon optimal control problem solved at k, is formulated as (5.6)-(5.12). Note that it takes two parameters: the current state x_k, as well as the risk allocated to the past $N-1$ time steps $\delta_{k-N+1}, \cdots \delta_{k-1}$. We assume that the current state x_k is known with certainty at time k. The designer of the controller chooses two constants, Δ and ϵ, so that $\epsilon \leq \Delta/N$. The optimization problem has two decision

variables: the control sequence,

$$\boldsymbol{u} := \left[u_{k|k} \cdots u_{k+N-1|k}\right],$$

and the risk allocation over the next N time steps,

$$\boldsymbol{\delta} := \left[\delta_{k|k} \cdots \delta_{k+N-1|k}\right].$$

Note that, in (5.11) below, δ_j is a given parameter that represents a past risk allocation determined in previous iterations, while $\delta_{j|k}$ is a decision variable that represents a future risk allocation.

$\mathcal{P}_k$: Finite-horizon optimal control problem

$$\min_{\boldsymbol{u},\boldsymbol{\delta}} \quad F(\bar{x}_{k+N|k}) + \sum_{\tau=k}^{k+N-1} f(\bar{x}_{\tau|k}, u_{\tau|k}) \tag{5.6}$$

$$\text{s.t.} \quad x_{\tau+1|k} = Ax_{\tau|k} + Bu_{\tau|k} + Ew_{\tau|k} \tag{5.7}$$

$$g(x_{\tau|k}) \preceq 0 \tag{5.8}$$

$$x_{k+N|k} \in \mathcal{R}_f(\epsilon) \tag{5.9}$$

$$\forall w_{\tau|k} \in \mathcal{W}(\delta_{\tau|k}), \forall \tau \in \mathbb{Z}_k^N$$

$$(C_N:) \quad \sum_{j=k}^{k+N-1} \delta_{j|k} \leq \Delta \tag{5.10}$$

$$(C_i:) \quad \sum_{j=i+k-N}^{k-1} \delta_j + \sum_{j=k}^{k+i} \delta_{j|k} \leq \Delta, \forall i \in \mathbb{Z}_1^{N-1} \tag{5.11}$$

$$u_{\tau|k} \in \mathcal{U}, \quad \delta_{\tau|k} \geq \epsilon, \quad \forall \tau \in \mathbb{Z}_k^N, \tag{5.12}$$

where

$$\mathbb{Z}_k^n = \{k, k+1, \cdots k+n-1\}.$$

For later convenience, the constraints (5.10) and (5.11) are labeled as C_i, with $i = 1 \cdots N$.

$\mathcal{W}(\delta)$ is a compact set that contains the origin in its interior and satisfies:

$$\Pr\left[w_k \in \mathcal{W}(\delta)\right] = 1 - \delta. \tag{5.13}$$

Of course, such a set $\mathcal{W}(\delta_k)$ is not unique. For now, let us assume that we can uniquely specify a set $\mathcal{W}(\delta_k)$ as a function of δ_k, with some additional conditions. In Section 5.6, we present a condition that specifies $\mathcal{W}(\delta_k)$ and guarantees the convexity of the finite-horizon optimal control problem.

In (5.9), $\mathcal{R}_f(\epsilon)$ is the ϵ-robust control invariant set. We formally define the ϵ-robust control invariant set as follows:

Definition 2 : ϵ-robust control invariant set

An ϵ-robust control invariant set, $\mathcal{R}_f(\epsilon) \subseteq \mathcal{R}$, is a closed set that has the following property:

$$x_k \in \mathcal{R}_f(\epsilon) \Longrightarrow \exists \kappa(x_k) \in \mathcal{U} : x_{k+1} \in \mathcal{R}_f(\epsilon), \forall w_k \in \mathcal{W}(\epsilon), \tag{5.14}$$

where

$$\mathcal{R} = \{x \in \mathbb{R}^{n_x} \mid g(x) \preceq 0\}.$$

We describe how to compute an ϵ-robust control invariant set in Section 5.7.

Like standard MPC, the proposed algorithm applies only the first control input $u_{k|k}$, although it computes $u_{k|k} \cdots u_{K+N-1|k}$. Hence, it takes only the risk allocated to the first time step $\delta_{k|k}$, although it computes $\delta_{k|k} \cdots \delta_{k+N-1|k}$.

A notable difference of $\mathcal{P}_k$ from existing RMPC algorithms is that the disturbance sets $\mathcal{W}(\delta_{\tau|k})$ are not fixed; they vary for different values of $\delta_{\tau|k}$. Compared to the joint chance-constrained finite-horizon optimal control developed by [15], $\mathcal{P}_k$ has three additional constraints: (5.9), (5.11), and $\delta_{\tau|k} \geq \epsilon$ in (5.12). These constraints are the key ingredient of $\mathcal{P}_k$ for guaranteeing probabilistic resolvability.

The next two subsections present the main results of this chapter.

5.5.2 Probabilistic Resolvability

In order to prove probabilistic resolvability for the proposed algorithm, we first prove the following lemma:

Lemma 3: If $\mathcal{P}_k$ has a feasible solution, then $\mathcal{P}_{k+1}$ has a feasible solution with at least probability $1 - \delta_k$.

Proof: Let $[u^\star_{k|k} \cdots u^\star_{k+N-1|k}]$ and $[\delta^\star_{k|k} \cdots \delta^\star_{k+N-1|k}]$ be a feasible solution to $\mathcal{P}_k$. Note that $\delta_k = \delta^\star_{k|k}$ (Line 5 of Algorithm 4). By definition,

$$\Pr[w_k \in \mathcal{W}(\delta_k)] \geq 1 - \delta_k.$$

We prove the lemma by showing that, if $w_k \in \mathcal{W}(\delta_k)$ is the case, then the following candidate solution is a feasible solution to $\mathcal{P}_{k+1}$:

$$[u^\star_{k+1|k} \cdots u^\star_{k+N-1|k} \ \kappa(x_{k+N|k})], \ [\delta^\star_{k+1|k} \cdots \delta^\star_{k+N-1|k} \ \epsilon].$$

If $w_k \in \mathcal{W}(\delta_k)$, then the candidate solution satisfies (5.8) in $\mathcal{P}_{k+1}$. Then it follows from (5.14) that the candidate solution also satisfies (5.9) in $\mathcal{P}_{k+1}$. The constraint C_i of $\mathcal{P}_{k+1}$ is satisfied for $i = 1 \cdots N-1$ because it is equivalent to C_{i+1} in $\mathcal{P}_k$. Finally, the satisfaction of C_N in $\mathcal{P}_{k+1}$ is implied from $\delta_k (= \delta_{k|k}) \geq \epsilon$ in (5.12) of $\mathcal{P}_k$:

$$\sum_{j=k+1}^{k+N-1} \delta^\star_{j|k} + \epsilon \leq \sum_{j=k}^{k+N-1} \delta^\star_{j|k} \leq \Delta.$$

■

The following theorem establishes probabilistic resolvability of the proposed algorithm:

Theorem 2: Probabilistic Resolvability
If $\mathcal{P}_k$ has a feasible solution, then $\mathcal{P}_{k+1} \cdots \mathcal{P}_{k+N}$ have feasible solutions with at least the probability of $1 - \Delta$.

Proof: By assumption, w_k and w_j are independent for $k \neq j$. By recursively applying Lemma 3, the probability that $\mathcal{P}_{k+1} \cdots \mathcal{P}_{k+N}$ have feasible solutions given the feasibility of $\mathcal{P}_k$ is:

$$\prod_{\tau=k}^{k+N-1} (1 - \delta_\tau) \geq 1 - \sum_{\tau=k}^{k+N-1} \delta_\tau \geq 1 - \Delta.$$

The second inequality follows from C_1 in $\mathcal{P}_{k+N-1}$. See Appendix for the proof of the first inequality. ■

5.5.3 Satisfaction of the Joint Chance Constraint

The following theorem holds:

Theorem 3: Feasibility

The Joint Chance-Constrained MPC (Algorithm 4) guarantees the satisfaction of the joint chance constraint (5.3).

Proof: Assume that $\mathcal{P}_k$ is feasible, and a solution (u_k, δ_k) is obtained at time step k. It follows from Lemma 3 and (5.8) of $\mathcal{P}_k$ that, with a probability of at least $1 - \delta_k$, $\mathcal{P}_{k+1}$ is feasible and the next state x_{k+1} satisfies the state constraints $g(x_{k+1}) \preceq 0$. By recursively applying this fact, the satisfaction of the joint chance constraint (5.3) at the time step $k + 1$ is guaranteed as follows:

$$\Pr\left[\bigwedge_{\tau=k+1}^{k+N} g(x_\tau) \preceq 0\right] \geq \prod_{\tau=k}^{k+N-1} (1 - \delta_\tau) \tag{5.15}$$

$$\geq 1 - \sum_{\tau=k}^{k+N-1} \delta_\tau \geq 1 - \Delta \tag{5.16}$$

The third inequality follows from C_1 of $\mathcal{P}_{k+N-1}$.[1] See Appendix for the proof of the

[1]Note that the constraints are tightened by bounding (5.15) with its first-order approximation, (5.16). We avoid imposing the constraint $\prod_{\tau=k}^{k+N-1}(1 - \delta_\tau) \geq 1 - \Delta$ because it is a nonconvex constraint. Alternatively, we can transform the nonconvex constraint into an equivalent convex form, $\sum_{\tau=k}^{k+N-1} \log(1 - \delta_\tau) \geq \log(1 - \Delta)$. However, we choose to use the first-order approximation (5.16) for two practical reasons. Firstly, linear constraints has an advantage in computation time. Secondly, since a very small value is chosen for the upper bound on the risk Δ in most practical applications, the approximation error is negligible.

second inequality. ■

Note that the proof of the theorem uses only C_1. Nonetheless, we need $C_2 \cdots C_N$ in order to recursively guarantee the feasibility of C_1 in the future, as shown in the proof of Lemma 3.

5.6 Convex Joint Chance-Constrained MPC

5.6.1 Conditions for Convexity

In this section, we show that $\mathcal{P}_k$ is a convex optimization problem if the following four conditions hold:

$A1$: f and F in (5.6) are convex functions.

$A2$: g in (5.8) is a convex function.

$A3$: $\mathcal{W}(\delta_k)$ is a circle with a radius r_k, defined as $\mathcal{W}(\delta_k) = \{w \in \mathbb{R}^{n_w} \mid \|w\| \leq r_k \}$.

$A4$: $r_\tau \geq \sqrt{n_w - 1}$.

Note that n_w is a dimension of w. $A1$ and $A2$ are standard assumptions. Regarding $A3$, it is common to assume that $\mathcal{W}$ is an ellipsoid (e.g., [2, 89, 11]). Since we assume standard Gaussian distributions as in (5.2), the level set of the probability distribution is a circle.

Compared to $A1$-$A3$, $A4$ would be an unfamiliar condition, but it plays a central role in proving the convexity. It requires that the radius of the disturbance sets is more than $\sqrt{n_w - 1}$. It turns out that $A4$ is a very mild condition. Since r_k is a monotonically decreasing function of δ_k, $A4$ is equivalent to imposing an upper bound on δ_k. The corresponding upper bound on δ_k is 0.61 for $n_w = 2$, 0.57 for $n_w = 3$, and 0.56 for $n_w = 4$. In practical applications the risk bound Δ is set to a very small value, typically below 1%. Therefore, $A4$ does not make the constraints tighter at all in most cases.

With regarding to $A2$, we approximate the convex constraint $g(x) \preceq 0$ by a set of linear constraints $Hx \preceq g$. Although our discussion below assumes this linear approximation, $\mathcal{P}_k$ is convex for a general convex function g because Pontryagin difference preserves convexity. Similarly, we approximate the ϵ-robust invariant control set $\mathcal{R}_f(\epsilon)$ by a set of linear constraints, $H_\epsilon x \preceq g_\epsilon$.

5.6.2 Convex Reformulation of $\mathcal{P}_k$

With $A1$-$A4$ and the linear approximation of g, we reformulate $\mathcal{P}_k$ as below. Note that the optimization problem involves the mean state $\bar{x}_{\tau|k}$, instead of $x_{\tau|k}$. We denote $\boldsymbol{r} := [r_{k|k}\ r_{k+1|k} \cdots r_{k+N-1|k}]^T$.

$\mathcal{P}'_k$: Convex finite-horizon optimal control problem

$$\min \quad F(\bar{x}_{k+N|k}) + \sum_{\tau=k}^{k+N-1} f(\bar{x}_{\tau|k}, u_{\tau|k}) \tag{5.17}$$

$$\text{s.t.} \quad \bar{x}_{\tau+1|k} = A\bar{x}_{\tau|k} + Bu_{\tau|k}, \quad \forall \tau \in \mathbb{Z}_k^N \tag{5.18}$$

$$H\bar{x}_{\tau|k} \preceq g - \Phi_H^\tau \boldsymbol{r}, \quad \forall \tau \in \mathbb{Z}_{k+1}^{N-1} \tag{5.19}$$

$$H_\epsilon \bar{x}_{k+N|k} \preceq g_\epsilon - \Phi_{H_\epsilon}^{k+N} \boldsymbol{r} \tag{5.20}$$

$$\sum_{j=k}^{k+N-1} \delta_{j|k} \leq \Delta \tag{5.21}$$

$$\sum_{j=\tau-N+1}^{k-1} \delta_j + \sum_{j=k}^{\tau} \delta_{j|k} \leq \Delta, \quad \forall \tau \in \mathbb{Z}_k^{N-1} \tag{5.22}$$

$$\delta_{\tau|k} \geq \xi_{n_w}(r_{\tau|k}), \quad \forall \tau \in \mathbb{Z}_k^N \tag{5.23}$$

$$r_{\tau|k} \geq \sqrt{n_w - 1}, \quad \forall \tau \in \mathbb{Z}_k^N \tag{5.24}$$

$$u_{\tau|k} \in \mathcal{U}, \quad \delta_{\tau|k} \geq \epsilon, \quad \forall \tau \in \mathbb{Z}_k^N \tag{5.25}$$

In (5.19) and (5.20), Φ_H^τ is an n_H-by-N matrix, where n_H is the number of rows in H. The element of Φ_H^τ at the ith row and jth column is:

$$\Phi_{H,ij}^\tau = \begin{cases} \|h_i A^{\tau-k-j} E\| & (j \leq \tau - k) \\ 0 & (\text{Otherwise}) \end{cases},$$

where h_i is the ith row vector of H. Such a matrix Φ_H^τ is obtained as follows. First, we recursively define a sequence of sets $\mathcal{X}_k, \mathcal{X}_{k+1}, \cdots$ as follows.

$$\mathcal{X}_k = \{x_k\}, \quad \mathcal{X}_{\tau+1} = A\mathcal{X}_1 \oplus B\{u_\tau\} \oplus E\mathcal{W}(\delta_\tau),$$

where $\oplus$ is a Minkowski sum. The Minkowski sum $\oplus$ of two sets, $\mathcal{A}, \mathcal{B} \in \mathbb{R}^n$, is defined as:

$$\mathcal{A} \oplus \mathcal{B} := \{x \in \mathbb{R}^n \mid \exists a \in \mathcal{A}, b \in \mathcal{B} \ : \ x = a + b\}.$$

By recursively applying the above equation and (5.18), we obtain:

$$\mathcal{X}_\tau = \{\bar{x}_\tau\} \oplus \sum_{j=1}^{\tau-k} A^{\tau-k-j} E\mathcal{W}(\delta_{k+j-1}).$$

In order to satisfy the state constraints with the specified risk bound, $\mathcal{X}_\tau$ must be included in the feasible state region, as shown in Figure 5-2. Note that $\mathcal{W}(\delta_\tau)$ is a circle with radius r_τ. Hence, by using the triangle inequality, a sufficient condition for satisfying the ith constraint is obtained as follows:

$$h_i \bar{x}_{\tau|k} \leq g - \sum_{j=1}^{\tau-k} \|h_i A^{\tau-k-j} E\| r_j.$$

Constraints (5.19) and (5.20) are equivalent to the above inequality. Roughly speaking, when $\|h_i\| = 1$, $\Phi_H^\tau \boldsymbol{r}$ specifies the distance between a constraint boundary and the mean state that is sufficient to guarantee the risk bound δ_τ, as shown in Figure 5-2.

The constraint (5.23) relates $r_{\tau|k}$ to $\delta_{\tau|k}$. The function $\xi_{n_w}(r)$ is obtained by solving the following equation [89]:

$$\begin{aligned} 1 - \xi_{n_w} &= \int_{w \in \mathcal{W}(\delta)} p_{n_w}(w) dw \\ &= \frac{1}{2^{n_w/2}\Gamma(n_w/2)} \int_0^{r^2} x^{n_w/2-1} e^{-x/2} dx, \end{aligned} \tag{5.26}$$

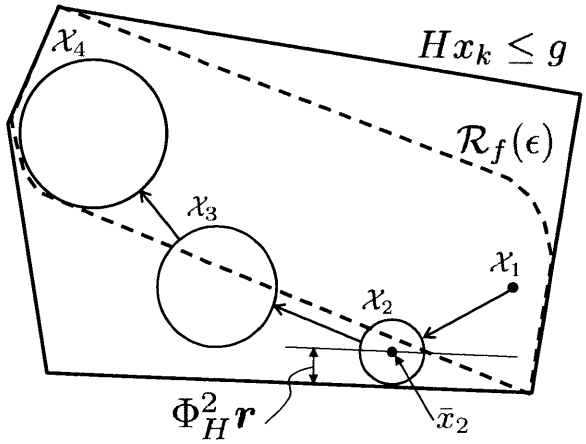

Figure 5-2: Illustration of the convex joint chance-constrained MPC. With an assumption that $\mathcal{W}(\delta_\tau)$ is a circle, the distance between a constraint boundary and the mean state that is sufficient to guarantee the risk bound δ_τ is obtained analytically.

where $p_{n_w}(\cdot)$ is the probability density function of the n_w-dimensional standard Gaussian distribution. This integral can be analytically computed for a given n_w. For example, the closed-form expressions for $\xi_{n_w}(r)$ with $n_w = 1 \cdots 4$ are listed below:

$$\begin{aligned} \xi_1(r) &= 1 - \mathrm{erf}\left(\frac{r}{\sqrt{2}}\right) \\ \xi_2(r) &= e^{-r^2/2} \\ \xi_3(r) &= 1 - \mathrm{erf}\left(\frac{r}{\sqrt{2}}\right) + \frac{re^{-r^2/2}}{2^{1/2}\Gamma(3/2)} \\ \xi_4(r) &= \frac{1}{2}(r^2+2)e^{-r^2/2}, \end{aligned} \tag{5.27}$$

where $\mathrm{erf}(\cdot)$ is the Gauss error function and Γ is the Gamma function.

5.6.3 Proof of Convexity

The following theorem holds:

Theorem 4: Convexity

$\mathcal{P}'_k$ is a convex optimization problem.

Proof: Since all constraints in $\mathcal{P}'_k$ are linear except for (5.23), it suffices to show that $\xi_{n_w}(r)$ is convex. Note that the domain of r is restricted to $r \geq \sqrt{n_w - 1}$ by

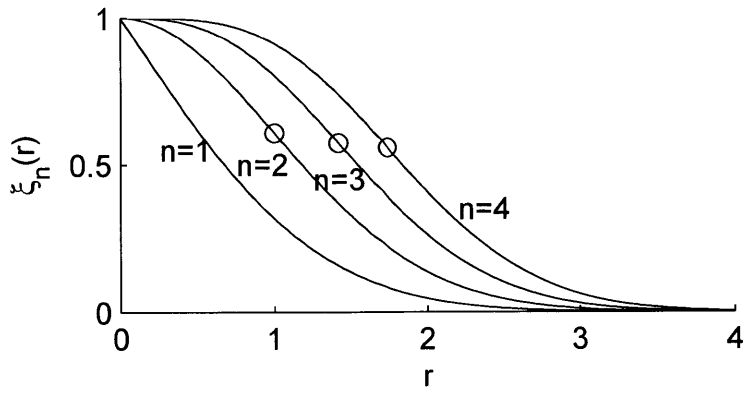

Figure 5-3: Plots of $\xi_{n_w}(r)$. The inflection points are marked by the circles. The constraint (5.24) limits the domain of r to the left of the inflection points.

(5.24). The second-order differential of $\xi_{n_w}(r)$ is obtained from (5.26) as follows:

$$\frac{d^2\xi_{n_w}}{dr^2} = 2(r^2 - n_w + 1)r^{n_w-2}e^{-r^2/2}.$$

Therefore, $\frac{d^2\xi_{n_w}}{dr^2} \geq 0$, and hence $\xi_{n_w}(r)$ is convex, for $r \geq \sqrt{n_w - 1}$. ■

Figure 5-3 shows the plots of $\xi_{n_w}(r)$ for $n_w = 1 \cdots 4$. Observe that the inflection points are at $r = \sqrt{n_w - 1}$.

5.7 Computation of ϵ-Robust Control Invariant Set

We next present a method for computing an ϵ-robust control invariant set.

In set-bounded RMPCs, a robust control invariant set can be efficiently computed by using an iterative method developed by Kerrigan [45]. The same method can be used to compute an ϵ-robust control invariant set $\mathcal{R}_f(\epsilon)$, by replacing the bounded set $\mathcal{W}$ with $\mathcal{W}(\epsilon)$ for a fixed ϵ. In order to use Kerrigan's method, it is more convenient if $\mathcal{W}(\epsilon)$ is a polytope rather than a circle, as assumed in $A3$.

From here, we explain how to find such a polytope. Let L be an n_L-by-n_w matrix, and set

$$\mathcal{W}(\delta) = \{w \in \mathbb{R}^{n_w} \mid Lw \preceq m\}.$$

We denote by L_i and m_i the ith row vector of L and ith element of m, respectively. We choose L_i so that $\mathcal{W}(\delta)$ is a closed set. Without loss of generality, we can assume that:

$$\|L_i\| = 1.$$

We also assume that $m_i \geq 0$, so that the origin point is included in $\mathcal{W}(\delta)$. With these assumptions, the following is a sufficient condition for $\delta \leq \epsilon$:

$$\sum_{i=1}^{n_L} \xi_1(m_i)/2 = \epsilon,$$

where ξ_1 is defined as (5.27). This condition is derived from Boole's inequality, and is closely related to the risk allocation approach presented in [72]. Typically, we choose m_i uniformly so that $\xi_1(m_i)/2 = \epsilon/n_L$, while choosing L so that $\mathcal{W}(\epsilon)$ is a regular polytope.

When both the feasible state space and $\mathcal{W}(\epsilon)$ are polytopes, the ϵ-robust control invariant set obtained by a finite number of iterations of Kerrigan's method is also a polytope. Such an ϵ-robust control invariant set can be directly used for (5.20).

5.8 Simulation Results

We demonstrate the proposed algorithm with a 2-D point-mass double-integrator plant with position uncertainty:

$$A = \begin{pmatrix} 1 & 0 & 1 & 0 \\ 0 & 1 & 0 & 1 \\ 0 & 0 & 1 & 0 \\ 0 & 0 & 0 & 1 \end{pmatrix}, B = \begin{pmatrix} 1/2 & 0 \\ 0 & 1/2 \\ 1 & 0 \\ 0 & 1 \end{pmatrix}, E = \begin{pmatrix} 0.1 & 0 \\ 0 & 0.1 \\ 0 & 0 \\ 0 & 0 \end{pmatrix}$$

We impose state constraints requiring that the position is within a square with its corners at $(5, 5)$, $(5, -5)$, $(-5, -5)$, and $(-5, 5)$. The control constraint is given by

$\|u_k\|_\infty \leq 1$. We use quadratic terminal and step costs:

$$F = \bar{x}_{k+N|k}^T P \bar{x}_{k+N|k}, \quad f_\tau = \bar{x}_{\tau|k}^T Q \bar{x}_{\tau|k} + u_{\tau|k}^T R u_{\tau|k},$$

where $Q = 10^{-4} \cdot I_4$ and $R = I_2$, with I_n being the n-dimensional identity matrix. We obtain the P matrix by solving the algebraic Riccati equation with Q and R. We set Q significantly smaller than R in order to make the finite-horizon optimal control problem nontrivial; since the controller tries to minimize the control inputs, optimal solutions tend to push against state constraint boundaries, making the chance constraints active.

Figure 5-4 shows simulation results with $N = 10$, $\epsilon = 10^{-5}$, and four different values of Δ. In all four cases, the proposed control algorithm successfully guides the states towards the origin point without violating the state constraints. Since the system is continuously subjected to disturbances, the states do not strictly converge to the origin. Figure 5-5 shows the risk allocation δ_k at the first 20 time steps with $\Delta = 0.1$. It allocates larger risk at the beginning in order to allow the state to go close to the state boundary so that the control effort is minimized.

Table 5.1 shows the total step cost for 10 time steps, $\sum_{k=1}^{10} f_k$, with different settings of Δ and ϵ. The values shown in the tables are the averages and the standard deviations of 100 simulations for each case with random initial conditions. The average computation time of the 1,200 simulations is 0.167 sec per step, and the maximum is 1.58 sec per step.

The table shows a tendency towards increasing cost as the risk bound Δ decreases. This is because the control algorithm becomes more risk-averse with smaller Δ. As shown in Figure 5-4, with smaller Δ, the control algorithm keeps the state away from the boundaries with larger margin by applying stronger control, which results in greater cost. Hence, the designer of the controller can conduct a trade-off between risk-aversion and efficiency by choosing Δ.

A choice of ϵ influences the cost in two ways. On the one hand, with a smaller ϵ, the constraint $\delta_{\tau|k} \geq \epsilon$ in (5.25) is relaxed, allowing more flexibility in risk allocation.

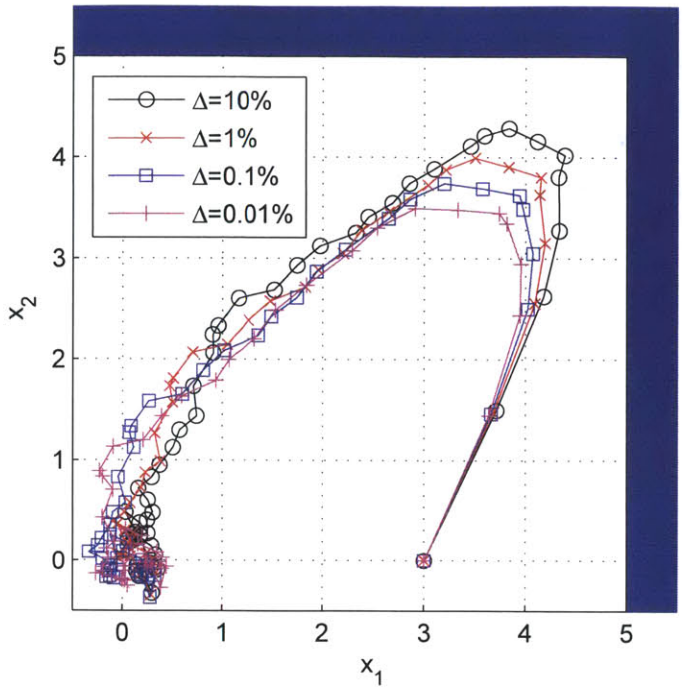

Figure 5-4: Simulation results of the proposed joint chance-constrained MPC with various risk bounds.

This is why $\epsilon = \Delta/10N$ results in less cost than $\epsilon = \Delta/N$. On the other hand, a smaller ϵ results in a smaller ϵ-robust invariant control set, making (5.20) tighter. This explains the slight increase in observed cost at $\epsilon = \Delta/100N, \Delta = 0.0001$, compared with $\epsilon = \Delta/10N, \Delta = 0.0001$. From Table 5.1 it appears that a good rule of thumb is to set $\epsilon = \Delta/10N$.

Table 5.1: The averages and the standard deviations of the total costs for different settings of Δ and ϵ. For each cases, 100 simulations are conducted with random initial conditions.

	$\epsilon = \Delta/N$	$\epsilon = \Delta/10N$	$\epsilon = \Delta/100N$
$\Delta = 0.1$	1.30 ± 0.46	1.28 ± 0.45	1.28 ± 0.45
$\Delta = 0.01$	1.42 ± 0.48	1.40 ± 0.47	1.40 ± 0.47
$\Delta = 0.001$	1.52 ± 0.50	1.50 ± 0.50	1.50 ± 0.50
$\Delta = 0.0001$	1.62 ± 0.52	1.608 ± 0.518	1.609 ± 0.518

Finally, in order to demonstrate probabilistic resolvability, we run the 10 time-

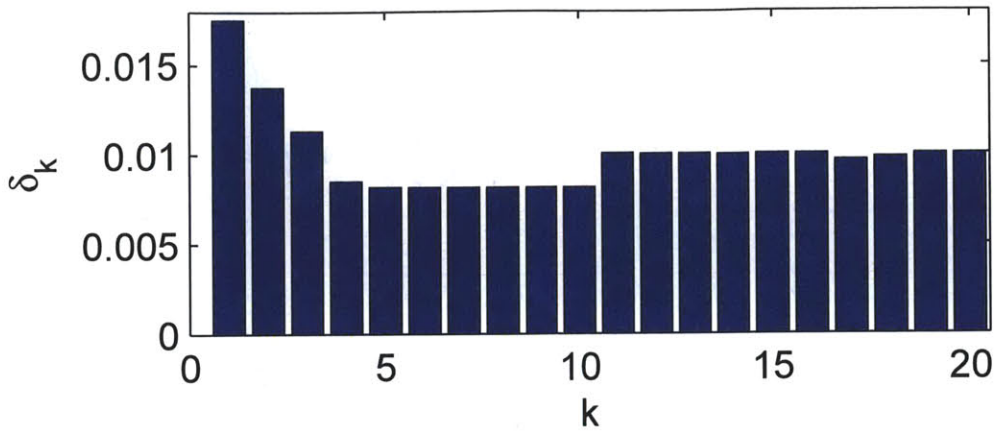

Figure 5-5: Resulting risk allocation with $\Delta = 0.1$.

step simulation 10,000 times, with $\Delta = 0.5$, $\epsilon = 0.005$, and $N = 10$. The initial state is chosen randomly. Out of the 10,000 runs, there are five unsuccessful runs where the finite-horizon optimal control problem becomes infeasible or the solution violates the state constraints. The 0.05% failure rate is lower than the specified risk bound, 50%, by a large margin. This result demonstrates the probabilistic resolvability of the proposed joint chance-constrained MPC algorithm, as predicted by the theory. However, it also means that the algorithm is overly conservative. Our future work is to develop a less conservative algorithm while guaranteeing probabilistic resolvability.

5.9 Conclusions

In this chapter we defined probabilistic resolvability, and developed a joint chance-constrained MPC approach that guarantees probabilistic resolvability. Establishing probabilistic resolvability requires that 1) the terminal state be in an ϵ-robust control invariant set, and 2) the risk allocated at each time step be greater than ϵ. We have also shown that, with moderate conditions, the finite-horizon optimal control problem of out MPC approach can be implemented as a convex optimization problem.

Appendix

The following bound is used in the proofs of Theorems 1 and 2:

$$\prod_{i=1}^{N}(1-\delta_i) \geq 1 - \sum_{i=1}^{N}\delta_i \quad (0 \leq \delta_i \leq 1, \forall i) \tag{5.28}$$

This inequality can be proved by induction as follows: *Proof:* It is trivial when $N = 1$. When (5.28) holds for $N = k$, it also holds for $N = k + 1$ because:

$$\begin{aligned}\prod_{i=1}^{k+1}(1-\delta_i) &\geq \left(1 - \sum_{i=1}^{k}\delta_i\right)(1-\delta_{k+1}) \\ &= 1 - \sum_{i=1}^{k+1}\delta_i + \left(\sum_{i=1}^{k}\delta_i\right)(\delta_{k+1}) \geq 1 - \sum_{i=1}^{k+1}\delta_i.\end{aligned}$$

■

Chapter 6

Policy Analysis

As we discussed in Chapter 1, a major technical challenge for a smart grid barrier is the uncertainty in renewable generation, climate, and human behaviors. Chapters 3 to 5 developed a decentralized risk-sensitive control system that can overcome this technical challenge. However, various social obstacles, such as lack of economic incentive, overregulation, and conflict of interest, can also prevent the implementation of smart grid technologies. While the role of technologies are to *enable* a higher level of renewable penetration into a grid, it is the role of policy to *realize* it by removing these obstacles. We first discuss in Section 6.1 the connection between policy and smart grid, with a particular focus on what policy is necessary to implement the proposed risk-sensitive control system. Then in Sections 6.2 and 6.3, we discusses key policy challenges and options that will enable our proposed risk-sensitive control technologies to be fully utilized. Specifically, we discuss the need for deregulation, as well as available policy options, by considering specific cases in Europe, Japan, and the U.S.

6.1 Policy Needs for Decentralized Risk-Sensitive Control of a Smart Grid

Recall that the proposed control system in Chapters 3 - 5 are distributed and risk-sensitive. The distributed architecture allows efficient and robust operation of a smart grid, while the risk-sensitive capability allows for a high penetration of renewables. However, traditional electrical grids are operated in a centralized manner by vertically-integrated power providers. Moreover, since the cost of renewable energy is higher than that of conventional energy in general, lack of economic incentive prevents penetration of renewables into a grid. In this section, we discuss the policy needed to deploy the proposed decentralized risk-sensitive control approach. More specifically, we discuss the need to decentralize the grid's operation, as well as the need to provide economic incentive for renewables.

6.1.1 Decentralization

Traditional electrical grids are centralized in two senses: vertical integration and one-way power distribution. We provide an overview of these two areas in this subsection.

Vertical integration

The proposed control system dispatches nominal and contingent power in a *distributed* manner through a market-based mechanism, as discussed in Chapter 3. Such a distributed system can achieve economic efficiency through competition. In contrast, traditional electrical grids are centralized, in the sense that they are typically operated by vertically integrated power providers. A vertically integrated power provider owns and operates all power plants within a region, as well as transmission and distribution networks. It behaves as a centralized decision maker, deciding the outputs of the plants as well as the power flow in the networks.

In the past two decades, electrical grids have become increasingly decentralized, particularly in the U.S. and in Europe. In contrast, in Japan, electrical grids are

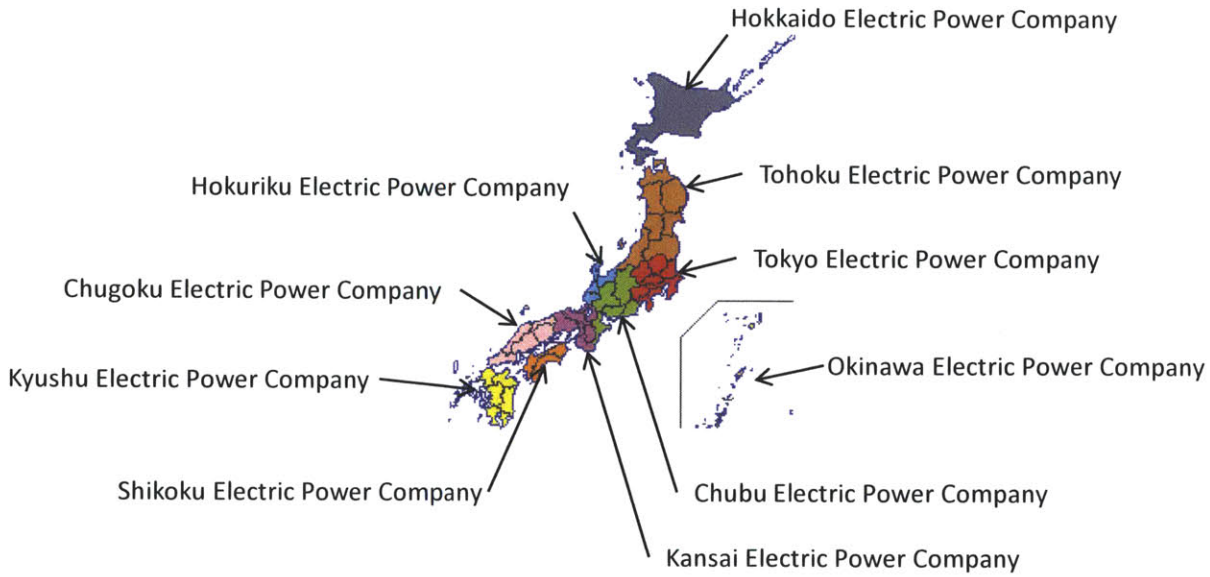

Figure 6-1: Vertically-integrated power companies in Japan

still operated mostly by vertically integrated power companies. As shown in Figure 6-1, there are ten vertically-integrated power companies in Japan, each of which is solely responsible for generation, transmission, and distribution within the designated region. Although the partial deregulation in 2005 introduced a market-based power dispatch at the newly established Japan Electric Power Exchange (JEPX), only 0.2% of the total electricity consumed in Japan was traded in JEPX in 2006[1]. In order to implement the proposed distributed control system, deregulation policy is necessary in order to allow distributed power production and market-based power exchange. We discuss this issue in detail in Section 6.2.3.

One-way power distribution

As we introduced in Section 1.1.2, each Connected Sustainable Home has its own generation capability through various power sources, such as the use of solar cells, micro combined heating and power (micro-CHP), and bio-mass. We envision a com-

[1] *Denryoku Jiyuuka no Seika to Kadai.* Satoshi Yamaguchi. 2007. National Diet Library Issue Brief Number 595 (2007. 9. 25).

munity of Connected Sustainable Homes that are connected to each other through a micro grid in order to maximize the overall energy efficiency of the community by exchanging power. In such a community, each Connected Sustainable Home is both a supplier and a consumer of electricity.

In contrast, current electricity distribution networks are designed as "one-way streets", where households are consumers who always buy electricity from centralized suppliers. For example, in Japan, local power interchange between households is prohibited by law. Therefore, again, deregulation of electricity distribution system is a key to realizing the distributed risk-sensitive control system. We discuss this matter in detail in Section 6.2.1.

6.1.2 Economic Incentives for Renewables

In Chapters 3 and 5 we develop risk-sensitive control algorithms that overcome a technical barrier of introducing renewables to a grid. However, there is also an economic barrier that must be overcome. More specifically, without any adequate policy to provide economic incentive, renewable energy production can hardly be competitive with conventional energy due to its relatively high production cost. For example, in the U.S., average levelized cost of conventional electricity is typically below \$100/MWh. According to [87], the estimated levelized cost in the U.S. in 2009 was \$66.1/MWh for conventional combined cycle gas and \$94.8/MWh for conventional coal. Although on-shore wind generation has competitive cost of \$97.0/MWh, the cost of off-shore wind power (\$243.2/MWh) and Solar PV (\$210.7/MWh) are significantly higher than conventional energies. Moreover, the cost structure of renewables are characterized by the large proportion of capital cost. For example, out of the \$97.0/MWh cost of on-shore wind, \$83.9/MWh is capital cost. This requirement for a large capital cost is another barrier to investment in new renewable generation facilities. Therefore, it is necessary to implement policies that create economical incentives, along with the implementation of risk-sensitive control technologies, in order to achieve high penetration of renewables. Available policy options are discussed in detail in Section 6.3. Additionally, existing regulations can also be a barrier to renewable penetration. We

discuss such regulations in Section 6.2.2.

6.2 Deregulation

Each nation has a legal system that regulates the operation of their electrical grid. As we discussed in the previous section, these regulatory systems were often designed decades ago, when electrical grids were operated by vertically-integrated power providers, who generate and deliver electricity in a centralized manner. In contrast, a fundamental principle of a smart grid is to achieve energy efficiency through *decentralized* operation of the grid, such as the market-based contingent energy dispatch algorithm proposed in Chapter 3. Hence, deregulation is key to realizing the vision of a smart grid. In this section we discuss the advantages and risks of deregulation by studying cases in Japan and the U.S.

6.2.1 Regulation of Distributed Generation and Transmission in a Micro-grid in Japan

Recently, a concept for a regional-scale smart grid, called a micro-grid, has been proposed [54, 92]. Micro-grids achieve energy efficiency by allowing flexible power interchange between individual residential and commercial buildings with small-scale generators, such as micro-CHPs (combined heat and power) and rooftop solar cells [39]. However, such local power interchange between individual buildings is restricted by a regulatory system in Japan[2]. Specifically, provisions of the Electricity Business Act[3] restrict energy distribution by unlicensed providers. The provisions also require stability in voltage amplitude and frequency, which imposes restrictions on reverse power flow and power interchange. By 2000, only ten companies had been licensed to sell electricity to households in Japan. A revision of the Electricity Business Act

[2] *Chiiki EMS Kadai Chousa Houkokusho* (Report on Regional Energy Management System). 2011. Kyushu Bureau of Economy, Trade and Industry. Available on-line at `http://www.kyushu.meti.go.jp/report/1104_ems/all.pdf` (Japanese, retrieved on Jan 11, 2012)

[3] *Denki Jigyou Hou*, Act No. 170 of July 11, 1964. English translation of the law is available at `http://eiyaku.hounavi.jp/eigo/s39a17001.php`. (Retrieved on Jan 11, 2012.)

in 2000 opened the electricity market for new energy providers, called Power Producer and Suppliers (PPSs). However, this deregulation does not allow market-based power interchange in a micro-grid because PPSs are allowed to sell electricity only to commercial-scale utility customers that consume more than 50 kW. Due to such restrictions, there are only 49 PPSs in Japan, as of January 5, 2012[4]. Currently, individual buildings with solar cells can sell energy to electricity companies by making a special contract. However, direct exchange of power between individual buildings is restricted. Therefore, in order to utilize micro-grid's capability to achieve energy efficiency, electricity retail market must be fully deregulated to allow power interchange between households.

6.2.2 Restrictions on the Construction of Wind Farms in Japan

Due to geographical limitations and concentrated population, suitable sites for wind farms are very limited in Japan. Two prospective locations for future large-scale wind farms are the ocean and national parks. However, both involve conflicts of interests between stakeholders.

Fishery Rights Offshore wind farms have been successfully deployed in a large scale in Europe, most notably in the U.K. and Denmark. However, such a large-scale introduction of offshore wind turbines is difficult in Japan partially because of conflict with fishery rights. For historical reasons, fisheries have strong legal rights over the use of ocean area around Japan. Specifically, the Fishery Act[5] grants licensed fishery unions an exclusive right to operate fishery business within designated water areas. Any activities that may cause loss to the fishery business are restricted.[6] Therefore, construction of an off-shore wind farm requires permission from the licensed fishery

[4]The list of PPSs are available at `http://www.enecho.meti.go.jp/denkihp/genjo/pps/pps_list.html`.

[5]*Gyogyou Hou*, Act No. 267 of 1949, revised most recently by Act No. 77 of 2007.

[6]Another area that is restricted by fishery rights is space development; since a rocket launch requires a large ocean area to be prohibited for safety reasons, it conflicts with the fishery rights. As a result, the number of annual launches from the Tanegashima Space Center in Japan is limited.

union, as well as compensation for their loss. Although fishery is still an important industry in Japan, such a biased distribution of rights over the use of ocean area must be adjusted in order to support sustainable development.

Preservation of the Local Environment in National Parks Suitable sites for wind generation are often located in national parks and quasi-national parks, which together cover about 9% of the land area in Japan. The Natural Parks Act[7] restricts activities that impair the scenery and harm the ecosystem of the parks. Construction of wind generators in national and quasi-national parks are subject to the regulation since they may impair the scenery of the parks and affect the ecology of birds. Although the law does not explicitly prohibit the construction of wind generators, ambiguities in the provisions, such as the definition of "impairing the scenery," had been an obstacle. These ambiguities was resolved in 2004 by the guideline published by the Ministry of the Environment[8]. The guideline rules prohibit the constructions of wind generators in Special Protection Zones and Class I Special Zones[9] in the parks, while permitting the constructions in Class II and III Special Zones with several restrictions.

6.2.3 Risk of Deregulation: California Electricity Crisis

Although deregulation can result in enhanced energy efficiency by allowing flexible operation of a grid and by removing obstacles to renewable energy production, it can also undermine the reliability of an electrical grid. The California Electricity Crisis, which occurred from 2000 to 2001 highlights the inherent risk of deregulation. California Assembly Bill No. 1980, passed by the State of California in 1996, promoted electricity deregulation in order to enhance competition and improve cost efficiency

[7]Shizen Kouen Hou, Act No. 161 of 1957, revised most recently by Act No. 47 of 2010.

[8]*Final report by the Kokuritsu, Kokutei Kouen-nai ni okeru Fuuryoku Hatsuden Shisetsu Secchi no Arikata ni Kansuru Kentoukai* (Committee on the Construction of Wind Generation Facilities in National and Quasi-National Parks). 2004. Available on-line at `http://www.env.go.jp/nature/wind_power/index.html` (Japanese).

[9]The area of each national and quasi-national park is divided into four categories of Special Zone that determine the degree of protection: Special Protection Zone, Class I Special Zone, Class II Special Zone, and Class III Special Zone.

[29]. The bill encouraged investor-owned utilities (IOUs) to sell their generation assets to independent power producers (IPPs), in an attempt to dismantle a vertically-integrated monopoly. It also deregulated the wholesale price of electricity. This means that the wholesale price is decided in a market. To protect consumers from price fluctuations and power shortages, the Bill included two regulations. First, the retail price of electricity was capped at the pre-deregulation level (6.7 cents per kWh), while the wholesale price cap was removed. Second, utility companies were required by law to meet demand by buying electricity from the wholesale market when faced with imminent power shortages.

This partial deregulation policy, which was intended to protect consumers from unregulated competition in the wholesale market, backfired. IPPs gained bargaining power in the wholesale market since the utility companies had to purchase electricity at any price to meet demand. This was price inelastic since the retail price was capped. The IPPs took advantage of this situation to manipulate the wholesale price by "economic withholding and inflated price bidding," [29] meaning that they suppressed the output level in order to raise the wholesale price. The Federal Energy Regulatory Commission (FERC) reported that Enron and other companies employed trading strategies that "violated the anti-gaming provisions of their FERC-approved tariffs." [29] The wholesale price, which had been kept below $50 per MWh, surged above $200 per MWh in 2000, as shown in Figure 6-2 [20]. Due to the resulting electricity shortage, the state experienced multiple large-scale blackouts, one of which affected 1.5 million people.

This case illustrates the uncertain nature of electricity deregulation. Despite the expectations of policymakers that the deregulation would decrease the price of electricity due to enhanced competition, it resulted in a price surge. The regulations placed on the utility companies, which were intended to avoid electricity shortages contributed to the large-scale blackouts.

As illustrated in this case, although deregulation is mandatory to deploy smart grid technologies, such as the risk-sensitive controllers presented in this thesis, deregulation policy must be carefully designed in order to avoid catastrophic market failure.

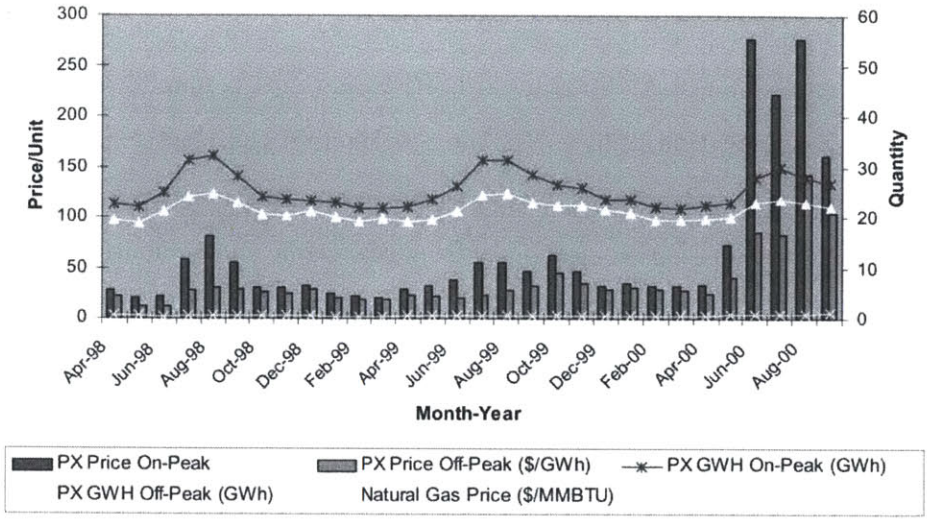

Figure 6-2: Monthly average of hourly PX day-ahead unconstrained prices in California, as well as the market clearing GWh by time-of-use (TOU) and monthly average of daily natural gas prices. The electricity price surged in 2000, although both the demand (PX GWH On-Peak and Off-Peak) and gas price where almost constant. Source: Woo, 2001 [20].

6.3 Policy Options to Enhance Renewable Energy

In Chapters 3 and 5, we presented risk-sensitive control algorithms that can allow high penetrations of renewables. Deregulation policies discussed in the previous section removes legal barriers to introducing renewables to a grid. However, since the price of renewable energy is relatively higher than conventional energy, profitability is an issue. Even if technologies and lows allow renewables to be connected to a grid, this economic barrier must be overcome to realize a large-scale introduction of renewables. Two major policies that are widely employed to accelerate investment in renewable energy technologies are a renewable portfolio standard (RPS) and a feed-in tariff (FIT). This section gives an overview of the mechanism of these two policies and discusses their advantage and disadvantages.

6.3.1 Renewable Portfolio Standard

The idea of a renewable portfolio standard (RPS) is to set a mandatory goal for renewable energy penetration, and to let the market find the least expensive way to achieve that goal [49]. It typically places an obligation on electricity suppliers to produce a specified fraction of their electricity from renewable energy sources. In order to motivate compliance, it imposes penalties on companies that fail to reach the specified targets. Many RPS programs have associated renewable energy certificate (REC; also known as green certificate) trading programs. A tradable certificate is granted to an electricity supplier for each unit of power generated by qualified renewable energy sources. Electricity suppliers that encounter difficulty increasing renewable generation can buy RECs from other suppliers who have less difficulty introducing renewables. This market mechanism can minimize the overall cost to achieve the RPS target. As of May 2009, 24 U.S. states and the District of Columbia have RPS policies in place[10]. Together these states account for more than half of the electricity sold in the United States[11].

Pros and Cons of RPS An advantage of RPS is that the price of renewable energy is automatically adjusted by an REC market. Hence, under the assumption of perfect market conditions this system should lead to the lowest renewable electricity generation cost at the target level of penetration [36]. However, choosing a reasonable target level is not a simple task since future technology development is difficult to predict, hence the extent of possible renewable penetration becomes unpredictable. If the target is too ambitious it imposes unaffordable costs on electricity suppliers through penalties; on the other hand, if it is set too low, RPS would fail to enhance the introduction of renewable energies. For example, the Japanese RPS program seems to have set a low target: it required 11,015 GWh of renewable production in 2010, accounting for only 1.2% of the total electricity consumption that year [12]. The

[10]Database of State Incentives for Renewable Energy (DSIRE)

[11]Web page of U.S. Department of Energy. Retrieved from `http://apps1.eere.energy.gov/states/maps/renewable_portfolio_states.cfm` on January 14, 2012.

[12]According to the statistics published by the Federation of Electric Power Companies of Japan, the total energy demand in 2010 was 9064,2000 GWh. The data is available on-

fact that this RPS goal was too easy is evident from the low market price of REC in Japan; it was just 5.2 Japanese Yen per kWh in 2010[13], which is about half the retail price of electricity. This price is considerably lower than other countries with RPS.

Example: The State of California California's RPS aims at achieving 20% renewable penetration by 2010. To this end, it obligates load serving entities (LSEs), such as investor-owned utilities (IOUs), energy service providers (ESPs) and community choice aggregators (CCAs), to achieve an annual target level, which is increased by 1% every year until 2010. Pursuant to the RPS legislation, the California Public Utilities Commission implemented flexible compliance rules that allow LSEs to bank excess renewable energy, and defer deficits in any year for up to three years. LSEs were allowed to defer their entire target for their first year of compliance for up to three years. LSEs with deficits are subject to penalties, 5 cents/kWh, up to $25 million per year per LSE[14].

Since the implementation of the RPS program in 2002, renewable generation capacity has grown significantly, as shown in Figure 6-3. However, the 20% RPS goal was not fully met. For example, the four large IOUs in California reported that they met 17.0% of their electricity demand with RPS-eligible generation in 2010. PG&E served 15.9% of its 2010 load with RPS-eligible renewable energy, SCE with 19.3%, and SDG&E with 11.9% [15]. Although these companies did not meet the 20% goal by 2010, the California Public Utilities Commission (CPUC) stated in September 2011 that "it has not issued any penalties for non-compliance because it has not made a determination that any LSE is out of compliance."[16] This is probably because the

line at `http://www.fepc.or.jp/library/data/demand/__icsFiles/afieldfile/2011/04/28/kakuho_fy2010.pdf` (Retrieved on January 14, 2012).

[13]Statistics by the Japanese Agency for Natural Resources and Energy. Available On-line at `http://www.rps.go.jp/RPS/new-contents/top/ugokilink-kakaku.html`. Retrieved on January 15, 2012.

[14]California Public Utilities Commission. `http://www.cpuc.ca.gov/PUC/energy/Renewables/compliance.htm` Retrieved on January 15, 2012.

[15]California Public Utilities Commission. Renewable Portfolio Standard Quarterly Report. 3rd Quarter, 2011. Available at `http://www.cpuc.ca.gov/NR/rdonlyres/2A2D457A-CD21-46B3-A2D7-757A36CA20B3/0/Q3RPSReporttotheLegislatureFINAL.pdf` Retrieved on January 15, 2012.

[16]California Public Utilities Commission. `http://www.cpuc.ca.gov/PUC/energy/Renewables/`

LSEs banked credits when the goal was low in the early years of the program, and used the credits in later years to avoid penalties.

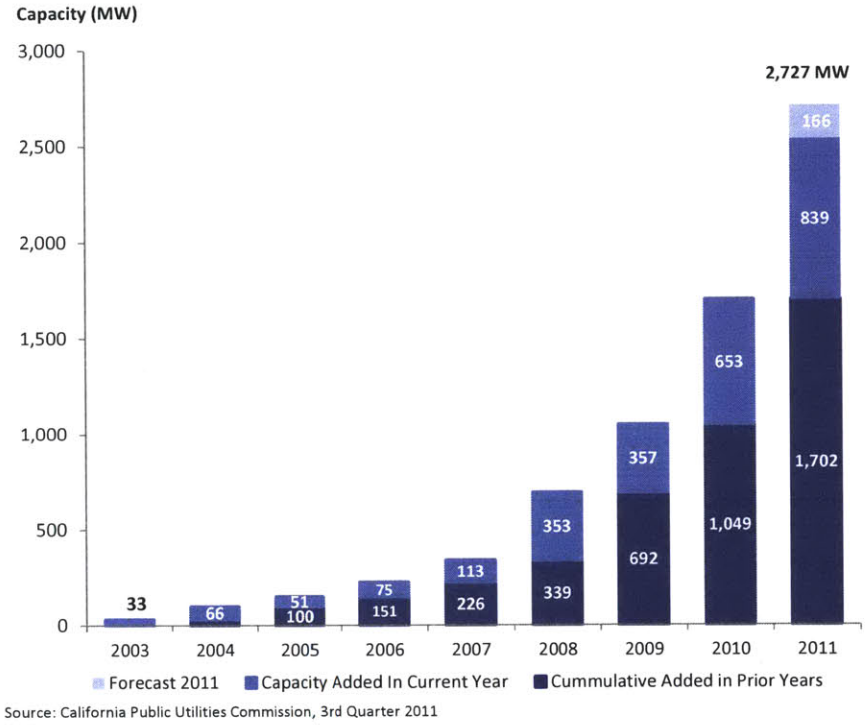

Figure 6-3: Growth in renewable generation capacity in California. Source: State-level RPS targets in the U.S. Source: Database of State Incentives for Renewable Energy (DSIRE). Source: California Public Utilities Commission, Renewable Portfolio Standard Quarterly Report. 3rd Quarter, 2011. [17]

6.3.2 Feed-in Tariff

Policy Overview

A feed-in tariff (FIT) is a policy mechanism, in which eligible renewable electricity producers are paid a fixed cost-based price for the renewable electricity they produce [36]. In other words, a federal or provincial government regulates the tariff rate of renewable electricity. The objective of FIT is to create generation-based, price-driven incentives. These usually take the form of either a fixed amount of money paid for

`compliance.htm` Retrieved on January 15, 2012.

renewable generation, or an additional premium on top of the market price paid to renewable electricity producers. In addition, most FIT policies set a guaranteed duration (typically 10-30 years) of the specified tariffs in order to create stronger incentives for long-term investments.

FIT policies began to attract attention in Europe in the late 1980s especially in Denmark, Germany, Italy, and, in the 1990s, in Spain. As of 2011, FIT policies have been enacted in over 50 countries[18]. Most notably, Spain, Germany, and Denmark achieved a large growth in wind power, which now accounts for 9%, 5%, and 20% of electricity in those countries, respectively [24]. The case of Germany is reviewed later in this section.

Case Study: Germany

The German FIT policy is considered to be one of the most successful, along with those of Spain, Portugal, and Denmark [23]. The current FIT system in Germany was established in several steps [36]. It was initially introduced to Germany in 1991 by the Electricity Feed-in Act. The act was replaced by the Renewable Energy Act in 2000, which uncoupled the tariff level from the retail price of electricity. Instead, it bound the tariff level to the cost of generation. This results in different tariff levels for different technologies (e.g., wind, solar, biomass, etc.), as well as for different locations, depending on cost. Moreover, the Act extended purchase guarantees for a period of 20 years. As shown in Figure 6-4, the tariff levels have been relatively high compared to other European nations, but they are reduced every year to encourage more efficient production of renewable energy.

Renewable electricity generation, particularly wind, has shown significant growth since the introduction of the FIT policy, as shown in Figure 6-5. In the first quarter of 2011, 19.2% of Germany's electricity was produced by renewable sources[19]. With

[18]REN21 Global Status Report, 2010. Available on-line at `http://www.ren21.net/REN21Activities/Publications/GlobalStatusReport/tabid/5434/Default.aspx` Retrieved on January 15,2012.

[19]Development of Renewable Energy Sources in Germany 2010. Federal Ministry for the Environmental, Nature Conservation and Nuclear Safety. Available on-line at `http://www.bmu.de/files/english/pdf/application/pdf/ee_in_deutschland_graf_tab_en.pdf` Retrieved on January 15,

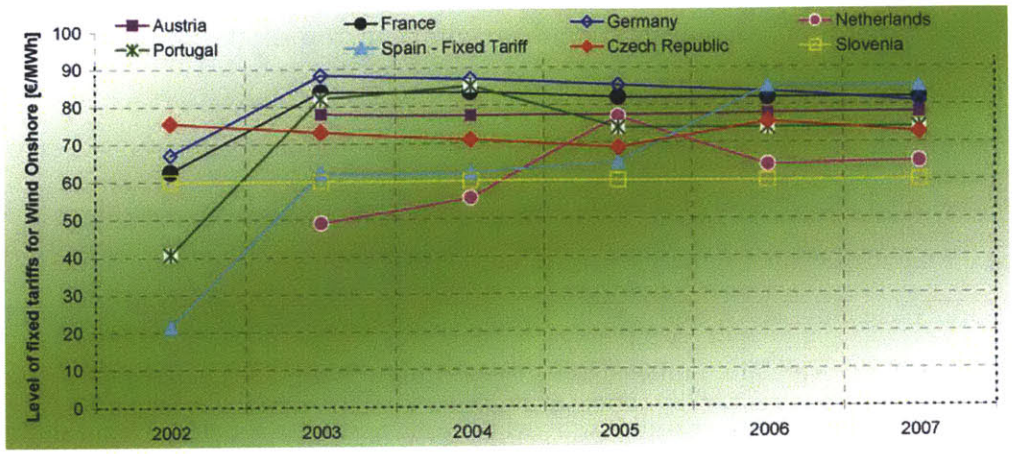

Figure 6-4: Comparison of FIT levels for on-shore wind generation by nations. Source: Haas et al. [36].

the successful FIT policy, Germany reduced emissions of greenhouse gases -21.3 % by the end of 2007, compared with 1990 levels[20]. The country set an ambitious goal to increase the proportion of gross electricity consumption attributable to renewables to at least 30 percent by the year 2020, and to 50 percent by 2050[21].

Pros and Cons of Feed-in Tariff

A remarkable advantage of FIT over RPS is that it reduces uncertainty in investment conditions. Under an RPS policy, investment in renewable generation facilities must be financed by selling RECs, whose price is uncertain because it is determined by a market. In contrast, with a FIT policy the price of renewable electricity is guaranteed by a government for a long period (typically for several decades). Moreover, in many countries the tariff rate is determined based on the cost for generation of each renewable technology. The price certainty with long-term contracts encourages

2012.

[20]Renewable Energy Sources in Figures. June 2009. Federal Ministry for the Environmental, Nature Conservation and Nuclear Safety. Available on-line at `http://www.bmu.de/files/english/renewable_energy/downloads/application/pdf/broschuere_ee_zahlen_en.pdf`. Retrieved on January 15, 2012.

[21]Renewable Energy Sources in Figures. June 2009. Federal Ministry for the Environmental, Nature Conservation and Nuclear Safety. Available on-line at `http://www.bmu.de/files/english/renewable_energy/downloads/application/pdf/broschuere_ee_zahlen_en.pdf`. Retrieved on January 15, 2012.

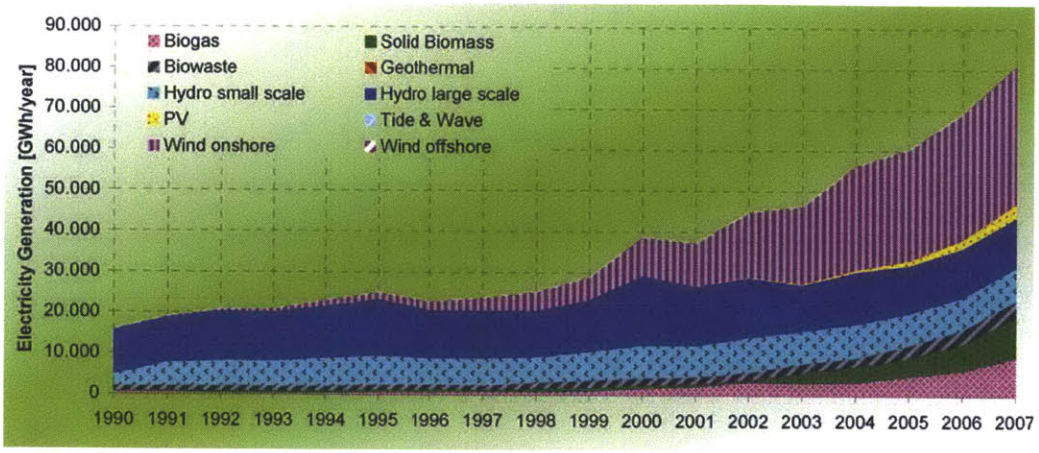

Figure 6-5: Renewable energy generation in Germany from 1990 to 2007. Data is based on International Energy Agency 2008. The graph is taken from [36].

investors to finance renewable energy.

A major criticism of FIT is that a too generous tariff rate results in market inefficiency. On the other hand, RPS can theoretically achieve a specified target penetration of renewable energy with minimum cost. This claim is based on an assumption that there is a multiplicity of buyers and sellers in a perfectly competitive REC market, where no single buyer or seller has enough market share to have a significant influence on prices [24]. In practice, markets are rarely perfectly competitive.

It appears that FIT policies have been quite successful in Europe. For example, Denmark, Germany, and Spain, which have operated FIT systems for two decades, have achieved much larger growth in wind generation than other European countries that do not employ FIT or were late to introduce it, as shown in Figure 6-6. Toke [24] assesses the effectiveness of the RPS policy in the U.K.[22] and conclude that it does not deliver renewable energy any more cheaply than a feed-in tariff. Haas et al. concludes [36] that "sufficiently generous FITs - set above the generation cost level - are quite effective in attracting investment in renewables."

However, it would not be appropriate to compare RPS and FIT with a single criterion, as the objectives of the two policies are different. While the focus of RPS is cost-efficiency, FIT puts more focus on rapid growth of renewable penetration. In

[22]In the U.K., RPS is called renewable obligation (RO)

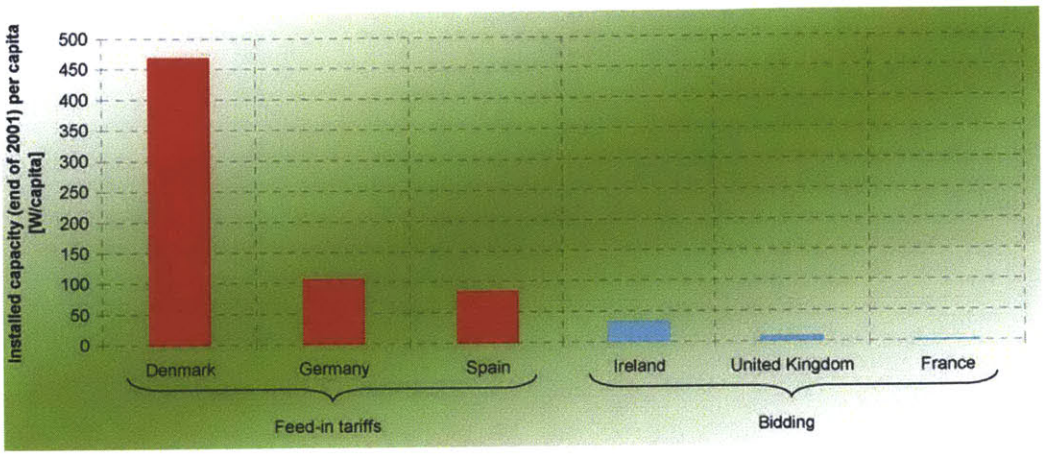

Figure 6-6: Comparison of wind power deployment by the policy options employed from 1990 to 2001. Source: Haas et al. [35]. The graph is created by [36].

terms of constrained optimization, RPS aims at minimizing cost with a lower bound on renewable penetration, while FIT seeks to maximize renewable penetration with an upper bound on cost, specified by the tariff rate. Hence, comparison of the two policy options reflect differences in philosophical viewpoints, as is the case in many other policy discussions.

6.4 Conclusions

In the first half of this chapter we reviewed several cases in Japan and the U.S. that highlight the need for, as well as the risk of, electricity deregulation. A careful design of deregulation policy is necessary in order to effectively implement a smart grid while avoiding potential risk, illustrated by the case of the California energy crisis. In the second half of this chapter we discussed the pros and cons of two major policy options to promote the introduction of renewable energies: the renewable portfolio standard (RPS) and the feed-in tariff (FIT). We provided an interpretation of the two policy options in terms of constrained optimization: RPS minimizes cost with a lower bound on renewable penetration, while FIT maximizes renewable penetration with an upper bound on cost.

Chapter 7

Conclusion

This thesis developed a distributed control system to enable a smart grid with sustainable homes, and discussed policy options to realize the vision.

The proposed control system is composed of three algorithms. The first algorithm is a Market-based Contingent Energy Dispatch for a smart grid, which finds the most efficient allocation of nominal and contingent power generation. Furthermore, it explicitly considers the uncertainty in the supply from renewables, such as wind and solar, and guarantees that the risk of power imbalance is within given risk bounds. The algorithm optimizes the allocation through a market mechanism. More specifically, a market optimizes the prices of nominal and contingent power, while each plant is responsible for finding the optimal output levels of nominal and contingent power. The maximum efficiency is achieved at the equilibrium place, where the supplies and demands are balanced. We demonstrated the algorithm's capabilities through simulations of an electrical grid with heterogeneous power plants.

The second algorithm is a risk-sensitive plan executive, p-Sulu On-Line or p-Sulu OL, which can optimally control the indoor temperature of a Connected Sustainable Home. It achieves significant reduction in energy consumption by controlling the incoming sunlight through a south-facing facade made of electrochromic glass windows, whose opacity can be changed. The residents specify their desired range of temperature through a temporal plan on state called chance-constrained qualitative state plan (CCQSP), which is optimally executed by p-Sulu OL. We demonstrated

that p-Sulu OL achieves significant reduction in energy consumption compared to a classical control approach, while successfully limiting the risk of failure to satisfy residents' requirements.

The third algorithm is a joint chance-constrained MPC, which can be applied to AC frequency control and building temperature control with uncertainty. Resolvability or recursive feasibility is an essential property for robust MPCs. However, when an unbounded stochastic uncertainty is present, it is generally impossible to guarantee resolvability. We proposed a new concept called *probabilistic resolvability*. An MPC algorithm is probabilistically resolvable if it has feasible solutions at future time steps with a certain probability, given a feasible solution at the current time. The proposed chance-constrained MPC algorithm guarantees probabilistic resolvability, as well as the satisfaction of a joint chance-constraint. Furthermore, with moderate conditions, we showed that the finite-horizon optimal control problem solved at each time step in the proposed algorithm is a convex optimization problem. The probabilistic feasibility of the proposed algorithm is validated by Monte-Carlo simulations.

Finally, we discussed key policy challenges and policy options to allow smart grid technologies to be fully utilized. The case studies in Japan showed that various regulations, such as the ones on electricity distribution, fishery right, and national park scenery, prevent flexible operation of a smart grid and introduction of renewable energy. On the other hand, the case study on the California energy crisis, where a large-scale blackouts occurred as a result of a market failure, illustrated the risk of deregulation. We also compared two policy options to enhance renewable energy production: a renewable portfolio standard (RPS) and a feed-in tariff (FIT). We provided an interpretation of the two policy options in terms of a constrained optimization that RPS minimizes cost with a lower bound on renewable penetration, while FIT maximizes renewable penetration with an upper bound on cost.

Bibliography

[1] B. Açikmeşe and J. M. Carson III. A nonlinear model predictive control algorithm with proven robustness and resolvability. In *Proceedings of American Control Conference*, 2006.

[2] B. Açikmeşe, J. M. Carson III, and D. S. Bayard. A robust model predictive control algorithm for incrementally conic uncertain/nonlinear systems. *International Journal of Robust and Nonlinear Control*, 21(5):563–590, 2011.

[3] R. Alur, T. Feder, and T. A. Henzinger. The benefits of relaxing punctuality. *Journal of the ACM*, 43, 1996.

[4] G. Andersson. Dynamics and control of electric power systems. Lecture not of 227-0528-00, ITET, ETH, 2011.

[5] S. C. G. A. Andreas Ulbig, Michèle Arnold. Framework for multiple time-scale cascaded mpc application in power systems. In *Proceedings of the 18th IFAC World Congress*, 2011.

[6] S. C. G. A. Andreas Ulbig, Michèle Arnold. Framework for multiple time-scale cascaded mpc application in power systems. In *Preprints of the 18th IFAC World Congress*, 20121.

[7] K. E. Atkinson. *An Introduction to Numerical Analysis, Second Edition.* John Wiley & Sons, 1989.

[8] F. Bacchus and F. Kabanza. Planning for temporally extended goals. *Annals of Mathematics and Artificial Intelligence*, (22):5–27, 1998.

[9] N. M. Barr. *Wind Models for Flight Simulator Certification of Landing and Approach Guidance and Control Systems.* University of Michigan Library, 1974.

[10] A. Ben-tal, A. Goryashko, E. Guslitzer, and A. Nemirovski. Robust solutions of uncertain linear programs. *Operations Research Letters*, 25:1–13, 1999.

[11] A. Ben-tal and A. Nemirovski. Robust solutions of uncertain linear programs. *Operations Research Letters*, 25:1–13, 1999.

[12] D. P. Bertsekas. *Nonlinear Programming.* Athena Scientific, 1999.

[13] L. Blackmore. *Robust Execution for Stochastic Hybrid Systems.* PhD thesis, Massachusetts Institute of Technology, 2007.

[14] L. Blackmore, H. Li, and B. C. Williams. A probabilistic approach to optimal robust path planning with obstacles. In *Proceedings of American Control Conference*, 2006.

[15] L. Blackmore and M. Ono. Convex chance constrained predictive control without sampling. In *Proceedings of the AIAA Guidance, Navigation and Control Conference*, 2009.

[16] L. Blackmore, M. Ono, A. Bektassov, and B. C. Williams. A probabilistic particle control approximation of chance constrained stochastic predictive control. *IEEE Transactions on Robotics*, 26(3), 2010.

[17] S. Boyd, N. Parikh, E. Chu, B. Peleato, and J. Eckstein. Distributed optimization and statistical learning via the alternating direction method of multipliers. *Foundations and Trends in Machine Learning*, 3(1):1–122, 2010.

[18] A. Charnes and W. W. Cooper. Chance-constrained programming. *Management Science*, 6:73–79, 1959.

[19] H. Chen, C. Scherer, and F. Allgower. A game theoretic approach to nonlinear robust receding horizon control of constrained systems. In *American Control*

Conference, 1997. Proceedings of the 1997, volume 5, pages 3073 –3077 vol.5, jun 1997.

[20] Chi-Keung and Woo. What went wrong in california's electricity market? *Energy*, 26(8):747 – 758, 2001.

[21] L. Chisci, J. Rossiter, and G. Zappa. Systems with persistent disturbances: predictive control with restricted constraints. *Automatica*, 37(7):1019 – 1028, 2001.

[22] B. Chowdhury and S. Rahman. A review of recent advances in economic dispatch. *Power Systems, IEEE Transactions on*, 5(4):1248 –1259, nov 1990.

[23] T. Couture and Y. Gagnon. An analysis of feed-in tariff remuneration models: Implications for renewable. *Energy Policy*, 2009.

[24] David and Toke. Renewable financial support systems and cost-effectiveness. *Journal of Cleaner Production*, 15(3):280 – 287, 2007. ¡ce:title¿Sustainable Development in Practice¡/ce:title¿.

[25] R. Dechter, I. Meiri, and J. Pearl. Temporal constraint networks. In *Proceedings of the first international conference on Principles of knowledge representation and reasoning*, pages 83–93, San Francisco, CA, USA, 1989. Morgan Kaufmann Publishers Inc.

[26] Electric Power Research Institute (EPRI), Palo Alto, CA. The green grid: Energy savings and carbon emissions reductions enabled by a smart grid, 2008.

[27] S. Elrod, G. Hall, R. Costanza, M. Dixon, and J. D. Rivieres. The responsive environment: Using ubiquitous computing for office comfort control and energy management. Technical report, XEROX Palo Alto Research Center, 1993.

[28] EPRI. The cost of power disturbances to industrial and digital economy companies. EPRI Technical report 1006274, 2001.

[29] Federal Energy Regulatory Commission (FERC). Final report on price manipulation in western markets, 2003.

[30] C. Feisst, D. Schlesinger, and W. Frye. Smart grid : The role of electricity infrastructure in reducing greenhouse gas emissions. Cisco Internet Business Solutions Group, 2008.

[31] M. Feldmeier and J. Paradiso. Personalized hvac control system. In *Internet of Things (IOT), 2010*, pages 1 –8, 29 2010-dec. 1 2010.

[32] C. E. Garcia, D. M. Prett, and M. Morari. Model predictive control: Theory and practice - a survey. *Automatica*, 25(3):335 – 348, 1989.

[33] P. Geibel and F. Wysotzki. Risk-sensitive reinforcement learning applied to control under constraints. *Journal of Artificial Intelligence Research*, 24:81–108, 2005.

[34] M. Gwerder and J. Todtli. Predictive control for integrated room automation. *8th REHVA World Congress for Building Technologies CLIMA*, (October), 2005.

[35] R. Haas, W. Eichhammer, C. Huber, O. Langniss, A. Lorenzoni, R. Madlener, P. Menanteau, P.-E. Morthorst, A. Martins, A. Oniszk, J. Schleich, A. Smith, Z. Vass, and A. Verbruggen. How to promote renewable energy systems successfully and effectively. *Energy Policy*, 32(6):833 – 839, 2004.

[36] R. Haas, C. Panzer, G. Resch, M. Ragwitz, G. Reece, and A. Held. A historical review of promotion strategies for electricity from renewable energy sources in eu countries. *Renewable and Sustainable Energy Reviews*, 15(2):1003 – 1034, 2011.

[37] H. Happ. Optimal power dispatch - a comprehensive survey. *Power Apparatus and Systems, IEEE Transactions on*, 96(3):841 – 854, may 1977.

[38] G. P. Henze, D. E. Kalz, S. Liu, and C. Felsmann. Experimental analysis of model-based predictive optimal control for active and passive building thermal storage inventory. *HVAC&R Research*, 11(2):189–213, 2005.

[39] C. Hernandez-Aramburo, T. Green, and N. Mugniot. Fuel consumption minimization of a microgrid. *Industry Applications, IEEE Transactions on*, 41(3):673 – 681, may-june 2005.

[40] A. G. Hofmann and B. C. Williams. Robust execution of temporally flexible plans for bipedal walking devices. In *Proceedings of the International Conference on Automated Planning and Scheduling (ICAPS-06)*, 2006.

[41] M. Huneault and F. Galiana. A survey of the optimal power flow literature. *Power Systems, IEEE Transactions on*, 6(2):762 –770, may 1991.

[42] F. Incropera, T. Bergman, A. Lavine, and D. DeWitt. *Fundamentals of Heat and Mass Transfer.* John Wiley & Sons, 2011.

[43] J. C. Jacobo, D. de Roure, and E. H. Gerding. An agent-based electrical power market. In *Proceedings of the 7th International Joint Conference on Autonomous Agents and Multiagent Systems (AAMAS): Demo Papers*, 2008.

[44] F. Kelly, A. Maulloo, and D. Tan. Rate control in communication networks: Shadow prices, proportional fairness and stability. *Journal of the Operational Research Society*, 49:237–252, 1998.

[45] E. C. Kerrigan. *Robust Constraint Satisfaction: Invariant Sets and Predictive Control.* PhD thesis, University of Cambridge, 2000.

[46] M. Khalid and A. V. Savkin. Model predictive control based efficient operation of battery energy storage system for primary frequency control. In *Proceeings of the 11th International Conference on Control, Automation, Robotics, and Vision*, 2011.

[47] S. Knight, G. Rabideau, S. Chien, B. Engelhardt, and R. Sherwood. Casper: space exploration through continuous planning. *Intelligent Systems, IEEE*, 16(5):70 – 75, sep-oct 2001.

[48] J. Z. Kolter and J. Ferreira. A large-scale study on predicting and contextualizing building energy usage. In *Proceedings of Twenty-Fifth AAAI Conference on Artificial Intelligence (AAAI-11), Special Track on Computational Sustainability and AI*, 2011.

[49] P. Komor. *Renewable Energy Policy.* iUniverse, 2004.

[50] M. V. Kothare, V. Balakrishnan, and M. Morari. Robust constrained model predictive control using linear matrix inequalities. *Automatica*, 32(10):1361 – 1379, 1996.

[51] Y. Kuwata, A. Richards, and J. How. Robust receding horizon control using generalized constraint tightening. *Proceedings of American Control Conference*, 2007.

[52] J. Kvarnstrom and P. Doherty. Talplanner: A temporal logic based forward chaining planner. *Annals of Mathematics and Artificial Intelligence*, (30), 2000.

[53] K. H. LaCommare and J. H. Eto. Cost of power interruptions to electricity consumers in the united states (us). *Energy*, 31(12):1845 – 1855, 2006.

[54] R. Lasseter and P. Paigi. Microgrid: a conceptual solution. In *Power Electronics Specialists Conference, 2004. PESC 04. 2004 IEEE 35th Annual*, volume 6, pages 4285 – 4290 Vol.6, june 2004.

[55] T. Léauté. Coordinating agile systems through the model-based execution of temporal plans. Master's thesis, Massachusetts Institute of Technology, 2005.

[56] T. Léauté and B. C. Williams. Coordinating agile systems through the model-based execution of temporal plans. In *Proceedings of the Twentieth National Conference on Artificial Intelligence (AAAI)*, 2005.

[57] D. J. Leith, M. Heidl, and J. V. Ringwood. Gaussian process prior models for electrical. In *Proceedings of the 8th International Conference on Probabilistic Methods Applied to Power Systems*, 2004.

[58] H. Li and B. C. Williams. Hybrid planning with temporally extended goals for sustainable ocean observing. In *Proceedings of Twenty-Fifth AAAI Conference on Artificial Intelligence (AAAI-11), Special Track on Computational Sustainability and AI*, 2011.

[59] H. X. Li. *Kongming: A Generative Planner for Hybrid Systems with Temporally Extended Goals.* PhD thesis, Massachusetts Institute of Technology, 2010.

[60] P. Li, M. Wendt, and G. Wozny. A probabilistically constrained model predictive controller. *Automatica*, 38:1171–1176, 2002.

[61] Y. Ma, F. Borrelli, B. Hencey, A. Packard, and S. Bortoff. Model predictive control of thermal energy storage in building cooling systems. In *Decision and Control, 2009 held jointly with the 2009 28th Chinese Control Conference. CDC/CCC 2009. Proceedings of the 48th IEEE Conference on*, pages 392 –397, dec. 2009.

[62] A. E.-D. Mady, G. M. Provan, C. Ryan, and K. N. Brown. Stochastic model predictive controller for the integration of building use and. In *Proceedings of Twenty-Fifth AAAI Conference on Artificial Intelligence (AAAI-11), Special Track on Computational Sustainability and AI*, 2011.

[63] D. Q. Mayne, J. B. Rawlings, C. V. Rao, and P. O. M. Scokaert. Constrained model predictive control: Stability and optimality. *Automatica*, 2000.

[64] MIT Mobile Experience Lab. Sustainable connected home brochure. Available on-line at `http://mobile.mit.edu/fbk_wp-uploads/2010/01/connected_home_brochure.pdf`. Retrieved on January 15,2012.

[65] W. J. Mitchell and F. Casalegno. *Connected Sustainable Cities.* MIT Mobile Experience Lab Publishing, 2008.

[66] N. Muscettola, P. Nayak, B. Pell, and B. C. Williams. Remote agent: to boldly go where no AI system has gone before. *Artificial Intelligence*, 103(1-2):5 – 47, 1998.

[67] F. Oldewurtel, C. N. Jones, and M. Morari. A tractable approximation of chance constrained stochastic mpc based on affine disturbance feedback. In *Proceedings of Conference on Decision and Control*, 2008.

[68] F. Oldewurtel, A. Parisio, C. Jones, M. Morari, D. Gyalistras, M. Gwerder, V. Stauch, B. Lehmann, and K. Wirth. Energy Efficient Building Climate Control using Stochastic Model Predictive Control and Weather Predictions. In *American Control Conference*, Baltimore, USA, jun 2010.

[69] F. Oldewurtel, A. Ulbig, A. Parisio, G. Andersson, and M. Morari. Reducing peak electricity demand in building climate control using real-time pricing and model predictive control. In *Proceedings of Conference on Decision and Control*, 2010.

[70] M. Ono. *Robust, Goal-directed Plan Execution with Bounded Risk*. PhD thesis, Massachusetts Institute of Technology, 2012.

[71] M. Ono and B. C. Williams. An efficient motion planning algorithm for stochastic dynamic systems with constraints on probability of failure. In *Proceedings of the Twenty-Third AAAI Conference on Artificial Intelligence (AAAI-08)*, 2008.

[72] M. Ono and B. C. Williams. Iterative risk allocation: A new approach to robust model predictive control with a joint chance constraint. In *Proceedings of 47th IEEE Conference on Decision and Control*, 2008.

[73] M. Ono and B. C. Williams. Decentralized chance-constrained finite-horizon optimal control for multi-agent systems. In *Decision and Control (CDC), 2010 49th IEEE Conference on*, pages 138 –145, dec. 2010.

[74] M. Ono and B. C. Williams. Market-based risk allocation for multi-agent systems. In *Ninth International Conference on Optimisation in Multi-Agent Systems*, 2010.

[75] K. S. Pandya and S. K. Joshi. A survey of optimal power flow methods. *Journal of Theoretical and Applied Information Technology*, 2008.

[76] A. Prékopa. The use of discrete moment bounds in probabilistic constrained stochastic programming models. *Annals of Operations Research*, 85:21–38, 1999.

[77] Z. Qiu, G. Deconinck, and R. Belmans. A literature survey of optimal power flow problems in the electricity market context. In *Power Systems Conference and Exposition, 2009. PSCE '09. IEEE/PES*, pages 1 –6, march 2009.

[78] SBI. Smart grid technologies, markets, components and trends worldwide. SB1926639, 2009.

[79] A. T. Schwarm and M. Nikolaou. Chance-constrained model predictive control. *AIChE Journal*, 45(8):1743–1752, 1999.

[80] P. O. M. Scokaert and D. Q. Mayne. Minmax feedback model predictive control for constrained linear systems. *IEEE Transactions on Automatic Control*, 43(8), 1998.

[81] N. Z. Shor. *Minimization Methods for Non-Differentiable Functions.* Springer-Berlag, 1985.

[82] D. Sontag, A. Globerson, and T. Jaakkola. Introduction to dual decomposition for inference. *Optimization for Machine Learning*, 2010.

[83] The U.S. National Research Council of the National Academies. Hidden costs of energy:, 2009.

[84] J. Tuinstra. *Price Dynamics in Equilibrium Models: The Search for Equilibrium and the Emergence of Endogenous Fluctuations.* Kluwer Academic Publishers, 2000.

[85] A. Ulbig, M. Galus, S. Chatzivasileiadis, and G. Andersson. General frequency control with aggregated control reserve capacity from time-varying sources: The case of phevs. In *Bulk Power System Dynamics and Control (iREP) - VIII (iREP), 2010 iREP Symposium*, pages 1 –14, aug. 2010.

[86] U.S. - Canada Power System Outage Task Force. Final report on the augus t 14, 2003 blackout in the united states and canada, April 2004.

[87] U.S. Energy Information Administration. Annual energy outlook 2010, 2010.

[88] F. Vallée, J. Lobry, and O. Deblecker. Impact of the wind geographical correlation level for reliability studies. *IEEE Transactions on Power Systems*, 22(4), November 2007.

[89] D. H. van Hessem. *Stochastic inequality constrained closed-loop model predictive control with application to chemical process operation.* PhD thesis, Delft University of Technology, 2004.

[90] R. Vastamäki, I. Sinkkonen, and C. Leinonen. A behavioural model of temperature controller usage and energy saving. *Personal Ubiquitous Comput.*, 9:250–259, July 2005.

[91] H. Voos. Agent-based distributed resource allocation in technical dynamic systems. In *Proceedings of IEEE Workshop on Distributed Intelligent Systems: Collective Intelligence and Its Applications*, 2006.

[92] Q. Wang, C. Lin, X. Yang, and J. Liu. Scheme of intelligent community based on distributed generation and micro-grid. In *Power System Technology (POWERCON), 2010 International Conference on*, pages 1 –6, oct. 2010.

[93] M. P. Wellman. A market-oriented programming environment and its application to distributed multicommodity flow problems. *Journal of Artificial Intelligence Research*, 1:1–23, 1993.

[94] L. Xiao, M. Johansson, and S. Boyd. Simultaneous routing and resource allocation via dual decomposition. *Communications, IEEE Transactions on*, 52(7):1136 – 1144, july 2004.

[95] H. Xu, U. Topcu, S. Low, C. Clarke, and K. Chandy. Load-shedding probabilities with hybrid renewable power generation and energy storage. In *Communication,*

Control, and Computing (Allerton), 2010 48th Annual Allerton Conference on, pages 233 –239, 29 2010-oct. 1 2010.

[96] F. Ygge and H. Akkermans. Power load management as a computational market. In *Proceedings of Second International Conference on Multiagent Systems*, 1996.